

MDM2 splice variants



Cellular localization and expression in a transgenic mouse model

Dissertation

zur Erlangung des akademischen Grades
doctor rerum naturalium (Dr. rer. nat.)

vorgelegt der

Mathematisch-Naturwissenschaftlich-Technischen Fakultät
Martin-Luther-Universität Halle-Wittenberg

angefertigt in der

Abteilung für Molekular Pharmakologie
St. Jude Children's Research Hospital, Memphis, TN

von Frau Dipl. Biochem. Katja Schuster

geboren am 31. Dezember 1975 in Cottbus (Brandenburg)

Gutachter:

1. Prof. Dr. rer.nat. Rainer Rudolph
2. PD Dr. rer. nat. Thilo Schlott

Verteidigung: 15. Dezember 2006

Memphis, den 24. Februar 2006

urn:nbn:de:gbv:3-000011042

[<http://nbn-resolving.de/urn/resolver.pl?urn=nbn%3Ade%3Agbv%3A3-000011042>]

No child should die in the dawn of life.

Danny Thomas (1914-1991)

In Erinnerung an meinen Großvater

Bruno Walter Gähler

Bibliographic description

Schuster, Katja

MDM2 splice variants – Cellular localization and expression in a transgenic mouse model

Martin-Luther-Universität Halle/Wittenberg, Dissertation, 2006
102 Pages, 131 References, 28 Figures, 6 Tables, 4 Appendix enclosures

Abstract:

The *MDM2* oncogene encodes a protein that is overexpressed and gene-amplified in several human tumors. In addition, more than 40 tumor *MDM2* splice variants have been identified, although, their main biological function is still undefined. This work evaluated the function of MDM2 splice variants *in vivo* and *in vitro*, and was divided into two major projects.

Project 1. *MDM2-A* is one of the most commonly occurring splice variants and therefore, an *Mdm2-a* transgenic mouse model was generated, and the *in vivo* function of MDM2-A was analyzed. Surprisingly, three of four founder mice contained mis-sense mutations within the *Mdm2-a* sequence. In addition, analysis of transgenic embryos suggested that wild-type MDM2-A is lethal for mouse development. Consistent with this observation, MDM2-A mediated growth inhibition *in vitro* that depended upon p53 and p21^{Waf1/Cip1} expression. Nevertheless, a single wild-type *Mdm2-a* transgenic mouse line was generated whose survival appeared dependent upon a lower level of MDM2-A and a restricted pattern of MDM2-A expression in tissues that can tolerate enhanced p53 function. Mutant and wild-type *Mdm2-a* transgenic mice did not show a tumorigenic phenotype; however, wild-type *Mdm2-a* transgenic mice showed reduced longevity probably due to the elevated p53 activity. In summary, a growth inhibitory function for MDM2-A was observed that is in contrast to transforming activities that have previously been determined for other MDM2 splice variants.

Project 2. Because cellular localization of proteins may provide information regarding their potential function, the expression of splice variants MDM2-A, B and FB26, and their co-expression with p53, full-length MDM2 and ARF were evaluated. All three splice variants localized to the nucleus in addition to faint cytoplasmic expression of MDM2-A and B. Nuclear localization of MDM2-A and B was controlled by a previously uncharacterized nuclear localization signal 2 (NLS2). Nucleoplasmic localization of FB26 was mediated both by the well-characterized NLS1 and a potentially novel NLS3 that was generated by aberrant splicing. p53 and full-length MDM2 co-localized with the splice variants in the nucleus. Since MDM2-A and B both contain a RING finger domain these results suggested that an interaction with full-length MDM2 in the nucleus is possible. FB26 was the only splice variant evaluated that contained a p53-binding domain implying that p53 and FB26 may also interact in the nucleus. ARF did not co-localize with the splice variants and was predominately expressed within the nucleoli. In summary, nuclear localization signals responsible for the nucleoplasmic distribution of MDM2 splice variants have been characterized. Co-localization of MDM2 splice variants with proteins such as p53 and full-length MDM2 is probably important for their function.

In conclusion, even though *MDM2* splice variants are usually found in human tumors, not all of them display transforming activities. It is possible that some MDM2 splice variants contribute to the development of tumors while others may have been generated because of defective splicing machinery as a consequence of tumorigenesis.

Table of Content

Title page

Bibliographic description	i
Table of Content	ii
Abbreviations	vi
1. Introduction	1
1.1. <i>MDM2</i> oncogene	1
1.2. Transcription and translation of <i>MDM2</i>	2
1.3. Posttranscriptional modifications	2
1.4. <i>MDM2</i> regulates the p53 tumor suppressor	3
1.5. p53-independent functions of <i>MDM2</i>	6
1.6. Introduction to splicing	8
1.7. <i>MDM2</i> splice variants	10
1.8. Aims of work	13
2. Materials	14
2.1. Technical instruments and materials	14
2.2. Chemicals	14
2.3. Cell culture media and materials	16
2.4. Enzymes	16
2.5. Kits	17
2.6. Antibodies	17
2.7. Plasmids	18
2.8. Oligonucleotides	19
2.9. Murine strains	21
2.10. Bacterial strains	21
2.11. Cell lines	21
2.12. Computer software and online applications	22

3. Methods	23
3.1. Molecular biology	23
3.1.1. Small scale isolation of plasmid DNA	23
3.1.2. Large scale isolation of plasmid DNA	23
3.1.3. Isolation of genomic DNA from mouse tail tips and tissue	23
3.1.4. Isolation of genomic DNA from paraffin sections	24
3.1.5. Isolation of total-RNA from mouse tissue	24
3.1.6. DNA and RNA concentration determination	24
3.1.7. Polymerase chain reaction	24
3.1.7.1. Polymerase chain reaction	24
3.1.7.2. Reverse transcriptase polymerase chain reaction	25
3.1.7.3. Sequencing reaction	25
3.1.8. Agarose gel electrophoresis	25
3.1.9. DNA fragment isolation of from agarose gel	26
3.1.10. Restriction endonuclease digestion	26
3.1.11. Ligation of DNA fragments	26
3.1.12. Preparation and transformation of chemical competent <i>E. coli</i>	27
3.1.13. Site directed mutagenesis	27
3.2. Mammalian cell culture	27
3.2.1. Maintenance and storage of cell lines	27
3.2.2. Cell counting	28
3.2.3. Transient transfection	28
3.2.4. Retroviral transduction	28
3.2.5. Adenoviral transduction	29
3.2.6. Flow cytometry	29
3.2.7. Growth rate analysis	30
3.3. Protein biochemistry	30
3.3.1. Preparation of protein extract from tissues and cells	30
3.3.2. Protein concentration determination	30
3.3.3. Polyacrylamide gel electrophoresis	31
3.3.4. Western blotting	31
3.3.5. Immunoprecipitation assay	32
3.3.6. Immunofluorescence	33

3.4.	Generation of transgenic mice	34
3.4.1.	Splicing by overlap extension	34
3.4.2.	Generation of the transgene	34
3.4.3.	Recovery of transgenic mice	35
3.4.4.	Maintenance of mouse colony	36
3.4.5.	Genotyping of transgenic mice	36
3.4.6.	Isolation of mouse embryonic fibroblasts	37
4.	Results: Expression of MDM2-A in a transgenic mouse model	38
4.1.	Generation of <i>Mdm2-a</i> transgenic mice	38
4.2.	Detection of mutations in the <i>Mdm2-a</i> transgene	39
4.3.	Decrease of wild-type <i>Mdm2-a</i> transgenic embryos during development	41
4.4.	Wild-type MDM2-A inhibits growth in mouse embryonic fibroblasts	43
4.5.	Growth inhibition of wild-type MEFs is dependent upon a wild-type <i>Mdm2-a</i> sequence	45
4.6.	Growth inhibition was p53- and p21 ^{Waf/Cip1} - dependent	46
4.7.	Mutant MDM2-A proteins are unable to bind full-length MDM2	48
4.8.	Factors affecting development of a wild-type <i>Mdm2-a</i> transgenic mouse	48
4.9.	Wild-type MDM2-A is expressed independently of full-length MDM2	50
4.10.	Survival of <i>Mdm2-a</i> transgenic mice	52
4.11.	Discussion	55
5.	Result: Cellular localization of MDM2 splice variants	60
5.1.	Introduction	60
5.2.	Generation of <i>Mdm2</i> splice variant constructs	61
5.3.	Expression of MDM2 splice variants and full-length MDM2 in mutant mouse embryonic fibroblasts	62
5.4.	Epitope tags do not influence the cellular localization for the fusion proteins	64
5.5.	Evaluation of alternate NLS sequences that could facilitate nuclear entry of MDM2 splice variants.	65
5.6.	Co-expression of MDM2 splice variants with MDM2 full-length	68
5.7.	Co-expression of MDM2 splice variants with p53	70
5.8.	Co-expression of MDM2 splice variants with p14 ^{ARF}	72

5.9.	Analysis of binding of full-length MDM2 and MDM2 splice variants to p14 ^{ARF}	72
5.10.	Discussion	75
6.	Summary	80
6.1.	English summary	80
6.2.	Deutsche Zusammenfassung	83
7.	References	87
8.	Appendix	96
	Acknowledgments	
	Curriculum vitae	
	List of Publications	
	Selbstständigkeitserklärung	

Abbreviations

A	Alanine
Ab	Antibody
ARF	Alternative reading frame of locus p16INKA
bp	Base pair
BSA	Bovine serum albumin
CAPS	3[cyclohexylamino]-1-propanesulfonic acid
CMV	Cytomegalovirus
DKOs	Double Knock Out
DMEM	Dulbecco's modification of eagle's medium
DMSO	Dimethyl sulfoxide
DNA	Deoxyribonucleic acid
<i>E. coli</i>	<i>Escherichia coli</i>
FBS	Fetal bovine serum
g	Gram
G	Glycine
GAPDH	Glyceraldehyde-3-phosphate dehydrogenase
GFAP	Glial fibrillary acidic protein
H	Histidine
Ig	Immunoglobulin
IgG	Immunoglobulin G
IP	Immunoprecipitation
K	Lysine
L	Leucine
<i>Mdm2</i>	Murine double minute 2 gene in the mouse
<i>MDM2</i>	Human homolog of the <i>Mdm2</i> gene
MDM2	Protein of human <i>MDM2</i> or murine <i>Mdm2</i> gene
MEFs	Mouse embryonic fibroblasts
MOPS	3(N-Morpholino) propanesulfonic acid
N	Asparagine
NES	Nuclear export signal
NLS	Nuclear localization signal

PCR	Polymerase chain reaction
PDVF	Polyvinylidenedifluoride
Q	Glutamine
R	Arginine
RNA	Ribonucleic acid
rpm	Rounds per minute
SDS	Sodium dodecyl sulfate
SOE	Splicing by overlapping extension
TKOs	Triple Knock Out
Tris	Tris (hydroxymethyl) methylamine
UV	Ultra violet
VC	Vector control

1. Introduction

1.1. MDM2 oncogene

The *Mdm2* cDNA was cloned from a transformed mouse 3T3 cell line, in which the gene was highly amplified¹. *Mdm2* was classed as an oncogene because overexpression of MDM2 protein in primary rodent NIH3T3 fibroblasts resulted in tumor formation when these cells were injected into nude mice². Since that time the human *MDM2* gene has been found to be amplified in several tumors including 30% of soft tissue sarcomas and osteosarcoma^{3,4}, neuroblastomas⁵ and gliomas⁶.

The human *MDM2* gene is located on chromosome 12q13-14 and encodes for a 90kDa (491 amino acids) phosphoprotein³. Both, the human and murine *Mdm2* gene comprise of 12 exons (Appendix 8.1). Sequence alignments of MDM2 genes of different species exposed three conserved regions CR1, CR2 and CR3 (Figure 1). The MDM2 protein contains a p53-binding domain within the N-terminal region^{7,8}, overlapping CR1. This domain encompasses amino acids 14-130 in the mouse⁹ and amino acids 19-102 in the human MDM2 protein¹⁰. The protein also comprises of a nuclear localization signal¹¹ that spans residues 181-185 and a nuclear export signal¹¹ that spans residues 191-209 of the human protein (Figure 1) and amino acids 184-192 of the murine protein. Furthermore, the MDM2 protein contains a central acidic domain (amino acids 237-299, CR2)¹², a zinc finger motif (human amino acids 305-319) and a RING finger domain (amino acids 435-489) at the C-terminus (CR3)^{12,13}. In addition, this RING finger domain includes a cryptic nucleolar localization signal NoLS¹⁴, residues 466-473 (Appendix 8.2).

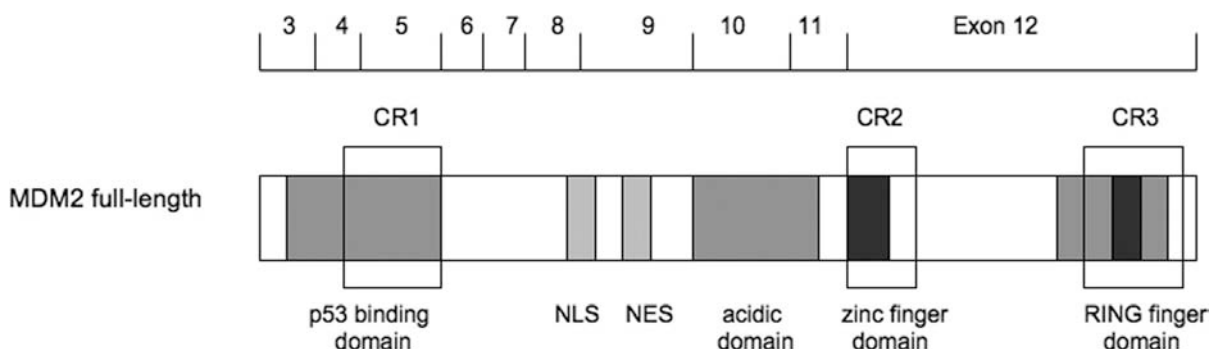


Figure 1
Schematic of full-length MDM2 protein. Specific domains are marked as shaded boxes. NLS – nuclear localization signal; NES – nuclear export signal; CR – conserved region shown as frames (Appendix 8.2)

1.2. Transcription and translation of MDM2

Transcription of the *MDM2* gene can occur from two different promoters, P1 is located upstream of exon 1, and the second promoter P2 lies within the first intron upstream of exon 2 and is responsive to the p53 tumor suppressor¹⁵. Different *MDM2* mRNA transcripts are expressed from the two promoters. For example, expression from P1 results in *MDM2* transcripts that containing exon 1 and exons 3-12, whereas expression from P2 results in *MDM2* transcripts that consist of exons 2-12¹⁶. Moreover, transcription rates from both promoters vary, as *Mdm2* mRNAs appear to be expressed at a much higher level from promoter P1 than *Mdm2* mRNAs from P2¹⁷. However, *in vitro* translation assays revealed that RNA expressed from P2 (p53 responsive) is translated at an eight-fold higher efficiency than RNA expressed from P1¹⁶. The p53 tumor suppressor arrests cells in G1 phase of the cell cycle¹⁸ or induces apoptosis¹⁹. MDM2 inhibits p53 function and thus supports the survival of the cell²⁰. MDM2 proteins are preferably translated from the first AUG codon within exon 3 independent of which promoter was used for transcription¹⁵. Thus, both mRNAs usually produce identical proteins. However, western blot analysis in murine myeloid leukemia cell lines showed that MDM2 proteins of different sizes are expressed because of alternative translation initiations¹⁵.

1.3. Posttranscriptional modifications

Posttranslational modification of MDM2 protein includes ubiquitination, sumoylation and phosphorylation²¹. Poly-ubiquitin-conjugation marks a protein for degradation in the proteasome, whereas mono-ubiquitination appears not to signal for immediate proteolytic degradation. MDM2 mediates ubiquitination of itself²² and other substrates²³ through its E3 ubiquitin ligase activity. The exact ubiquitination sites within MDM2 are not known. Posttranslational modifications such as sumoylation can alter the ligase activity of MDM2 resulting in an increased level of proteins that are substrates of MDM2 mediated ubiquitination, such as p53²¹. The E2 enzyme Ubc9 mediates sumoylation of MDM2 by binding to the N-terminal region (amino acids 40-59)²⁴. Miyauchi *et al.* (2002)²⁵ proposed that MDM2 is sumoylated during nuclear import by RanBP2 (SUMO-E3 ligase), a nuclear pore protein, and further within the nucleus by members of the PIAS family (SUMO ligase). p14^{ARF} mediates SUMO-conjugation of human MDM2 and particularly targets lysine residues within the N-terminal region of MDM2 (amino acids 134-212)²⁶. Co-expression of p14^{ARF} with MDM2 promoted an increase in sumo-conjugated MDM2, but did not affect human MDM2 expression levels²⁶.

Phosphorylation sites for MDM2 have been described within two regions of the MDM2 protein, the amino-terminal region (1-193) and within the central region (194-293)²⁷. The DNA-activated protein kinase (DNA-PK) was shown to phosphorylate serine 17 of MDM2 *in vitro*²⁸, which is suggested to cause weakening of the MDM2/p53 association. Another phosphatidylinositol 3-kinase family member, ATM, directly phosphorylates MDM2 at serine 395 in response to gamma-radiation or carcinogens²⁹ and interferes with MDM2-mediated nuclear export of p53³⁰. The protein tyrosine kinase c-Abl mediates phosphorylation of human MDM2, and as a consequence hinders p53 degradation and improves p53 transactivational activity^{31,32}. A study in 293 cells supplied evidence that c-Abl is responsible for phosphorylation on multiple sites; however, tyrosine 394 was recognized to be the most important site for c-Abl-dependent phosphorylation of MDM2³³. A study by Zhang *et al.* (2001) evaluated phosphorylation abilities of different cyclin/cyclin-dependent kinase (CDK) complexes to phosphorylate MDM2³⁴. Cyclin A bound to CDK2 phosphorylated MDM2 at threonine 216 *in vitro*. Cyclin A/CDK1 modified MDM2 in a similar manner. CDK complexes formed with cyclins E, D1 and B had impaired phosphorylational abilities towards MDM2 but not other phosphorylation targets such as histone H1 and pRb. This suggests that cyclin A/CDK is the cyclin/CDK complex that predominantly phosphorylates MDM2³⁴. This phosphorylation weakens the binding of MDM2 to p53. The protein kinase Akt targets serine residues for phosphorylation that are located close to the nuclear localization and nuclear export signal of MDM2 (166 and 186),³⁵. Data suggest that phosphorylation of these sites promotes relocation of human MDM2 from the cytoplasm to the nucleus in cultured MCF-7 or MDM2^{-/-}, p53^{-/-} double knock out MEF cells^{35,36}. Phosphorylation on both 166 and 186 serine residues can enhance MDM2-mediated degradation of p53 by promoting stronger binding to p300 and preventing the interaction of MDM2 to the tumor suppressor ARF³⁵.

In summary, the mechanisms by which MDM2 gene expression and protein stability are regulated are complex and occur at the point of transcription or via posttranslational modification that may influence MDM2-protein interactions and cellular localization²¹. The importance to control MDM2 function is evident in various studies that show a growth promoting and tumorigenic potential of MDM2 *in vivo* and *in vitro*.

1.4. MDM2 regulates the p53 tumor suppressor

The p53 tumor suppressor plays a critical role in the regulation of cell growth and survival^{18, 19}. p53 is induced by stress signals such as hypoxia³⁷, activation of oncogenes,

depletion of ribonucleoside triphosphates³⁸, spindle poisons and DNA damage due to UV- or gamma-radiation^{39, 40}. p53 transcriptionally activates or represses downstream targets that initiate programs such as cell cycle arrest¹⁸, apoptosis¹⁹, or senescence⁴¹ to ensure genomic integrity. However, if p53 function is inhibited, a damaged cell can divide, which can potentially lead to neoplasia and tumor formation. Mutations within the p53 tumor suppressor have been found in a variety of malignancies of the lung, liver, breast, brain, esophagus, colon, reticuloendothelial and the hematopoietic tissue⁴². Germ-line mutations within one allele of the p53 tumor suppressor gene have been identified in families with the Li-Fraumeni syndrome^{43, 44}, an autosomal dominant disease. Individuals that inherited these mutations are predisposed to the development of breast cancer, soft tissues sarcomas, and other tumors⁴⁵, emphasizing the importance of functional p53 in regulating cell proliferation.

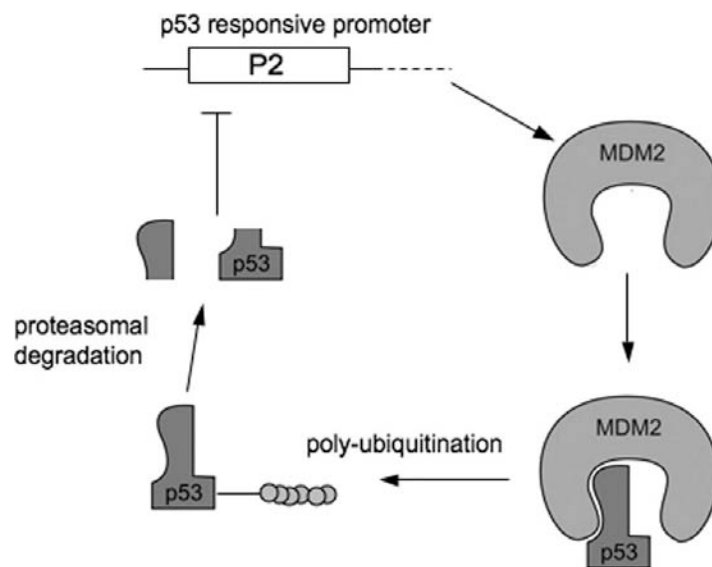


Figure 2
Model of the auto-regulatory feedback loop of MDM2 and p53, modified from Bartel *et al.* (2002)⁴⁶.

The best-characterized function of MDM2 is its regulation of p53 activity. Both proteins are controlled in an auto regulatory feedback loop. As shown in Figure 2, wild-type p53 transactivates MDM2 expression by binding a p53-responsive element⁴⁰ within the P2 promoter of the *MDM2* gene^{47, 48}. Following translation, MDM2 (Figure 2) binds to the transactivation site of p53. This p53-binding domain forms a trough that contains hydrophobic amino acids on the inside⁴⁹. The p53 region that binds to MDM2 forms an α -helix containing hydrophobic amino acids that get hidden in the gap⁴⁹. This interaction inhibits the transcriptional activity of p53^{10, 50}. In addition, MDM2 acts as an E3 ubiquitin

ligase²² that ubiquitinates p53 for degradation within the proteasome (refer to Figure 2). Ubiquitination of p53 by MDM2 requires the proteins E1, ubiquitin-conjugating enzyme and ubiquitin²³. MDM2 mediates either mono- or polyubiquitination of p53⁵¹. The shift towards one or the other depends on the level of MDM2 within the cell whereby increasing MDM2 levels promote polyubiquitination⁵¹. Monoubiquitination affects cellular localization of p53 by moving it to the cytoplasm and does not promote proteasomal degradation of p53⁵¹. In contrast, polyubiquitinated p53 is immediately degraded within the nucleus⁵¹. Proteasomal degradation after polyubiquitination occurs when MDM2 and p53 form a ternary complex with p300/CBP⁵². p300 unites the catalytic and regulatory proteins essential for p53 degradation⁵² in the 26s proteasome.

The importance of the interactions between MDM2 and p53 is demonstrated by studies with knock out mice. The MDM2 null genotype is lethal and the mice die early during embryonic development^{53, 54}. Mouse embryos lacking p53 develop normally but tumor formation is observed within 3 months of birth⁵⁵. p53 and MDM2 double knockout mice are viable and develop a similar phenotype than p53^{-/-} mice^{56, 57} demonstrating that loss of p53 rescues the lethal phenotype of the MDM2^{-/-} mice. More than 75% of mice of either phenotype develop malignant lymphomas. However, p53 null mice develop more sarcomas (about 42%) compared to the MDM2 and p53 double knockout mice (<10%)^{56, 57}.

The p53 signaling pathway is modulated by proteins interacting with MDM2 such as the ARF tumor suppressor (murine p19^{ARF}, human p14^{ARF})⁵⁸. ARF is expressed from the INK4a/ARF locus from an alternative reading frame, which encodes INK4a⁵⁹. ARF sequesters MDM2 within the nucleolus thereby releasing p53 from the MDM2/p53 binding complex⁶⁰. ARF also inhibits the nuclear export of MDM2⁶¹. The interaction of MDM2 with ARF leads to stabilization of p53 protein and inhibition of MDM2-mediated p53 degradation⁵⁸.

A MDM2-related protein, MDMX (also known as MDM4) binds MDM2 through RING finger domains in both proteins^{62, 63}, and as a consequence stabilizes the MDM2 protein in the complex⁶⁴. This interaction has been suggested to stimulate MDM2-mediated ubiquitination of p53 leading to its degradation⁶⁵. As noted in Section 1.3, MDM2 is post-translationally phosphorylated by a variety of different kinases, which can influence the MDM2/p53 interaction. Phosphorylation of MDM2 by Cyclin A/CDK1, ATM, DNA-PK or c-Abl enhances p53 stability and activity^{28, 30, 32, 34}, whereas MDM2 phosphorylation by Akt promotes p53 degradation³⁵.

In summary, MDM2 and p53 are regulated by an auto-regulatory feedback loop, which controls both, MDM2 function and p53 activity. As a result unrestrained proliferation and growth suppression are prevented. Posttranslational modifications and binding partners of MDM2 influence this balanced interaction.

1.5. p53-independent functions of MDM2

The majority of studies has been focused on the regulatory function of MDM2 towards p53, however there are significant data suggesting a p53-independent role for the MDM2 oncoprotein^{66,67}.

Soft tissue sarcomas, bladder and esophageal carcinoma samples have been evaluated for their p53 and MDM2 status; surprisingly, some of these tumors contained both mutations within p53 and MDM2 gene amplification⁶⁸⁻⁷⁰. In addition, the occurrence of these tumors correlated with a more aggressive disease than tumors showing either one of these changes^{68,69}. It is needless for a tumor to have two mechanisms to diminish the function of p53 and this fact supports a p53-independent role for MDM2.

Further evidence for a p53-independent role of MDM2 is that MDM2 gene amplification and p53 mutations preferentially occur in tumors developed from different types of tissues as reviewed in a report by Momand *et al.* (1998)⁷¹. For example, MDM2 amplifications were detected at the highest frequency in soft tissue sarcoma and osteosarcoma whereas p53 mutations were detected predominantly in tumors of the lung, ureter and pancreas⁷¹. These data suggest that alternative MDM2 functions could trigger the growth of tumors with MDM2 overexpression in specific cellular backgrounds⁶⁶.

Another indication that MDM2 functions independently of p53 is the identification of MDM2 splice variants in a variety of different tumors⁷²⁻⁷⁷. Some of these splice variants lack part of the p53 binding domain and it has been demonstrated that these isoforms cannot interact with the p53 protein. The role of these splice variant is still enigmatic; however, growth promoting functions have been confirmed both *in vitro*⁷² and *in vivo*^{78,79}. A detailed overview describing the function of MDM2 splice variants is contained within Section 1.7.

Various studies have produced evidence for a p53-independent function of MDM2. For example, a study by Jones *et al.* (1998)⁸⁰ evaluated the effect of MDM2 overexpression on tumor formation in a transgenic mouse model. The mice expressed MDM2 transcripts at a level 2-fold higher than wild-type control mice. The main tumor type observed was sarcoma (38%). When these mice were bred into a p53 null mouse strain the same percentage of sarcomas developed (38%), compared to only 9% in the original p53 null mouse strain. The

investigators concluded that MDM2 mediates tumor formation independent of p53 in mesenchymal cells ⁸⁰.

MDM2 interacts with the tumor suppressor Rb (retinoblastoma) in a p53-independent manner. Rb is a nuclear protein that suppresses transcription of genes necessary for the progression of the cell cycle from G1 into S phase ⁸¹ (Figure 3). Functional Rb is hypophosphorylated and binds transcription factors such as E2F family members, thereby inhibiting E2F mediated transactivation of S phase specific genes ^{81, 82}. The retinoblastoma protein forms stable complexes with MDM2 *in vivo* ⁸³. This interaction stimulates E2F activity and promotes cell cycle progression ⁸³.

In addition, MDM2 interacts directly with E2F to regulate the cell cycle independently of p53. E2F family members form heterodimers with DP family members, which are also directly modulated by MDM2 ⁸⁴. The E2F1/DP1 complex mediates apoptosis *in vitro* ⁸⁵. In cells negative for p53, MDM2 expression reduced the number of apoptotic cells when E2F1 was coexpressed with DP1 ⁸⁴. The anti-apoptotic function of MDM2 was dependent on the presence of the DP subunit but not on p53. Additionally, MDM2 stimulated DNA synthesis and colony formation when coexpressed with the heterodimer E2F1/DP1, implying that cells expressing all three factors have a growth advantage ⁸⁴.

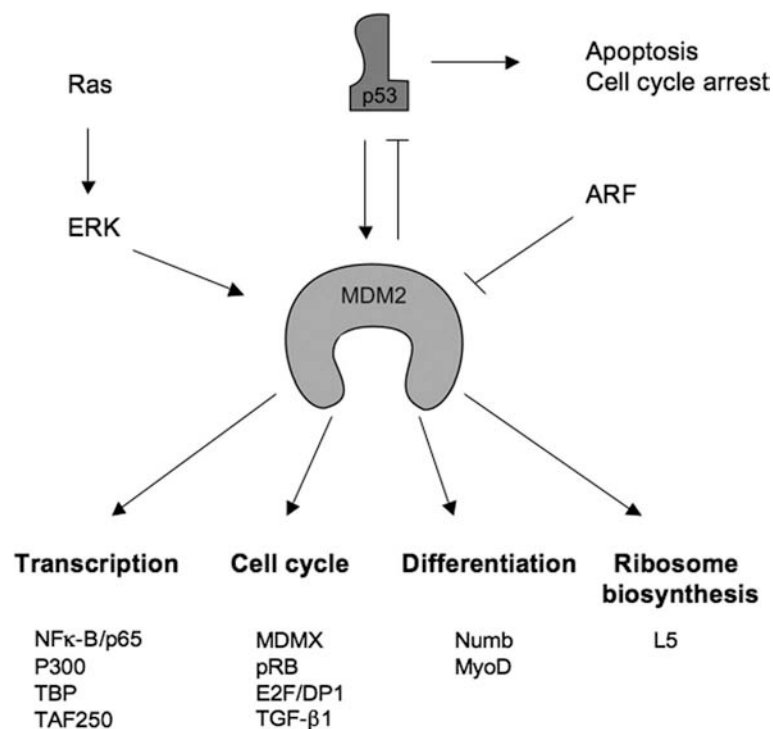


Figure 3
Schematic of the different p53-independent roles of MDM2, modified from Ganguli *et al.* (2003) ⁶⁷

Besides MDM2's p53-independent role in cell cycle regulation, it has been proposed that MDM2 functions in cell differentiation and transcription (Figure 3). The Numb gene encodes a protein which is mandatory for neural cell differentiation and cell fate during organogenesis^{67,86}. MDM2 binds Numb, significantly decreasing its stability and resulting in relocation of Numb from the cytoplasm to the nucleus⁸⁶. The Numb-binding site of MDM2 overlaps the p53-binding domain at the N-terminal region suggesting that Numb-MDM2 interactions may prevent p53 binding.⁸⁶

An example of when MDM2 influences transcription is its ability to enhance NF- κ B activity. The NF- κ B family are transcription factors that control expression of genes involved in immune and inflammatory response, cellular transformation and apoptosis⁸⁷. The most abundant form of NF- κ B is a heterodimer consisting of p50 and p65 (RelA) subunits. However, only the p65 subunit is responsible for regulating the transcription of downstream targets⁸⁷. In acute lymphoblastic leukemia (ALL) cell lines, overexpression of MDM2 induced p65 expression and caused resistance to the chemotherapeutic drug Doxorubicin⁸⁷. The investigators of this report confirmed that MDM2 directly binds the Sp1 sites in the p65 promoter and mediates its transcription⁸⁷.

In summary, the oncoprotein MDM2 modulates proteins other than the p53 tumor suppressor and promotes cell growth and tumor formation by mechanisms that are both dependent and independent of p53.

1.6. Introduction to splicing

Splicing is an important cellular mechanism to generate variable protein isoforms for normal development. However, inappropriate splicing caused by mutations has been associated with several human diseases for example Parkinson's disease⁸⁸, Cystic fibrosis⁸⁸, Spinal muscular atrophy^{88,89} and cancer⁹⁰.

The autosomal recessive disease Spinal muscular atrophy causes loss of motor neurons within the spinal cord. Interruption of the nerve supply to skeletal muscle leads to weakness and paralysis of voluntary muscles. The majority of patients has lost the survival of motor neuron gene 1 (*SMN1*) on both alleles. *SMN2*, a duplicated gene at the same chromosomal locus can potentially encode exactly the same protein. However, silent mutations in *SMN2* disrupt an exonic splicing enhancer within exon 7 that causes exon 7 to be spliced out and results in expression of a nonfunctional truncated protein⁸⁸.

Incorrect splicing of a variety of human genes has been linked to the development of cancer. For example, splicing of the *ATM* gene is caused by the generation of a mutation within intron 10. As a consequence, exon 11 is spliced out incorrectly resulting in a frame shift and a truncated protein⁹¹. This mutation has been associated with a higher risk in developing breast cancer in women⁹¹. Another example for the creation of a splice variant linked to cancer development is the DNA repair gene *MLH1*. A mutation within intron 1 causes the next exon to be spliced out incorrectly⁹². The resulting truncated *MLH1* protein is non-functional and one of the causes for hereditary colorectal cancer⁹².

Primary RNA transcripts of human genes are processed by 5'capping, 3'cleavage, polyadenylation and splicing to generate mature mRNA molecules, which are then translated into proteins. Introns are excised by the spliceosome, a giant ribonucleic protein complex that contains small nuclear ribonucleic protein particles (snRNP)^{93,94}. There are five snRNPs; U1, U2, U4, U5 and U6, each of which binds several proteins and other splicing factors⁹³. Splicing occurs predominantly at conserved 5' or 3' sequences located directly on exon-intron boundaries. The majority of introns is bordered with dinucleotides GU at their 5'terminus and AG at their 3'end⁹⁰. In addition, a branch point, usually an adenosine residue, is located 20-40 bp upstream from the 3'end of the intron, which also contributes to splice site recognition⁹⁴.

Two forms of abnormal splicing processes have been described: alternative and aberrant. Alternative splicing uses the same pre-mRNA molecules and employs some but not all of the exon-intron junctions resulting in transcripts lacking one or more exons⁹⁰. An investigation that evaluated 10,000 human genes from 50 tissues samples and cell lines implied that about 74% of the analyzed genes were alternatively spliced⁸⁹. Examples of alternative splicing are the transcripts of the fibroblast growth factor receptor 2 gene (*FGFR2*). Exons 1-7 and exon 10 of *FGFR2* are expressed constitutively. However, exon 8 is found only in transcripts expressed in epithelial cells, and exon 9 is included only in mature mRNAs expressed in fibroblasts⁸⁹.

Aberrant splicing is mainly caused by mutations. These mutations occur either directly at the flanking dinucleotides of 5' or 3' splice sites, within the consensus sequence of the splice sites, or at cryptic splice sites within exons or introns⁹⁰. Aberrant splicing also occurs at short base pair repeats that function as splice sites⁹⁵. The transcripts generated from the aberrant splicing process either contain additional intron sequences, or have parts of exons deleted, which can result in a frame shift and truncation of the translated protein. Examples of aberrant splicing are the genes *ATM* and *MLH1*, as described above. Another example is the

estrogen receptor gene. A cryptic splice site (AT to GT) has been described within an intron of this gene resulting in an aberrantly spliced transcript. This splice variant contains an additional 69 nucleotides within its reading frame and is associated with breast cancer⁹⁰.

In summary, splicing is an important cellular process to generate variable protein isoforms for normal development; however, abnormal splicing has been linked to human disease.

1.7. MDM2 splice variants

To date, more than 40 splice variants of *MDM2* have been documented in several types of tumors including ovarian cancer, bladder carcinoma⁷², glioblastoma^{73, 74}, invasive breast cancer⁷⁶, liposarcoma⁷⁷, soft tissues sarcoma⁹⁵ and rhabdomyosarcoma⁷⁵ (Figure 4A). Expression of alternative *MDM2* splice variants often correlates with a more advanced tumor stage^{72, 73} and in a study of invasive breast cancers the presence of aberrant splice forms was associated with decreased patient survival⁷⁶.

Different *MDM2* transcripts are generated by both alternative and aberrant splicing^{46, 76} as described above. An example of an aberrant *MDM2* splice variant is *MDM2-PM2*, which has been detected in rhabdomyosarcomas⁹⁵. This splice form is generated using a repeated sequence as a splice site. The motif 5'-TGAAAGAG-3' is repeated three times within the *MDM2* gene sequence. These are base pairs 149-155, 278-285 and 1232-1239; according to the *MDM2* mRNA Genbank sequence number AX057138 (refer to Appendix 8.1). Aberrant variant *MDM2-PM2* (Figure 4B) is spliced at this repeat motif, within exon 4 and exon 12, and as a consequence exons 5-11 and two of the three 5'-TGAAAGAG-3' motifs are spliced out⁹⁵. As a result, *MDM2-PM2* protein lacks half of the p53-binding site, the nuclear localization signal (NLS), nuclear export signal (NES), the ARF binding site and the Zinc finger domain⁹⁵. In general, splice variants of the *MDM2* gene lack major parts of the N-terminal and/or C-terminal regions that contain important domains as described in Section 1.1 (refer also to Figure 1). Therefore, it is presumed that the resulting truncated *MDM2* proteins have altered biological functions and properties. The functions of *MDM2* splice variants are still unclear. Data are contradictory as to whether *MDM2* splice variants contribute to the development of malignancies or if they are created as a consequence of the deregulation of a tumor cell. In addition, there are studies that have detected *MDM2* splice variants in normal lymphocytes and tissues of breast epithelia, parenchyma, spleen, kidney, intestine, and stomach^{76, 96}, indicating that *MDM2* splice transcripts are expressed in normal tissues and suggesting that they may play a normal physiological role.

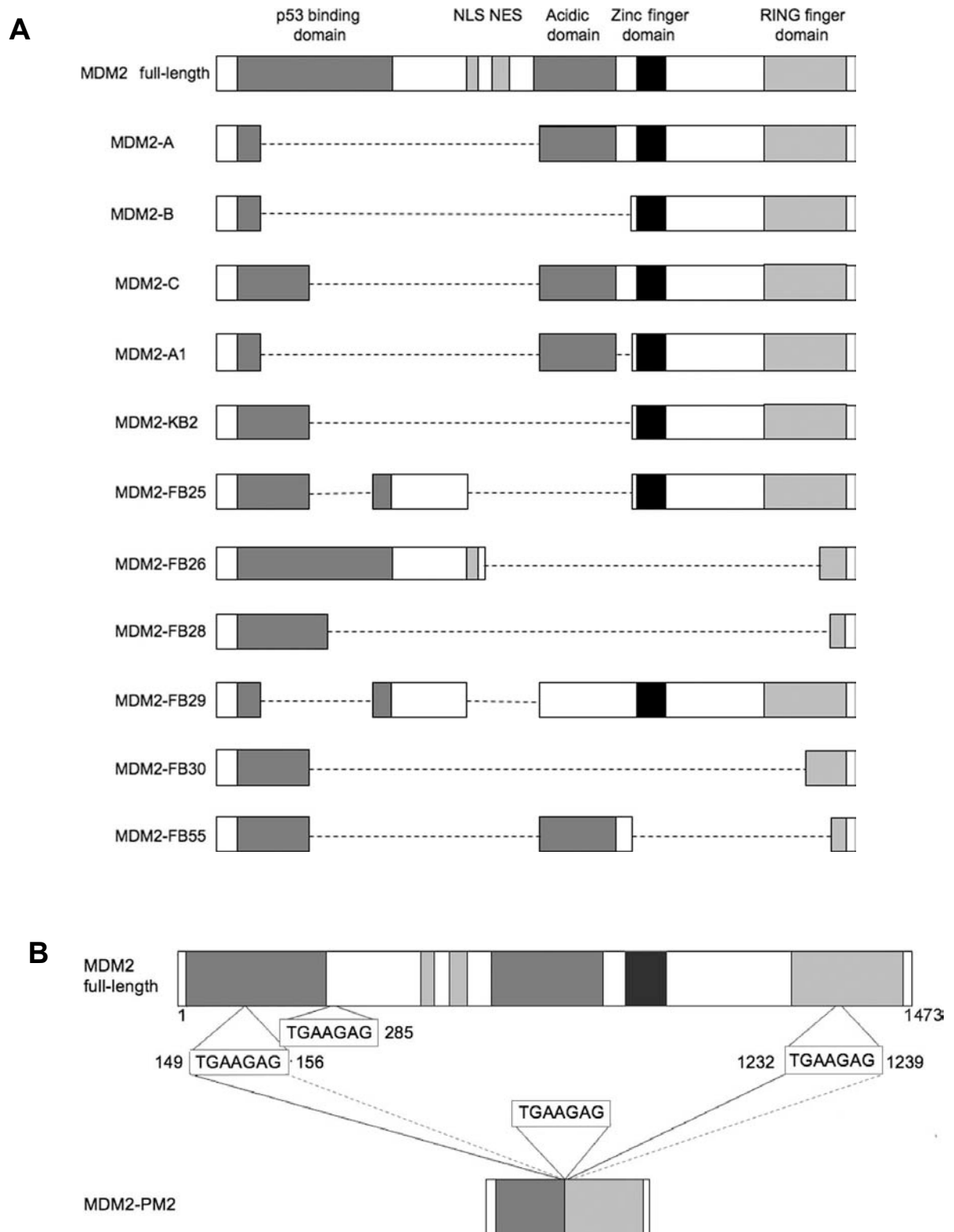


Figure 4

(A) Schematic of the full-length and spliced MDM2 mRNA transcripts detected in pediatric rhabdomyosarcoma samples and cell lines modified from Bartel *et al.* (2000)⁷⁵. (B) Diagram of the splicing pattern of splice variant MDM2-PM2, modified from Bartel *et al.* (2000)⁷⁵. NLS - nuclear localization signal, NES - nuclear export signal, MDM2-FL - full-length MDM2 mRNA. Numbers symbolize the numbers of nucleotides in the sequence.

Several published studies have evaluated the function of MDM2-B, the splice variant most commonly found in human cancers^{78, 79, 97}. MDM2-B has also been referred to as MDM2-ALT1⁹⁷ and Mdm2-Δ28-298⁷⁸. In a study by Fridman *et al.* (2003), MDM2-B accelerated lymphomagenesis in an Eμ-myc transgenic mouse model⁷⁸ in a similar manner compared to full-length MDM2. However, in the same study MDM2-B expressed in p53+/+ fibroblasts failed to form colonies in soft agar unlike full-length MDM2⁷⁸, suggesting that this splice variant may only have a weak oncogenic potential. *In vivo*, the tumorigenic potential of MDM2-B was observed in an *Mdm2-b* transgenic mouse model. These mice developed B-cell lymphoma and myeloid sarcomas between the age of 1 and 2 years⁷⁹. The authors suggested a p53-independent function for MDM2-B involving the transcription factor NF-κB⁷⁹. MDM2-B increases NF-κB activity by increasing the level of subunit RelA and decreasing levels of the NF-κB-inhibitor IκBα. Consequently, expression of MDM2-B reduced the proportion of apoptotic cells after cytotoxic agent treatment in response to activated NF-κB⁷⁹.

In contrast to its growth promoting functions, p53-dependent growth inhibitory activity has been described for splice variants with an intact C-terminal RING finger domain. MDM2-B has been shown to bind full-length MDM2 and sequester it in the cytoplasm⁹⁷. Binding of MDM2-B in this manner prevents the binding of p53 to full-length MDM2, resulting in increased p53 activity⁹⁷. Similar results were observed when evaluating the function of truncated murine isoforms of MDM2 that interact with full-length MDM2⁹⁸. Five of six murine MDM2 splice variants evaluated lacked part of the p53-binding domain but retained the complete carboxyl-terminus. Binding of these splice variants to full-length MDM2 protein through their RING finger domains resulted in p53-mediated growth inhibition⁹⁸.

MDM2 splice variants have been found predominantly in tumor samples, however their main physiological function is still unclear because both growth promoting and growth inhibitory phenotypes have been demonstrated. Therefore additional studies are required in order for the differences observed *in vivo* and *in vitro* to be understood.

1.8. Aims of work

MDM2 splice variants have been primarily identified in human tumors, however their function is still unclear. Therefore, the overall goal of this study was to characterize MDM2 splice variants both *in vivo* and *in vitro*. This research study was divided into two major projects: the first part was to generate a transgenic mouse model expressing a common MDM2 splice variant and to evaluate its phenotype. The second part focused on the cellular localization of MDM2 splice variants, and how their localization might be altered by expression of known binding partners.

Project 1. A recent study in the laboratory had determined that *MDM2-A* was the most frequently found *MDM2* splice variant in rhabdomyosarcoma primary tumors. Therefore, the main goal of this work was to evaluate the function of splice variant *MDM2-A* *in vivo* and *in vitro*. The objectives for this project were: (1) to generate the murine equivalent of human *MDM2-A* cDNA for cloning into a mammalian expression vector and microinjection into mouse embryos; (2) to generate a *Mdm2-a* transgenic mouse and evaluate its phenotype, with respect to tumor development or other abnormalities; (3) to evaluate the phenotype of *MDM2-A* *in vitro* when expressed in wild-type and mutant mouse embryonic fibroblasts.

Project 2. The goal of this project was to evaluate the cellular localization of MDM2 splice variants *in vitro*. The objectives for this project were: (1) to determine whether the lack of domains such as the p53 binding domain or the N-terminal nuclear localization signal influenced the localization of different MDM2 isoforms when expressed in mouse fibroblasts; (2) to evaluate whether co-expression of these MDM2 isoforms with the known binding proteins full-length MDM2, p53 and p14^{ARF} altered their localization within the cell.

2. Materials

2.1. Technical instruments and materials

BioMax MR Film	Kodak, Rochester, NY
Biosafety cabinet	Baker Company, Sanford, MA
Centrifuge 5415C	Eppendorf, Westbury, NY
Centrifuge Avanti™ J-25	Beckmann, Fullerton, CA
Centrifuge J-6B	Beckmann, Fullerton, CA
CO ₂ -Incubator	Forma Scientific, Marietta, OH
Horizon® 11-14 Gel Electrophoresis	Gibco, Carlsbad, CA
Immobilon-P, 0.45µm PVDF	Millipore, Bedford, MA
Incubator Shaker	New Brunswick, Edison, NJ
Mastercycler gradient	Brinkmann, Westbury, NY
Micro Hybridization incubator 2000	Robbins Scien., Sunnyvale, CA
Microfuge tube 0.5ml, 1.5ml	Midwest Scientific, St.Louis, MO
Microfuge tube 2.0ml	Ambion, Austin, TX
Nytran SuPerCharge, 045µm	Schleicher&Schuell., Keene, NH
Petridishes 100mm	Fisher, Fair Lawn, NJ
Phosphorimager, Molecular Dynamic	Amersham Corp, Piscataway, NJ
Pipettes, 1ml, 200µl, 100µl	Rainin, Oakland, CA
Pipette-tips	Rainin, Oakland, CA
Power pac 3000	BioRad, Hercules, CA
Scintillation counter LS6500	Beckmann, Fullerton, CA
Steriflip®, 0.45µm PVDF	Millipore, Bedford, MA
Tris-Glycine, precast gels 4-20%, Novex®	Invitrogen, Carlsbad, CA
Turbo Blotter pack	Schleicher&Schuell., Keene, NH
Vortex Genie2	Fisher, Fair Lawn, NJ
Water bath	Precision, Winchester, VA

2.2. Chemicals

2-Mercapthoethanol	BioRad, Hercules, CA
2-propanol	Fisher, Fair Lawn, NJ
Acidic acid, glacial, A.C.S.	Fisher, Fair Lawn, NJ
Agarose	Invitrogen, Carlsbad, CA

Albumin from bovine serum 98%	Sigma, St. Louis, MO
Ampicillin	Sigma, St. Louis, MO
Boric acid	BioRad, Hercules, CA
CAPS	Sigma, St. Louis, CA
Carbenicillin disodium salt	Invitrogen, Carlsbad, CA
Chloramphenicol	Sigma, St. Louis, MO
Chloroform	Fisher, Fair Lawn, NJ
dNTP (dATP, dCTP, dGTP, dTTP)	Promega, Madison, WI
ECL-Western Blotting Reagent	Amersham Biosciences Corp, Piscataway, NJ
EDTA	BioRad, Hercules, CA
Ethanol, 200 proof, 190 proof	Fisher, Fair Lawn, NJ
Formaldehyde	Fisher, Fair Lawn, NJ
Hydrochloric acid, A.C.S.	Fisher, Fair Lawn, NJ
Kanamycin	Sigma, St. Louis, MO
LB-Agar Miller	EMD Chem., Gibbstown, NJ
LB-Broth Lennox	EMD Chem., Gibbstown, NJ
LB-Broth Miller	EMD Chem., Gibbstown, NJ
Methanol A.C.S.	Fisher, Fair Lawn, NJ
MOPS	Sigma, St. Louis, MO
Nonfat dry Milk Carnation®	Nestle, Solon, OH
Protein assay	BioRad, Hercules, CA
Redivue deoxycytidine 5'-[α - ³² P] triphosphate, triethylammonium salt	Amersham Biosciences Corp, Piscataway, NJ
Sodium chloride	Fisher, Fair Lawn, NJ
Sodium dodecylsulfate	Fisher, Fair Lawn, NJ
Sodium hydroxide	Fisher, Fair Lawn, NJ
Tris	Fisher, Fair Lawn, NJ
Triton®-X-100	Fisher, Fair Lawn, NJ
Trizma®, Tris-HCL	Sigma, St. Louis, MO
Tween20	Fisher, Fair Lawn, NJ
X-Gal	Roche, Indianapolis, IN

2.3. Cell culture media and materials

15ml conical tubes, polypropylene	Sarstedt, Newton, NC
2-Mercaptoethanol for cell culture	Gibco, Carlsbad, CA
2-well chamber culture slides	Nalge Nunc Intern, Naperville, IL
50ml Falcon® conical tubes, polypropylene	B. Dickinson, Franklin Lakes, NJ
Costar® Culture flasks, 162, 75, 25mm ²	Corning Inc, Corning, NY
Cryo vials 1.5ml	Nalge Nunc Intern, Naperville, IL
Disposable cups	Sarstedt, Newton, NC
DMEM (Dulbecco's modified Eagle's Medium)	Mediatech Inc, Herndon, VA
Fetal bovine serum	HyClone, Logan, UT
Fugene	Roche, Indianapolis, IN
Gentamicin	Gibco, Carlsbad, CA
Hank's balanced salt solution	Gibco, Carlsbad, CA
L-Glutamine	Mediatech Inc, Herndon, VA
Nonessential amino acids	Gibco, Carlsbad, CA
PBS	HyClone, Logan, UT
Penicillin/Streptomycin Mix	Gibco, Carlsbad, CA
Screw cap tubes 1.5ml	Sarstedt, Newton, NC
Trypsin EDTA 1x	Mediatech Inc, Herndon, VA

2.4. Enzymes

Antipain	Invitrogen, Carlsbad, CA
Aprotinin	Invitrogen, Carlsbad, CA
HotStarTaq™ DNA Polymerase	Qiagen, Valencia, CA
Leupeptin	Invitrogen, Carlsbad, CA
Platinum® Pfx DNA polymerase	Invitrogen, Carlsbad, CA
PMSF	Sigma, St. Louis, MO
Proteinase K 50µg/µl	Epicentre, Madison, WI
Restriction endonucleases (<i>EcoRI</i> , <i>XhoI</i> , <i>SstI</i> , <i>PstI</i> , <i>HincII</i>)	Invitrogen, Carlsbad, CA
Sodium fluoride	Sigma, St. Louis, MO
Sodium orthovanadate	Sigma, St. Louis, MO

2.5. Kits

Cloned AMV First-Strand cDNA Synthesis Kit	Invitrogen, Carlsbad, CA
Easy-DNA	Invitrogen, Carlsbad, CA
EndoFree® Plasmid Maxi Kit	Qiagen, Valencia, CA
EX-WAX™ DNA Extraction Kit	Serologicals Corp, Norcross, GA
HotStarTaq® Master Mix Kit	Qiagen, Valencia, CA
QIAprep® Spin Miniprep Kit	Qiagen, Valencia, CA
QIAquick® Gel Extraction Kit	Qiagen, Valencia, CA
QuikChange® Multi Site-Directed Mutagenesis	Stratagene, La Jolla, CA
Rapid DNA Ligation Kit	Roche, Indianapolis, IN
RNase-Free DNase Set	Qiagen, Valencia, CA
RNeasy® Mini Kit	Qiagen, Valencia, CA
TOPO TA cloning® Kit	Invitrogen, Carlsbad, CA
Zero Blunt™ TOPO® PCR cloning Kit	Invitrogen, Carlsbad, CA

2.6. Antibodies

Anti- α Tubulin B-7	Santa Cruz Santa Cruz, CA
Anti-FLAG M2 mouse	Sigma, St. Louis, Missouri
Anti-FLAG rabbit	Sigma, St. Louis, Missouri
Anti-MDM2 2A10 mouse	M. Roussel, St. Jude, Memphis, TN
Anti-MDM2 C-18 rabbit	Santa Cruz Biotech. Santa Cruz, CA
Anti-MDM2 rabbit	R&D Systems, Inc,
Anti-MDM2 SMP14 mouse	Santa Cruz, Santa Cruz, CA
Anti-MYC mouse	Invitrogen, Carlsbad, CA
Anti-p14 ^{ARF} mouse	Oncogene
Anti-p21 F-5	Santa Cruz Santa Cruz, CA
Anti-p53 Ab-7	Oncogene
Anti-V5 mouse	Invitrogen, Carlsbad, CA
Anti-IgG2a mouse	Jackson Inc., West Grove, PA
Anti-IgG1 mouse	Jackson Inc., West Grove, PA
Anti-Ig rabbit (Fraction, normal)	Acc. Chem. & Scien. Corp., Westbury, NY
Anti-IgG mouse	Santa Cruz Santa Cruz, CA

Anti-goat	Horseradish peroxidase conjugated	Pierce, Rockford, IL
Anti-mouse	Horseradish peroxidase conjugated	Amersham Bio. Corp, Piscataway, NJ
Anti-mouse	Fluorescein FITC conjugated	Jackson Inc., West Grove, PA
Anti-mouse	Rhodamine TRITC conjugated	Jackson Inc., West Grove, PA
Anti-rabbit	Horseradish peroxidase conjugated	Amersham Bio. Corp, Piscataway, NJ
Anti-rabbit	Fluorescein FITC conjugated	Jackson Inc., West Grove, PA
Anti-rabbit	Texas Red® conjugated	Jackson Inc., West Grove, PA
Anti-sheep	Horseradish peroxidase conjugated	Pierce, Rockford, IL

2.7. Plasmids

MSCV-IRES-GFP	Persons <i>et al.</i> 1997
pCAGGS	Niwa <i>et al.</i> 1991
pcDNA4/V5-His B	Invitrogen, Carlsbad, CA
pcDNA6/myc-His© B	Invitrogen, Carlsbad, CA
pCR®2.1-TOPO®	Invitrogen, Carlsbad, CA
pCR®-Blunt II-TOPO®	Invitrogen, Carlsbad, CA
pEQECO	Dr. Peter Houghton, St. Jude
pSRαMSVtkCD8	Dr. Martine Roussel, St. Jude

2.8. Oligonucleotides

Name	Sequence 5' to 3'	Function	Reference
Mouse5end Mouse3end	CCGAATTCGCCAATGTGCAATACCAACAT CCGCTCGAGGCTAGTTGAAGTAACTTAGCACA	Multiplex PCR	N
Super3ex Super10ex	CTTACGCCATCGTCAAGATCCAGAGTCTCTTGTTCCGAAG CTTCGGAACAAGAGACTCTGGATCTTGACGATGGCGTAAG	SOE	N
5primeFLAG	GGAATTCATGGACTACAAGGACGACGATGACAAGATGTGCAATACCAACATGTCTG	Fusion-epitope-tag	N
pCAGGS5 pCAGGS3	CCATGTTTCATGCCTTCTTC CTTTATTAGCCAGAAGTCAG	Sequencing	N
REFsense REFanti	CCACAGTCCATGCCATCAC CAGGAAATGAGCTTGACAAG	Multiplex PCR	N
HPRT-sense HPRT-anti	GTAATGATCAGTCAACGGGGGAC CCAGCAAGCTTGCAACCTTAACCA	RT-PCR	99
MSCVsense MSCVanti	CCTGAACCTCCTCGTTCG GACAAACGCACACCGGCC	Sequencing	N
SeqMsense SeqManti	CTTAGCTGACTATTGGAAGTG GAATAGTCGTCACTCTCCTG	Sequencing	N
SeqM3 SeqM4	GCTTGGATGTGCCTGATGG CTTCTTCTGCCTGAGCTGAG	Sequencing	N
MutAS182/183	CTGGTGAACGACAAAGAAATGGCCACAAATCTGATAG	Mutagenesis within NLS1	N
MutAS469/470	GCAAAGAAGCTAAATTGAAAGGAATAAGCCCTGCCC	Mutagenesis within NLS2	N
MutAS466/467	GGCCTGCTTTACATGTGCAAATCAGCTAAATGAAAGG	Mutagenesis within NLS2	N
MutA325	CCTTAGCTGACTATTGGAATGCACCTTCATGCAATG	Mutagenesis	N
MutA586	CACAATCACAAGAAAGTGAAGACTATTCTCAGCC	Mutagenesis	N

To be continued on next page.

Name	Sequence 5' to 3'	Function	Reference
MutA742	CCTTGTGTGATTTGTCAAG <u>G</u> TCGACCTAAAAATGG	Mutagenesis	N
MutFL1	GCCCCTTAATGCCA <u>T</u> TGAACCTTGTGTGATTTG	Mutagenesis	N
Mut26FB394	GTGTCACCTTGAAGGT <u>G</u> GGAGTGATCAAAAGG	Mutagenesis	N
Mut26FB491	CCTCATCTAGAAGGAGAG <u>C</u> AATTAGTGAGACAG	Mutagenesis	N
MutB25	ACCAACATGTCTGTAC <u>C</u> CTACTGATGGTGCTG	Mutagenesis	N
MutB308	GTGAATGATTCCAGAGAGTCATCATGTGTTG <u>A</u> GGAAAATGATG	Mutagenesis	N
MutB407	TATAGCAGCCAAG <u>A</u> AGATGTGAAAGAGTTTGAAAGGG	Mutagenesis	N
MdmKS1	GTGGAATTCGCAAATGTGCAATACCAACATG	Fusion-epitope-Tag	N
MdmKS2	GAACCGCGGGCA* T ATTCCTTTCTTTGACTT		
MdmKS3	GAACCGCGGCACA* T AGGGGAAATAAGTTAGC		

Table 1

All primers were synthesized at the Hartwell Center, St. Jude Children's Research Hospital, Memphis. Restriction sites are underlined, transcription start and termination signal are shown in bold, sequences for epitope tags such as FLAG, V5 or HA are shown in italic, nucleotides changed during site-directed mutagenesis are underlined and shown bold, * change of amino acid to eliminate stop codon, N - oligonucleotides generated in this study, NLS- nuclear localization signal. Refer to Appendices 8.3 and 8.4 for hybridization sites of the most commonly used oligonucleotides.

2.9. Murine strains

The mouse inbred strain FVB/NJ was used to generate *Mdm2-a* transgenic animals. This strain is suitable for the production of transgenic mice because of the large pronuclei in the fertilized mouse egg¹⁰⁰ and because of the large litters they produce (means 10-12 pups). The mice are homozygous for the retinal degeneration allele *Pde6b^{rd1}* and appear albino¹⁰⁰. The transgene fragment *Mdm2-a* was sent to the Transgenic Core Unit (TCU) at St. Jude Children's Research Hospital in Memphis, TN, and microinjected into the pronuclei of one-cell stage embryos. These embryos were transferred into pseudo-pregnant female mice. Mouse tails of the resulting offspring were provided by the TCU, St. Jude for further analysis.

2.10. Bacterial strains

DH5 α Maximum efficiency	Invitrogen, Carlsbad, CA
DH5 α Sub-efficiency	Invitrogen, Carlsbad, CA
TOP10 chemical competent cells	Invitrogen, Carlsbad, CA
XL10-Gold® ultra competent cells	Stratagene, La Jolla, CA

2.11. Cell lines

Identification	Growth conditions	Reference
293T	DMEM, 10% FBS, 4mM L-Glutamine	MA. Bjornsti, St. Jude
MEF (DKO) p53 ^{-/-} , MDM2 ^{-/-}	DMEM, 10% FBS, 4mM L-Glutamine	G. Zambetti, St. Jude
MEF p21 ^{-/-}	DMEM, 10% FBS, 4mM L-Glutamine	P. Houghton, St. Jude
MEF p53 ^{-/-}	DMEM, 10% FBS, 4mM L-Glutamine	P. Houghton, St. Jude
MEF MDM2-A +/-	DMEM, 10% FBS, 2mM L-Glutamine, 0.1mM 2-Mercapthoethanol, 100U/ml Penicillin/Streptomycin, 1x Non-essential amino acids	N
MEF wild-type	DMEM, 10% FBS, 2mM L-Glutamine, 0.1mM 2-Mercapthoethanol, 100U/ml Penicillin/Streptomycin, 1x Non-essential amino acids	N
MEF (TKO) p53 ^{-/-} , MDM2 ^{-/-} , p19 ^{ARF} ^{-/-}	DMEM, 10% FBS, 4mM L-Glutamine, 10%CO ₂	G. Zambetti, St. Jude
C2C12	DMEM and Ham F12 media (1:2), 10% FBS, 10%CO ₂	P. Potter, St. Jude
NIH3T3	DMEM, 10% FBS, 4mM L-Glutamine, 10%CO ₂	

Table 2

Cell lines. All cells were grown at 37°C and 10%CO₂, N- cell line generated in this study. DMEM-Dulbecco's modification of eagle's medium, FBS-fetal bovine serum

2.12. Computer software and Online applications

Adobe® Photoshop® CS	Adobe Systems Inc., San Jose CA
IPLab Gel	Scanalytics Inc., Fairfax, VA
KaleidaGraph® Mac v.3.6x	Synergy Software, Reading, PA
Prism4	GraphPad Software Inc., San Diego, CA
www.ncbi.nlm.nih.gov	Blast search
www.dict.tu-chemnitz.de	English-German dictionary

All materials or research items that were not included in the Material Section will be named and identified in the Method Section. All aqueous solutions were prepared using de-ionized ultra pure water generated with the Milli-Q cartridge filter (Millipore).

3. Methods

3.1. Molecular Biology

3.1.1. Small scale isolation of plasmid DNA

Bacterial overnight cultures were prepared by picking a single *E. coli* colony from a LB-agar petridish and inoculating 10ml of LB-broth containing a selectable marker, if appropriate. The QIAprep® Miniprep Kit was used for plasmid purification. Overnight cultures (1-5ml) were centrifuged at 3000rpm for 5min, and plasmid DNA was isolated following the microcentrifuge-protocol in the manufacturer's manual.

3.1.2. Large scale isolation of plasmid DNA

LB-broth (800ml) containing a selectable marker was inoculated with 1ml of bacterial overnight culture. The culture was grown over night in an incubator shaker at 37°C and 280rpm. The next day, plasmid DNA was isolated using the EndoFree® Plasmid Maxi Kit with an altered protocol. LB-broth was poured into a 1l bottle (Nalgene® Labware) and centrifuged for 30min at 4°C at 3000rpm. The supernatant was discarded and the bacterial pellet was resuspended in 10ml of P1 buffer. The sample was then transferred to an autoclaved 50ml screw cap tube (Nalgene® Labware) and 10ml of P2 buffer was added. After mixing, 10ml of chilled P3 buffer was added and the sample was mixed and incubated on ice for 20min. The sample was then spun down for 30min at 13000rpm at 4°C to separate precipitated proteins and debris from the plasmid containing supernatant. The supernatant was transferred to a new autoclaved 50ml tube and spun down for another 15min, as described above. Next, a Qiagen-tip 500 column was equilibrated by applying 10ml of QBP buffer. Immediately after the last centrifugation, the supernatant was added to the column. The column was washed twice with 30ml of QC buffer and plasmid DNA was eluted with 15ml of QN buffer into two sterile 13ml tubes (Sarstedt). To precipitate DNA, 10ml of 2-propanol were added to the supernatant. To collect DNA, the sample was spun down at 9500rpm at 4°C for 30min. The DNA pellet was washed in 75% ethanol and then dried. The pellet was resuspended in TE buffer prior to use.

3.1.3. Isolation of genomic DNA from mouse tail tips and tissue

The Easy-DNA™ Kit was used to isolate genomic DNA from mouse tails and mouse tissues. The protocol for mouse tails was slightly altered. In a microfuge tube, a fresh or frozen mouse tail tip (1cm) was mixed with 320µl TE, 20µl lysis solution A, 10µl precipitation solution B and 1µl proteinase K (50µg/µl) and incubated at 60°C for at least 4h. After the protein digest, 300µl of solution A and 120µl of solution B were added and

vortexed. Next, 750µl of chloroform were added to the sample and mixed. The samples were centrifuged for 10min at 12000rpm at 4°C to separate the aqueous from the organic phase. The upper aqueous phase was transferred to a fresh tube, and DNA was precipitated with 1ml of 100% ice-cold ethanol. The genomic DNA was pelleted by centrifugation at 12000rpm for 10min at 4°C. The supernatant was discarded and the DNA pellet washed in 80% ice-cold ethanol. The resulting DNA pellet was air-dried and then resuspended in 50µl TE containing 2µg of RNase. For small samples, for example embryos, the protocol was followed exactly as described by the manufacturer.

3.1.4. Isolation of genomic DNA from paraffin sections

Three to four 0.4µm sections of paraffin embedded tissue were scraped from glass-slides, using an individual sterile scalpel (Becton Dickinson) for each individual specimen. Tissue was collected in a 1.5ml microcentrifuge tube. To isolate genomic DNA, the EX-WAX™ DNA Extraction Kit was used as described by the manufacturer.

3.1.5. Isolation of total-RNA from mouse tissue

Mouse tissues were snap frozen in liquid nitrogen and stored at -80°C until use. Tissues were ground under liquid nitrogen and collected in a microcentrifuge tube. The RNeasy® Mini kit was used to isolate total RNA by following the protocol (Animal Cells I). After adding RLT buffer, the sample was homogenized using a syringe and a 20-gauge needle (0.9mm diameter, Becton Dickinson). The lysate was passed through the syringe at least 5 times. RNA was extracted following the protocol as described in the manual. A DNase digestion step was included to eliminate all traces of genomic DNA. The RNase-Free DNase protocol was followed as described in the manufacturer's manual.

3.1.6. DNA and RNA concentration determination

To determine the concentration of nucleic acids in solution, light absorption was measured at 260nm and 280nm with a spectrophotometer. An $A_{260\text{nm}}$ (absorption at 260nm) of 1 equals 50µg/ml for double strand DNA and 40µg/ml for single strand RNA. Purity of a nucleic acid containing sample was determined by dividing the $A_{260\text{nm}}$ through the $A_{280\text{nm}}$. This value should lie between 1.8 and 2.0 to indicate pure nucleic acids.

3.1.7. Polymerase chain reaction

3.1.7.1. Polymerase chain reaction

Polymerase chain reaction (PCR) was used to amplify specific gene sequences for different experiments as described in the results. Platinum® Pfx DNA polymerase with a proofreading 3' to 5' exonuclease activity was used to ensure accurate amplification of the

desired template. In general for a 50µl reaction, plasmid or genomic DNA was mixed with 25pmol of each oligonucleotide primer together with 150µM of each dNTP, 50mM MgSO₄, 5µl of 10x amplification buffer, 5µl of 10x enhancer solution and 2.5U of the Pfx DNA polymerase. The reaction was carried out by denaturation of the DNA at 94°C for 2min followed by 30 rounds of denaturation of the DNA at 94°C/1min, annealing of the oligonucleotides at 56 to 60°C (depending on the primer)/1min and elongation 68°C/1min. A final elongation step at 68°C at 8min was carried out.

HotStarTaq DNA polymerase was used for difficult amplifications, for example Multiplex-PCR and any other problematic PCR reactions. In brief, for a 50µl reaction, template DNA was mixed with 5µl of 10x amplification buffer, 5µl of 5x Q-solution, 2.5mM of MgCl₂, 150µM of each dNTP, 25pmol of each oligonucleotide, and 2.5U of the polymerase. The following reaction steps were carried out: initial activation for 15min at 95°C followed by 35 rounds of denaturation for 1min at 94°C, annealing for 1min at 58°C and extension for 1min at 72°C. An additional final extension for 10min at 72°C was carried out. The samples were cooled and held at 4°C prior to analysis by agarose gel electrophoresis.

3.1.7.2. Reverse transcriptase polymerase chain reaction

Purified total RNA was used for cDNA synthesis using the cloned AMV First-Strand cDNA synthesis kit. Following the manufacturers instructions, 5µg RNA were used per reaction. The oligo(dT)₂₀ primer was used for elongation of the cDNA. To demonstrate that the RT-PCR product was derived for RNA and not from any contaminating genomic DNA in the sample, a second similar reaction was prepared excluding the cloned AMV Reverse Transcriptase. Any PCR product detected in this sample would have been derived from genomic DNA.

3.1.7.3. Sequencing reaction

For sequencing, a reaction of 12µl was prepared containing 200-500ng of DNA, 14pmol of oligonucleotide and water. The samples were sent to the Hartwell Center, St. Jude Children's Research Hospital for sequencing analysis. The Hartwell Center uses Big Dye® Terminator (v.3) Chemistry (Applied Biosystems) and the Applied Biosystem 3700 DNA Analyzer. The sequence data obtained was analyzed on the NCBI database (www.ncbi.nlm.nih.gov) using the pairwise blast search.

3.1.8. Agarose gel electrophoresis

Agarose gel electrophoresis was used to visualize and analyze nucleic acids. DNA or RNA samples were electrophoretically separated based on their size. A 1.5% agarose gel

contained 1.5g agarose, 100ml 1x TBE buffer and 5 μ l of ethidium bromide solution (1mg/ml, Sigma). The nucleic acid samples were mixed with DNA loading buffer and loaded into the gel slots. TBE buffer (1x) was used as the running buffer. Samples were electrophoresed at 80-100V. Nucleic acid bands were visualized with ultra violet light on an UV-transluminator (302nm). DNA markers were used to determine sizes of the nucleic acid.

TBE 10x	0.89M Tris 0.88M boric acid 20mM EDTA (ph8.0)
DNA loading buffer 10X	40% (w/v) Sucrose 100mM EDTA Bromophenol blue (Sigma)
DNA marker	5 μ g λ DNA/HindIII (Gibco) 5 μ g ϕ X 174 RF DNA HaeIII (Invitrogen) 13 μ l Buffer 3 (Gibco, 10x) 100 μ l water, sample was heated for 5 min at 65°C 13 μ l DNA loading buffer (10x), added last

3.1.9. DNA fragment isolation from agarose gel

DNA fragments were cut out of the agarose gel with a sterile scalpel, and transferred to a microcentrifuge tube. Extraction of the DNA was performed following the instruction of the QIAquick® Extraction kit. After gel isolation, the DNA was stored at 4°C.

3.1.10. Restriction endonuclease digestion

Plasmid or genomic DNA was digested using restriction endonucleases. The most efficient temperatures and salt reaction conditions were chosen based on the recommendation of the manufacturer for each enzyme.

3.1.11. Ligation of DNA fragments

Two separate ligation kits were used to insert DNA fragments into linearized plasmid DNA. In general, PCR fragments were cloned using the TOPO®-activated vector of the TOPO® TA or Zero blunt® TOPO® PCR cloning kit. In each reaction, 4 μ l of purified PCR product were used. Ligation was performed following the instruction of the manufacturers manual.

For other ligation reactions, plasmid DNA and DNA fragment were digested with restriction endonucleases to generate cohesive 5' and 3' ends (refer to Section 2.4). Then, the 5'-phosphate residues of the linearized plasmid were removed using calf intestinal alkaline phosphatase (Roche) as recommended by the manufacturer. Elimination of the 5'-phosphate

residues prohibits the re-ligation of the 5' and 3' ends to each other. The rapid DNA ligation kit was used to insert the DNA fragment into the linearized plasmid as recommended by the manufacturer. In general, a concentration ratio of 3:1 DNA fragment to plasmid DNA was used. The ligation sample was transformed into chemical competent *E. coli*.

3.1.12. Preparation and Transformation of chemical competent *E. coli*

Commercially available chemical competent *E. coli* were thawed on ice. The plasmid or ligation sample was diluted 5-fold with TE to generate DNA concentrations of approximately 1-10ng/ μ l. The competent cells were aliquoted into 14ml Polypropylene round bottom tubes (FALCON®, Becton Dickinson). Approximately 20ng of DNA was added to 50 μ l of competent cells and incubated on ice for 30min. Next, the reaction was heat-shocked for 30sec at 42°C and chilled for 2min on ice. SOC media (500 μ l) (Invitrogen) was added, and the bacterial sample was incubated at 37°C at 235rpm for 1h in an incubator shaker. The transformation mixture was plated out in dilutions on LB-agar plates containing appropriate antibiotics and incubated over night at 37°C.

3.1.13. Site directed Mutagenesis

The QuikChange® Multi Site-Directed Mutagenesis Kit was used to generate mutations or correct PCR-introduced mutations within a DNA sequence. Oligonucleotides were generated with a melting temperature (T_m) at or above 75°C. The formula $T_m = 81.5 + 0.41(\%GC) - 675/N - \%mismatch$ (N number of nucleotides in primer) was used to calculate the correct T_m . The Hartwell Center (St. Jude Children's Research Hospital) synthesized the primers, which were phosphorylated at the 5' end. The primers used for mutagenesis are listed in section 2.8. Mutagenesis reactions were carried out as directed in the instruction manual.

3.2. Mammalian cell culture

3.2.1. Maintenance and storage of cell lines

Viable cells were taken from liquid Nitrogen and thawed in a 37°C water bath. The contents of the vial were then added to a T162 cell culture flask containing complete media. Cells were incubated at 10% CO₂ at 37°C. To harvest a monolayer of cells, cells were washed twice in Hank's salt solution, then trypsin was added and cells were incubated for 1min. Cells were gently knocked off the flask surface and immediately resuspended in complete media. Cells were replated into culture flasks, slices or dishes as required, using a fraction of the harvested population or a specific number of cells.

Cell lines were stored for long-term in liquid Nitrogen. Cells were harvested as described above. The resuspended cells were then centrifuged at 1500rpm for 5min and the supernatant was discarded. Cells were resuspended and washed in Hank's salt solution. These steps were repeated. Pelleted cells were resuspended in freezing media containing 50% FBS, 40% complete media and 10% DMSO (Sigma), and placed into a cryo-vial. The tube was placed in a cryo-container with 2-propanol in the outer shell, and then slowly frozen at -80°C over night. The tube was transferred to the liquid Nitrogen tank 24h later.

3.2.2. Cell counting

To determine cell numbers, cells were harvested as described in section 3.2.1. Cell-containing media (200µl) was added to a disposable 20ml cup (Sarstedt). Then, 1ml of Hypertonic solution, 120µl of Lysing solution and 15ml of sterile Saline solution were added. The cup was placed into the coulter counter (Z2, Beckman Coulter, Hialeah, FL) and cells contained within 0.5ml of media were measured. The cell number per ml was calculated by multiplying the count with the dilution factor (81.6) and then multiplied by 2 because only 0.5ml of cells were counted.

Hypertonic solution	10mM Hepes 1.5mM Magnesium chloride pH 7.4
Lysing solution	13mM Ethylhexadecyldimethylammoniumbromide 3% v/v Acetic acid, glacial (17.4N)
Saline solution	154mM Sodium Chloride

3.2.3. Transient transfection

Fugene transfection reagent was used in a ratio 3:1 v/w with DNA. Transfection media (MEM, minimal essential medium, Gibco) (970µl) was added to a reaction tube, together with 30µl of Fugene reagent and 10µg DNA. A negative control was also prepared containing no DNA. After gently mixing, the reaction was incubated at room temperature for 1h. The mixture was then dropped evenly onto the cells. The cells were grown for 48h prior to analysis for cellular protein expression and localization (Immunofluorescence).

3.2.4. Retroviral transduction

To create ecotropic retroviral particles, the MSCV-IRES-GFP (MSCV-murine stem cell virus, IRES-internal ribosomal entry site, GFP-green fluorescent protein) ¹⁰¹ or the pSRαMSVtkCD8 viral vector (Dr. Martine Roussel, St. Jude) containing the cDNA of the

gene of interest (MDM2 splice variants or p14^{ARF}), was co-transfected with the helper plasmid pEQECO (Peter Houghton, St. Jude) into 293T packaging cells (Mary-Ann Bjornsti, St. Jude). Replication-incompetent retroviral particles were collected 48h post transfection. Fresh media was added to the 293T cells and new retroviral particles could be collected after another 24h. The media was either used immediately for transduction or stored at -80°C.

Fibroblasts were plated at a sub-confluent density and growth media was removed. The supernatant containing retroviral particles was filtered with a Steriflip® filter (0.22µm) to remove all cell debris. The supernatant was diluted 1:2 with complete media, and Polybrene (1mg/ml, Sigma) was added to a final concentration of 1µg/ml, to enhance virus-host interaction. After 24h, cells transduced with MSCV-IRES-GFP were analyzed for GFP expression to confirm viral transduction and then incubated for another 24h prior to western blot analysis or immunofluorescence assay. The internal ribosomal entry site allows polycistronic expression of multiple genes. Consequently, GFP is expressed from the same message as the gene of interest and is an excellent marker for transduction efficiency.

The pEQECO helper vector contains the cDNA of the glycoprotein gp70. This protein is recognized by an ecotropic receptor that is found only on rodent cells. These retroviral particles cannot infect human cells.

3.2.5. Adenoviral transduction

Cells were plated at 70% confluency and growth media removed. Virus particles containing the cDNA of the gene of interest (p53) were used at the concentration of 100 pfu/cell (plaque forming units/cell) in mouse embryonic fibroblast. Cells from a duplicate flask were counted and the number of virus particles used for the experiment was based on that cell number. The virus was diluted into 2ml of adenoviral transduction media (media containing only 2% fetal bovine serum) and added to the cells. After a two-hour incubation at 10%CO₂ and 37°C, complete growth media was added. The culture media was changed after 24h and the cells were incubated for a further 24h prior to western blot analysis and immunofluorescence assays.

3.2.6. Flow cytometry

Cells were washed in Hank's salt solution and pelleted. Next, 1ml of propidium iodide solution (0.05mg/ml propidium iodide, 0.1% sodium citrate and 0.1% Triton) was added to an aliquot of 1x10⁶ cells, and the suspension vortexed. Cells were sent to the Flow Cytometry Lab at St. Jude Children's Research Hospital for cell cycle analysis, which was performed

using the Becton Dickinson FACScan flow cytometer (Becton Dickinson, San Jose, CA). Fluorescence was measured after laser excitation at 488nm.

3.2.7. Growth rate analysis

Fibroblasts were transduced with retroviral vectors as described in Section 3.2.4. Cells were harvested after 48h and sent to the Flow cytometry Lab at St. Jude for sterile cell sorting. GFP sorted cells of each retroviral vector were plated into three wells of multiple 6-well plates. The cell numbers of three wells of each retroviral vector were counted the next day and every other day for a period of up to six days. The growth rates of the cells were plotted using KaleidaGraph® Mac v.3.6x software (Synergy Software, Reading, PA).

3.3. Protein biochemistry

3.3.1. Preparation of protein extract from tissues and cells

Frozen mouse tissues (50mm³) or cultured cell pellets (2x10⁶) were used to isolate cellular protein. One ml of prechilled sonication buffer containing proteinase inhibitors was added to a homogenizer containing the animal material. The tissue was homogenized until a homogeneous mixture was obtained. This mixture was then sonicated twice at 10μ peak to peak distance for 15 seconds to ensure that the cells and the DNA had been disrupted. The lysed cells were then centrifuged at 13000rpm for 10 min at 4°C. The supernatant was transferred to a new 1.5ml tube and held on ice.

Sonication buffer	50mM Tris (pH8.0)
	300mM NaCl
	1mM EDTA
	0.5mM DTT
	0.1% NP40 (Roche)
	10μg/ml Leupeptin, Aprotinin, Antipain,
	1mM Sodium orthovanadate
	200μM PMSF
	1mM NaF

3.3.2. Protein concentration determination

The protein concentration was estimated using the Protein Assay solution (Bradford solution, BioRad). A standard curve was prepared in triplicate, using samples of bovine serum albumin (BSA) in concentrations ranging from 0.1 to 1 mg/ml. The standards (20μl of each) were mixed with 1ml of Bradford solution and incubated at room temperature for 15 min. The

absorption at 595nm was measured and the value used to plot a standard curve. The protein concentrations of tissue and cell samples were calculated from the standard curve.

3.3.3. Polyacrylamide gel electrophoresis

A sample containing 50µg of total protein was pipetted into a microcentrifuge tube and mixed with Sample buffer to a final concentration of 1x. Samples were heated at 95°C for 10min, centrifuged at 13000rpm for 2min and then loaded immediately into well slots of a Novex® 4-20% gradient Tris-Glycine gel (Invitrogen) in the electrophoresis chamber (Hoefer Mighty Small II, Pharmacia Biotech, San Francisco, CA). The ProSieve® color protein marker (10µl) was also loaded to determine the molecular weight of the separated proteins. Running buffer (1x) was used to electrophorese the protein samples at 180-200V for 1-2h.

Sample buffer 4x	1M Tris pH 6.8, 40% Glycerol (Sigma), 8% SDS (w/v) 20% 2-Mercaptoethanol Bromophenol blue
Running buffer 10x	0.25M Tris 1.9M Glycine (BioRad) 35mM SDS

3.3.4. Western blotting

Proteins were electroblotted to a PVDF membrane (polyvinylidenedifloride 0.45µm Immobilon-P) for western blotting. The membrane was first washed in methanol for 10 sec, then rinsed twice in water and finally washed in 1x Transfer buffer. A blotting sandwich was prepared stacking one prewetted sponge, one prewetted sheet of blotting paper (Amersham), one protein gel, the PVDF membrane, another prewetted sheet of blotting paper and another prewetted sponge in the gel cassette. The sandwich cassette was placed in the Transphor Electrophoresis Unit (Hoefer Pharmacia Biotech), so that the protein gel was directed towards the cathode (-) and the PVDF membrane towards the anode (+). The proteins were transferred at 200mA for 1.5h. Following transfer, the membrane was air-dried.

For immunodetection of proteins, membranes were washed three times in 1xTBS-T for 5min each. Membranes were blocked with Blotto for 1h at room temperature to inhibit non-specific binding of antibodies. Primary antibodies (Ab) were diluted in Blotto to the appropriate concentration and added to the membranes. Incubation duration varied between 1h and overnight, and at room temperature or 4°C, respectively. Following three 5min-washes with 1x TBS-T, the secondary antibodies (diluted in Blotto) conjugated with Horseradish

peroxidase (HRP) were added and the membranes incubated at room temperature for 1h. The membranes were then washed three times in 1xTBS-T for 15min each.

Next, the ECL Western Blotting Reagent kit was used for protein detection. The two reagents provided were mixed 1:1 and added to the membranes for 5min. Chemiluminescence was generated through the oxidation of luminol (excited state) with hydrogen peroxide and HRP. The membranes were wrapped in Saran wrap and exposed to BioMax MR film for 30sec to 30min depending on the intensity of the signal.

The antibodies were stripped off the membranes by adding Stripping solution and incubating the membranes in a 50°C water bath for 10min. The PVDF was then washed twice in water and three times in 1xTBS-T prior to addition of another primary antibody.

10x transfer buffer	100mM CAPS pH 11.0 (Sigma) (1x buffer contains 10% Methanol)
10x TBS-T (11)	0.2M Tris pH 7.6 1.37M NaCl 10ml of Tween 20 (Sigma)
Blotto	5% dry milk in 1x TBST
Stripping solution	2% SDS 62.5mM Tris-HCL pH6.7 100mM 2-Mercapthoethanol

3.3.5. Immunoprecipitation assay

For immunoprecipitation (IP), pelleted cells were re-suspended in cooled IP-Lysis buffer. Samples were incubated on dry ice for 5min and thawed for 5 min in a 37°C water bath. These two steps were repeated 4 more times. The samples were centrifuged for 10min at 13000rpm and the supernatant was transferred to a new microfuge tube. Protein concentration was determined as described in Section 3.3.2. A FLAG-tag specific antibody, Anti-FLAG-M2 agarose affinity gel (Sigma, St. Louis, MO) was used to precipitate FLAG-tagged fusion proteins and their binding proteins from 200µg of total protein. IP samples were incubated with the antibody for 1-2h at room temperature. IP complexes were washed three times in ice-cold IP-lysis buffer. After a 2min-centrifugation at 7000 rpm, the wash buffer was aspirated, and the sample pellet was resuspended in 1x Sample buffer. Proteins were separated by electrophoresis and transferred to PDFV membranes as described in section 3.3.3 and 3.3.4.

IP Lysis buffer	20mM Hepes (Sigma) pH 7.5 150mM Sodium Chloride 0.1% Tween 20 10% Glycerol
------------------------	---

3.3.6. Immunofluorescence assay

For immunofluorescence staining, the cells (3×10^4 /well) were plated into chamber slides and incubated at 37°C and 10% CO₂ for 24h prior to analysis. Cells in chamber slides were fixed with 1% paraformaldehyde (Sigma) in FA-buffer (Difco, Fisher), and permeabilized with 0.25% Triton (Surfact-Amps® X-100, Pierce) in FA at room temperature. The slides were blocked with 10% swine serum (DAKO, Carpinteria, CA) in FA and stained with antibodies as shown in Table 3. The antibody staining was carried out as described elsewhere⁶⁰. Negative control antibodies were used to determine if the staining is specific. The nuclei were visualized using a 30µM Hoechst 33342 staining solution (Promega). Cells were visualized with the Fluorescence microscope Zeiss Axioplan 2 imaging at a magnification of 40 or 63x (Carl Zeiss Vision GmbH, Hallbermoos/Germany).

Primary Antibody	Secondary conjugated Antibody	Absorption/Emission in nm
Anti-V5 mouse		
Anti-MYC mouse	Anti mouse	FITC conjugated
Anti-MDM2 rabbit		492/520
Anti-MYC goat	Anti goat	
Anti-FLAG-M2 mouse	Anti mouse	
Anti-p14 ^{ARF} rabbit	Anti rabbit	Texas Red conjugated
Anti-MDM2 rabbit	Anti rabbit	596/620
Anti-p53 rabbit	Anti rabbit	
Anti-IgG2a mouse		492/520
Anti-IgG1 mouse	Anti mouse	FITC conjugated
Anti-IgG mouse		
Anti-Ig rabbit	Anti rabbit	Texas Red conjugated
		596/620

Table 3
List of all primary and secondary antibodies used for immunofluorescence, Absorption and Emission wavelengths were taken from Jackson ImmunoResearch antibody catalogue.

To distinguish between ARF, p53 and the MDM2 proteins, a secondary antibody conjugated with FITC (fluoresces green at 520nm) was used to detect the primary antibody against the MDM2 splice variant V5 tag and the full-length MDM2 MYC tag, whereas a

p14^{ARF} antibody, the primary p53 antibody or the primary antibody against the full-length MDM2 MYC tag (Anti-c-Myc-epitope rabbit, Affinity Bioreagents, Inc., Golden, CO).

3.4. Generation of transgenic mice

3.4.1. Splicing by overlap extension

The cDNA of *Mdm2-a* was created through “Splicing by overlapping Extension” (SOE) ¹⁰² using the murine full-length *Mdm2* cDNA (obtained from Dr Lozano, M.D. Anderson Cancer Center, Houston, TX) as a template. Exons 4 through 9 (Δ 28-220 amino acids) were deleted from the cDNA to mimic the human *MDM2-A* sequence (GenBank accession number U33199). The cDNA was amplified in two separate PCR-reactions (Figure 5) using two different oligonucleotides pairs, Mouse5end/Super3ex and Super10ex/Mouse3end. The primers Super3ex and Super10ex contained sequences of the junction between Exon3 and Exon10. Their 5'-ends consisted of either Exon3 or 10 sequences whereas their 3' ends consisted of complementary sequences from the opposite side of the break point. The resulting PCR products were used as templates for a third PCR-reaction with their complementary ends acting as primers to elongate a new recombinant cDNA of the *Mdm2-a* splice variant (Figure 5).

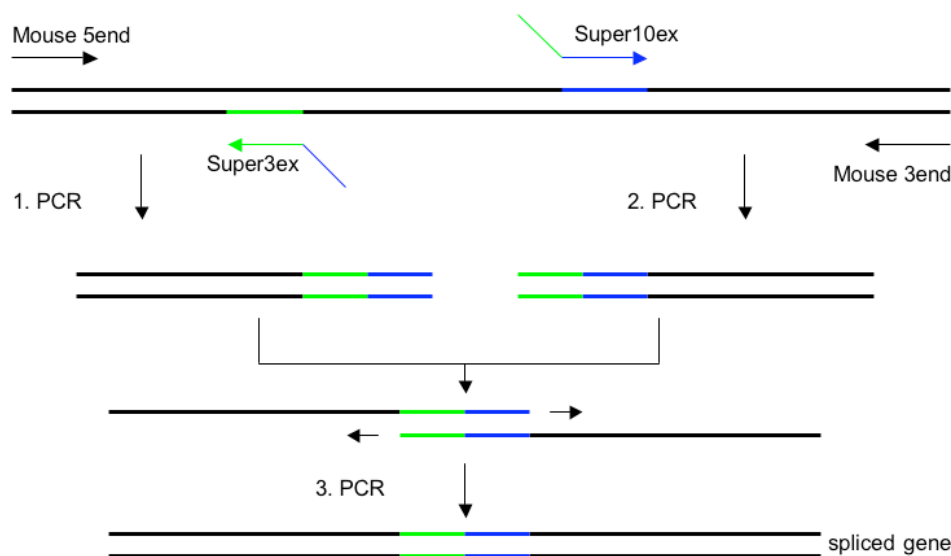


Figure 5
Splicing by overlap extensions-SOE. PCR- polymerase chain reaction. For primers refer to Table 1 and Appendix 8.4.

3.4.2. Generation of the transgenic mouse construct

The PCR product of *Mdm2-a* cDNA generated by the SOE method was cloned into EcoRI/XhoI restriction sites of the pCAGGS/MCS, a mammalian expression vector (Figure

6), that contains a constitutive chicken actin promoter, CMV enhancer and rabbit beta-globin polyadenylation signal¹⁰³. The vector is suited for high-level expression in several cell types¹⁰³.

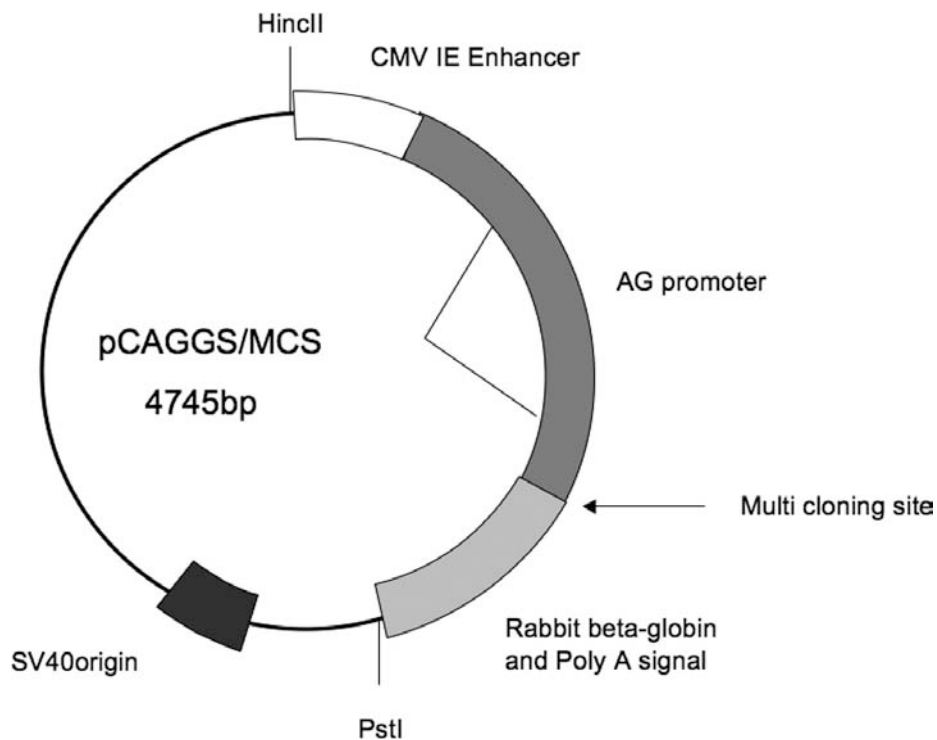


Figure 6
pCAGGS/MCS mammalian expression vector, CMV IE enhancer - cytomegalovirus enhancer; AG-promoter - modified chicken β -actin promoter

To confirm, that the *Mdm2-a* sequence in the plasmid contained no mutations, 200ng of plasmid DNA were sequenced by the Hartwell Center sequencing facility at St. Jude. The DNA sequence was confirmed by comparison to GenBank reference sequence (U40145).

The plasmid DNA (20 μ g) was digested with the restriction enzymes *HincII* and *PstI* to isolate only those sequences required for MDM2-A expression. The other plasmid sequences were removed to minimize cytotoxic DNA during the generation of transgenic mice. A 3.1kb fragment was obtained containing only the promoter, enhancer, cDNA and the polyA-signal. This DNA was separated from the remaining plasmid on an agarose gel. The excised gel piece containing the transgenic DNA fragment was given to Transgenic Core Unit at St. Jude, where it was eluted to a final concentration of 1-2ng/ μ l and microinjected into the pronuclei of fertilized one-cell stage mouse embryos (FVB/NJ mouse strain).

3.4.3. Recovery of transgenic mice

Potential *Mdm2-a* transgenic founder mice were genotyped by analysis of their tail tip DNA. Mouse tail biopsies were performed using sterilized scissors, and genomic DNA was

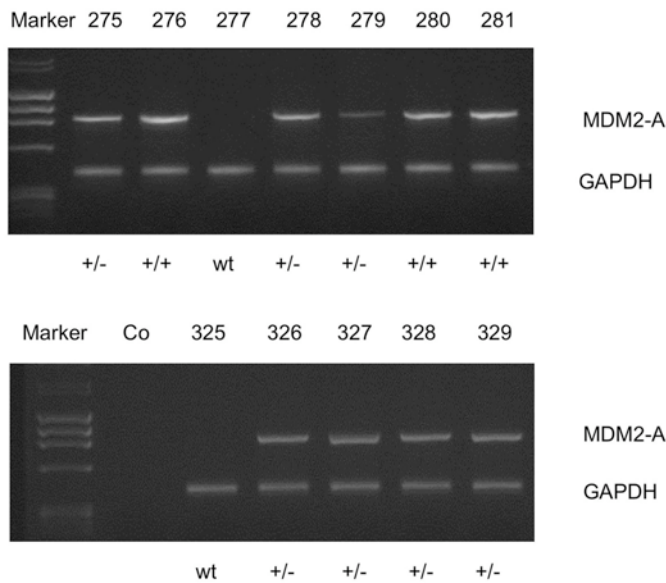
extracted from approximately 1cm of mouse tail. To determine which mice stably integrated the *Mdm2-a* transgene within their genome, multiplex PCR was performed to amplify the *Mdm2-a* transgene (900 base pairs) and the reference gene *GAPDH* (glyceraldehyde 3-phosphate dehydrogenase, GenBank M32599, 400 base pairs) in one reaction. HotstarTaq DNA polymerase was used as previously described (Section 3.1.7.1). In a 50 μ l reaction, 30 pmol of primer Mouse5end and Mouse3end, 10pmol of reference primer REFsense and REFantisense, and 300 μ g of genomic DNA were used. The templates were amplified in 32 cycles without final extension. A negative control was included in each PCR.

3.4.4. Maintenance of mouse colony

The founder mice were bred with wild type FVB/NJ mice to generate the heterozygous F1 offspring. Transgenic animals of the F1 generation were mated with each other (brother-sister mating) to generate homozygous offspring in the F2 generation. The transgenic mice were bred at the Animal Resource Center at St. Jude. The Institutional Animal Care and Use Committee (IACUC) approved all animal work and all experiments conform to the relevant regulatory standards.

3.4.5. Genotyping of the transgenic mice

To determine the genotype of the F2 generation of the transgenic mice, multiplex PCR analysis was performed as described in Section 3.1.7.1 and 3.4.3. The conditions were chosen to compare the intensity of both amplification products with each other in the logarithmic phase of the reaction (Figure 7). The intensities of the bands to each other were evaluated with the IPLab Gel software from Scanalytics, Inc (Fairfax, VA). Background values of the negative control were subtracted from the intensities of each amplification product. The resulting intensity values of the transgene bands were divided by the intensities of the corresponding reference gene bands. These values were used to determine the genotype of each mouse.

**Figure 7**

Genotype analysis of the *Mdm2-a* transgenic mice. Top panel shows Multiplex PCR reactions generated with different numbers of cycles. A reaction with 32 cycles was chosen for the genotype analysis. Bottom panel shows a representative multiplex PCR agarose gel of genotyped mice. The intensity of the bands to each other was evaluated to determine the genotypes. Wt- wild-type; +/- heterozygous mice; +/+ homozygous mice.

3.4.6. Isolation of mouse embryonic fibroblasts and embryos

Pregnant female mice were sacrificed at day 10-13 of their pregnancy using CO₂. Their bodies were cleaned with 70% ethanol and a small incision was made into the abdomen. The abdominal cavity was opened and the uterus including embryos was taken out and placed into a small dish containing sterile PBS. Each embryo was separated from the uterus and transferred to a fresh dish. Membranes were gently removed.

Embryos to be used for paraffin-sections were washed 3 times in PBS for 5 min. Only the tail was removed under an inverted microscope for genotyping. The embryos were then transferred to a 6-well plate and fixed in 10% formalin solution for at least 24h at room temperature. The embryos were taken to the Diagnostic Laboratory at the Animal Resource Center at St. Jude. In general, serial sections were cut at 4-5µm thickness and placed on glass-microscope slides. Tissues were stained with hematoxylin and eosin. Dr. Kelli Boyd (Pathologist, Veterinarian) at the Animal Research Center (ARC) evaluated the embryos.

To isolate mouse embryonic fibroblasts, day E13 embryos were harvested as described above, and the head and inner organs were removed. The remaining body parts were placed into a 6-well plate and 500µl trypsin-EDTA was added for digestion of the connective tissue. After an incubation time of 5min, the mixture was drawn through a syringe and a G18 needle. The body fragments were dispersed by pipetting and DMEM media was added containing 10% FBS, 2mM L-Glutamine, 0.1mM 2-Mercapthoethanol, 100U/ml Penicillin/Streptomycin and 1x non-essential amino acids. The cells were incubated at 37°C and 10%CO₂ and cultured like any other mammalian cell type *in vitro*.

4. Results: Expression of MDM2-A in a transgenic mouse model

4.1. Generation of *Mdm2-a* transgenic mice

The murine *Mdm2-a* cDNA was generated based on the human *MDM2-A* sequence (GenBank U33199) as described in Methods section 3.4.1. A schematic of the MDM2-A protein is shown in Figure 8. The *Mdm2-a* cDNA was cloned into pCAGGS¹⁰³ for constitutive expression in all tissues. After multiple rounds of microinjection, four out of 75 potential founders tested positive for the transgene. Even though microinjection usually results in 10-40% transgenic mice¹⁰⁴, a transgenic founder rate of only 5% was achieved in this study. This finding suggested that expression of MDM2-A might be detrimental to development.

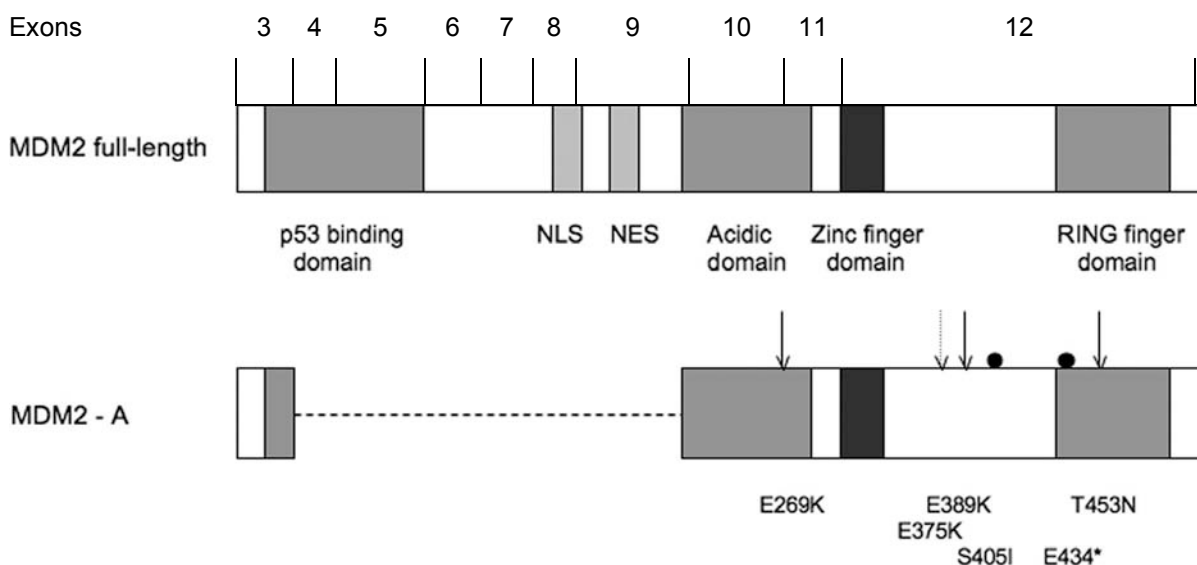


Figure 8

Schematic of murine full-length MDM2 and MDM2-A protein. Specific domains are marked as shaded boxes. Mutations detected in the *Mdm2-a* transgene are symbolized as arrows and shown in detail (mouse line A1, solid arrows; mouse line A2, broken arrow and mouse line A3, filled circles). Mouse line A4 does not contain mutations.

Three of the transgenic founders (founder A1, A3 and A4) were bred with wild-type animals, to generate heterozygous offspring (F1-generation). The other transgenic founder (founder A2) was a runt that died at the age of 6 weeks; the cause of death was unknown. Then heterozygous animals were mated with each other to generate homozygous offspring (F2-generation) containing two alleles of *Mdm2-a*. The genotype of the offspring was determined by Multiplex PCR as described in the Method section (refer to 3.4.3). The *Mdm2-a* transgene (900 base pairs) and the reference gene *GAPDH* (glyceraldehyde 3-phosphate dehydrogenase, 400 base pairs) were amplified in one reaction, and the intensity of the

resulting amplification products was compared. Figure 7 in Method section 3.4.5 shows a representative agarose gel of Multiplex PCR reactions for genotyping.

To date, 63 heterozygous transgenic and 36 homozygous transgenic mice have been evaluated from the first transgenic founder A1. For the third founder A3 were evaluated 41 heterozygous and 30 homozygous transgenic mice. For mouse line A4, 64 heterozygous animals but no homozygous offspring were generated.

4.2. Detection of mutations in the *Mdm2-a* transgene

The *Mdm2-a* transgene in all four founder mice was analyzed by PCR using genomic tail tip DNA as a template. Amplification products were sequenced, and results were confirmed by analysis of additional independent PCR reactions. Even though the *Mdm2-a* cDNA used in the microinjection appeared to consist of wild-type sequence, unique mis-sense mutations were detected within the *Mdm2-a* sequence of founders A1, A2 and A3. As shown in Figure 9, the sequence of *Mdm2-a* in founder line A1 contained three mutations. These were within the acidic domain (E269K), the region between the zinc finger and RING finger domain (E389K), and within the RING finger domain (T453N) (Figure 8). Founder line A2 contained one mutation in the sequence of the transgene located in the region between the zinc finger and RING finger domain (E375K) (Figures 8 and 9). Two mutations were detected in transgenic founder A3. The first mutation (S405I) was located in the region between zinc finger and RING finger domain; the second mutation (E434*) was located within the RING finger domain and resulted in a premature termination signal (Figures 8 and 9). Transgenic founder A4 did not contain any mutations within its transgene sequence. The number of copies of the transgene incorporated into the genome was extremely low (1-2 copies) for each of the mice generated, as determined by Southern analysis (data not shown). Only the mutant *Mdm2-a* sequence was present for mice A2 and A3. However, mouse A1 contained both wild-type and mutant transgene sequences observed as double peaks on the electropherogram of the sequencing data (refer to Figure 9).

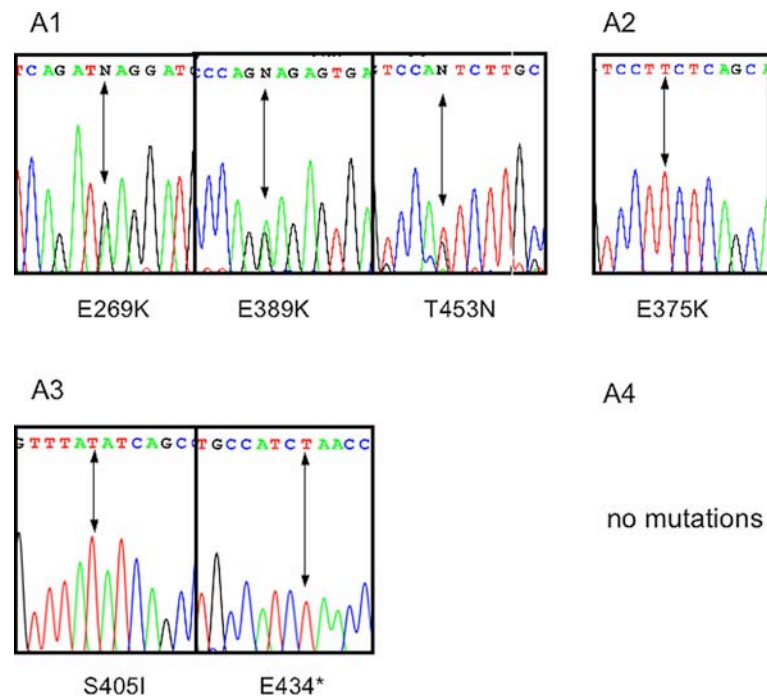


Figure 9
Schematic of electropherograms of *Mdm2-a* sequencing reactions of founder mice A1, A2, A3 and A4. Mutations are indicated as arrows. Numbers represent the amino acids that would be changed within the MDM2 protein. E-glutamic acid, K-lysine, T-threonine, N-asparagine, S-serine, I-isoleucine, V-valine, H-histidine, Y-tyrosine, Q-glutamine, R-arginine, F-phenylalanine, D-aspartic acid, *-termination signal

Upon subcloning the genomic DNA PCR product (mouse line A1) and sequencing the plasmids isolated from 18 individual colonies, it was determined that 50% of the *Mdm2-a* sequences in the plasmids contained all three mutations and 50% were wild-type. These data confirmed the presence of a mutant sequence that contained all three point mutations and one that was wild-type integrated into the genome for mouse line A1. The same results were also generated from the analysis of DNA isolated from different tissues: heart, skeletal muscle, salivary gland and liver. In addition, similar analysis of RNA by RT-PCR confirmed that both wild-type and mutant sequences were expressed. For mouse line A3, liver, skeletal muscle and heart were analyzed, and the same two mutations were identified. These data suggested that the mutant *Mdm2-a* transgenes were integrated into the genome of the one cell stage embryo and distributed to each cell type during development.

The mechanism by which these mutations arose in the transgenic mice is unclear. The data imply either that the DNA used for the microinjection procedure contained copies of mutant *Mdm2-a* cDNA in addition to wild-type *Mdm2-a* cDNA, or that the mutations were generated during embryonic mouse development. Because the transgene was present in

multiple tissues including the germ line it seems extremely unlikely that the mutations were generated within the one-cell stage embryo.

To determine whether the mammalian expression vector used for microinjection contained both mutant and wild-type copies of the *Mdm2-a* cDNA, the original transgenic plasmid pCAGGS/*Mdm2-a* was retransformed into DH5 α *E. coli* (Invitrogen, Carlsbad, CA), and 29 individual colonies were picked for overnight cultures and plasmid preparation. Sequencing of the isolated plasmids revealed no mutations within the *Mdm2-a* cDNA. Therefore, the DNA was at least 97% mutation free. However, if a very low proportion of plasmids did contain mutant *Mdm2-a* cDNA and there was selection during embryonic development against expression of wild-type MDM2-A, survival of mice expressing mutant MDM2-A can be explained.

4.3. Decrease of wild-type *Mdm2-a* transgenic embryos during development

To determine whether the expression of wild-type MDM2-A protein was being selected against during embryonic development, additional microinjections of one-cell-stage embryos were carried out using the *Mdm2-a* cDNA. Embryos at different developmental stages were harvested, their DNA isolated, amplified by PCR, and the amplification products sequenced.

After analysis of 37 embryos, seven *Mdm2-a* transgenic embryos were identified and dissected at day E10.5. Sequence analysis revealed that 5 of these embryos contained the wild-type *Mdm2-a* sequence. The sixth embryo contained the *Mdm2-a* cDNA with a single mis-sense mutation (H450Y), located within the RING finger domain (Table 4). Interestingly, the seventh embryo contained two *Mdm2* amplification products, one of which was wild-type for *Mdm2-a* and the other of which encoded the murine variant equivalent to human MDM2-B. Following analysis of 15 embryos at E11.5, one *Mdm2-a* transgenic embryo was obtained. Sequencing analysis identified three mis-sense mutations within the *Mdm2-a* sequence of this embryo: one within the portion of the p53 binding domain (J19T) and two between the acidic and the Zinc finger domains (Q280R and F289S).

Identification	Founder line	Transgenic animals / total number of animals	Mutation
Adult mice		4/75	
A1	Yes		E269K, E389K, T453N
A2	No		E375K
A3	Yes		S405I, E434*
A4	Yes		No mutation
Embryos at stage E10.5		7/37	
EB15	No		H450Y
EB39	No		No mutation in <i>Mdm2-a</i> , <i>Mdm2-b</i> ¹
Embryos at stage E11.5 - E12.5		4/26	
EB57	No		I19T, Q280R, F289S
EB22	No		<i>Mdm2-b</i> ¹
EB28	No		N431D, S458*

Table 4

Mutations discovered in the *Mdm2-a* transgenic mice and embryos. Numbers and letters refer to the following: ¹ - murine equivalent to the human *MDM2-B* splice variant, E-glutamic acid, K-lysine, T-threonine, N-asparagine, S-serine, I-isoleucine, V-valine, H-histidine, Y-tyrosine, Q-glutamine, R-arginine, F-phenylalanine, D-aspartic acid *-termination signal.

Following analysis of a total of 11 embryos collected at day E12.5, three were *Mdm2-a* transgenic embryos. One of these three embryos contained the wild-type *Mdm2-a* sequence. The second embryo contained two mis-sense mutations, one within the region between Zinc finger and RING finger domains (N431D) and the other within the RING finger domain (S458*). The third embryo contained no point mutations but lacked exons 4-11, equivalent to human *MDM2-B*. The mutation analysis for the embryos is summarized in Table 4.

Obtaining embryos for this study was difficult due to the low transgenic frequency observed. To obtain these eleven transgenic embryos, 63 embryos from eleven litters, were screened for the presence of the *Mdm2-a* transgene. Although the numbers evaluated are small, the proportion of transgenic embryos containing wild-type *Mdm2-a* decreased from 71% (5/7) at E10.5 to 25% (1/4) post E10.5, which is the same proportion obtained as live births (total 2/8). These data suggest that expression of wild-type MDM2-A might be detrimental to embryonic development beyond day E10.5. However, a small proportion of wild-type *Mdm2-a* transgenic embryos developed beyond this embryonic stage suggesting

that the selective pressure against the development of MDM2-A expressing embryos was absent in these mice.

Mdm2-a embryos were embedded in paraffin and serial sections were stained with hematoxylin and eosin. None of the wild-type *Mdm2-a* embryos evaluated showed identifiable developmental abnormalities compared to non-transgenic control or mutant transgenic embryos. Therefore, the exact cause of embryonic lethality could not be determined.

4.4. Wild-type MDM2-A inhibits growth in mouse embryonic fibroblast

To evaluate the function of different MDM2-A splice forms *in vitro*, retroviral vectors were generated containing the cDNAs of each *Mdm2-a* variant identified from the viable transgenic founders for transduction of wild-type mouse embryonic fibroblasts (MEFs) (FVB/NJ). Following transduction (48h), cells were sorted for GFP expression and GFP positive cells were plated in triplicate, and counted over a period of 6 days. Expressed mutant proteins are referred to as MDM2-A₁ (mouse line A1) and MDM2-A₃ (mouse line A3). The non-mutant protein is referred to as wild-type MDM2-A (mouse line A4).

As controls, MEFs were transduced with retroviral vectors containing either full-length *Mdm2* cDNA or a C-terminal fragment encoding only the MDM2 RING finger domain (MDM2-M3)⁹⁸. As expected, cells expressing full-length MDM2 grew faster than MEFs transduced with the vector control retrovirus due to the well-documented inhibition of p53 by full-length MDM2⁹⁸. As previously described, fibroblasts expressing MDM2-M3 grew slower than the control MEFs⁹⁸ (Figure 10).

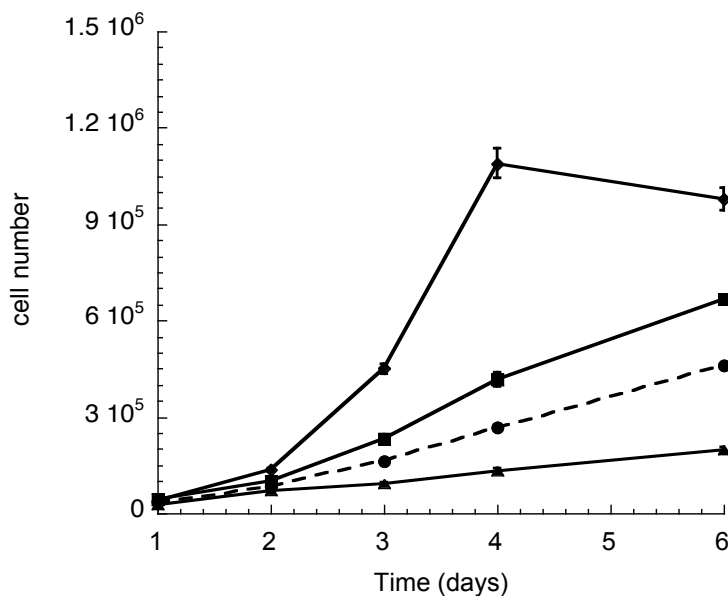


Figure 10
Growth curve of wild-type MEFs transduced with retroviral vectors expressing different MDM2 proteins. Wild-type MDM2-A inhibits growth in wild-type MEFs. Symbols refer to the following: (●) wild-type MDM2-A; (■) vector control; (◆) full-length MDM2; (▲) MDM2-M3 truncated protein.

This result was mediated by the binding of MDM2-M3 to endogenous full-length MDM2, preventing p53 from binding to full-length MDM2 and enhancing p53 function⁹⁸. Similarly, MEFs expressing wild-type MDM2-A grew at a slower rate than MEFs transduced with the vector control retrovirus (Figure 10). This result was also observed in NIH3T3 cells and in C2C12 murine myoblasts that express wild-type p53 (Figures 11A and 11B, respectively). These findings suggested that like MDM2-M3, wild-type MDM2-A contains an intact RING finger domain that binds full-length MDM2, leading to p53-mediated growth inhibition.

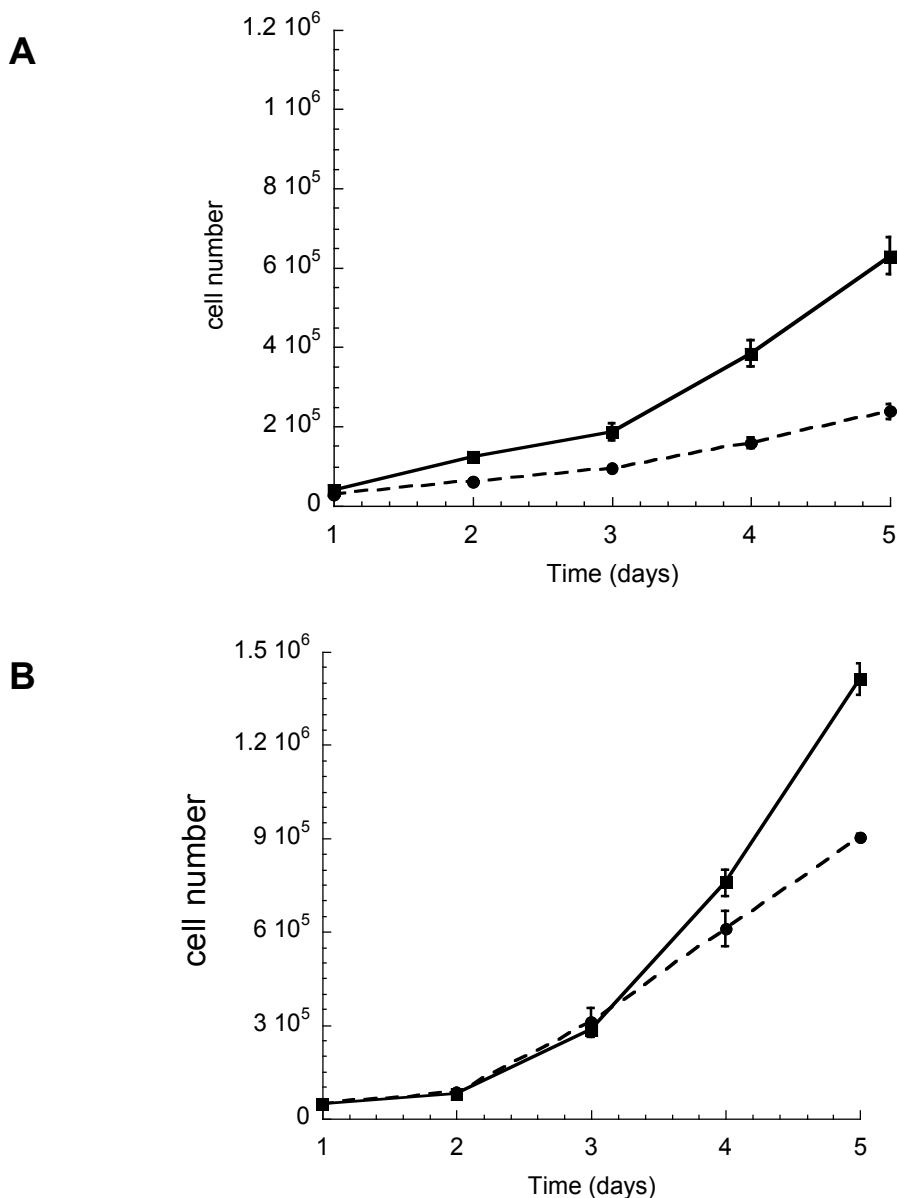


Figure 11
Growth curve of murine (A) NIH3T3 fibroblasts and (B) C2C12 myoblasts transduced with retroviral vectors expressing vector control and wild-type MDM2-A protein.
Wild-type MDM2-A inhibits growth in both NIH3T3 fibroblast and C2C12 myoblasts when compared to vector control cells. Symbols refer to the following: (●) wild-type MDM2-A, (■) vector control.

To determine the mechanism for the observed growth inhibition in wild-type MEFs, retrovirally transduced cells were sorted for GFP expression, and cell cycle analysis was performed after 48h. Figure 12 shows G1/S phase ratios for the cells following retroviral exposure. The G1/S ratio for cells expressing wild-type MDM2-A was greater (5.3) than that for vector control transduced MEFs (3.5), indicating that a higher proportion of MDM2-A expressing cells were in the G1 phase and less were in the S phase of the cell cycle (Figure 12). As controls, MEFs expressing either MDM2-M3 or full-length MDM2 were analyzed. As expected, the G1/S phase ratio of the slower growing cells expressing MDM2-M3 was greater (6.5) compared to the vector control transduced cells. In contrast, the G1/S phase ratio of the faster growing cells expressing full-length MDM2 was lower (2.4) than that for the control cells (3.5). The proportion of cells with a sub-G1 DNA content, indicative of apoptosis, was < 1% for all four viral exposures (data not shown) demonstrating that the lower cell number counted for the wild-type MEFs expressing the MDM2-A and MDM2-M3 splice variants was due to growth arrest and not apoptosis.

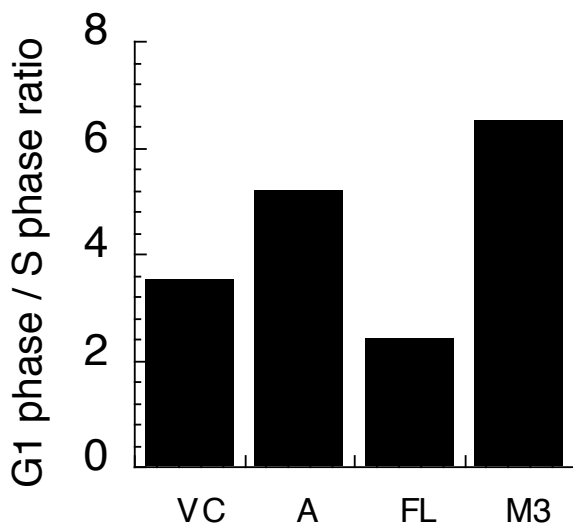


Figure 12
Representative cell cycle analysis of wild-type MEFs following retroviral transduction. G1/S phase ratio of cells expressing MDM2-A is higher than in cells expressing vector control and full-length MDM2. VC-vector control, A-wild-type MDM2-A, FL-full-length MDM2, M3-MDM2-M3.

4.5. Growth inhibition of wild-type MEFs is dependent upon expression of a wild-type *Mdm2-a* sequence.

To determine whether the observed growth inhibition in MEFs following expression of wild-type MDM2-A could also be mediated by the mutant MDM2-A proteins that were generated in the viable transgenic founder mice the growth of wild-type MEFs expressing the mutant cDNAs MDM2-A₁ and A₃ was evaluated (Figure 13). MEFs expressing mutant MDM2-A₁ and A₃ grew at a slightly faster rate than fibroblasts expressing wild-type MDM2-

A. Therefore, the mutations within splice variants MDM2-A₁ and A₃ that were present in transgenic mouse lines A1 and A3 provided a slight growth advantage to the MEFs in comparison to wild-type MDM2-A.

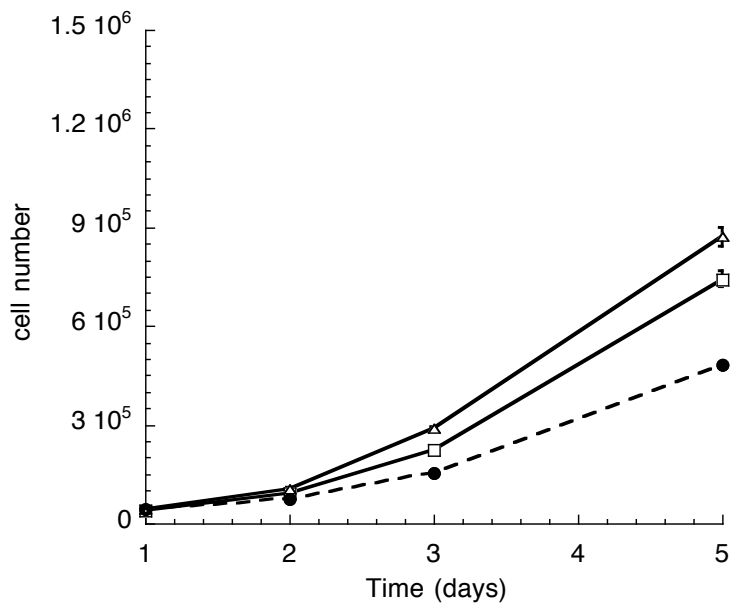


Figure 13
Growth curve of wild-type MEFs transduced with retroviral vectors expressing different MDM2-A proteins. Mutant MDM2-A proteins do not inhibit growth in wild-type MEFs. Symbols refer to the following: (●) wild-type MDM2-A, (□) mutant MDM2-A₁, (△) mutant MDM2-A₃.

4.6. Growth inhibition was p53- and p21^{Waf1/Cip1} –dependent.

Because MDM2-A expressing wild-type MEFs grew slower than control cells, we proposed that enhanced p53 activity was responsible. To determine if the growth inhibition mediated by the expression of wild-type MDM2-A was p53-dependent, the different MDM2-A variants were expressed in p53-null MEFs. Figure 14A shows, that regardless of the MDM2-A protein expressed, all retrovirally transduced p53-null fibroblasts grew at the same rate, indicating that p53 was responsible for the growth inhibition observed in wild-type MEFs following wild-type MDM2-A expression.

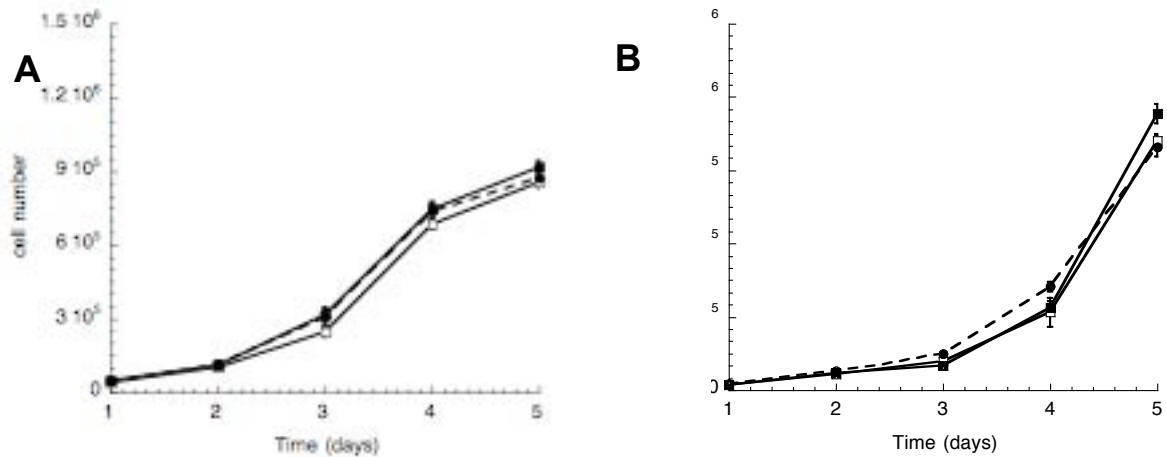


Figure 14

Growth curves of p53 null (A) and p21 null (B) MEFs transduced with retroviral vector expressing different MDM2-A proteins. (A) Wild-type MDM2-A mediated growth inhibition is dependent upon p53. (B) MDM2-A mediated growth inhibition is dependent upon p21. Symbols refer to the following: (●) wild-type MDM2-A, (□) mutant MDM2-A₁, (■) vector control.

It was also evaluated whether inhibition of cell growth was dependent on the p53-down-stream target p21^{Waf1/Cip1}, a cyclin dependent kinase inhibitor that arrests cells in G1 phase of the cell cycle. Results generated from growth analysis of p21-null MEFs demonstrated that cells expressing wild-type MDM2-A grew at a similar rate compared to vector control cells (Figure 14B). These data, demonstrate that the inhibition of proliferation mediated by wild-type MDM2-A was both p53 and p21 dependent. Wild-type, p53- and p21-null MEFs all expressed comparable levels of the different MDM2-A proteins (Figure 15).

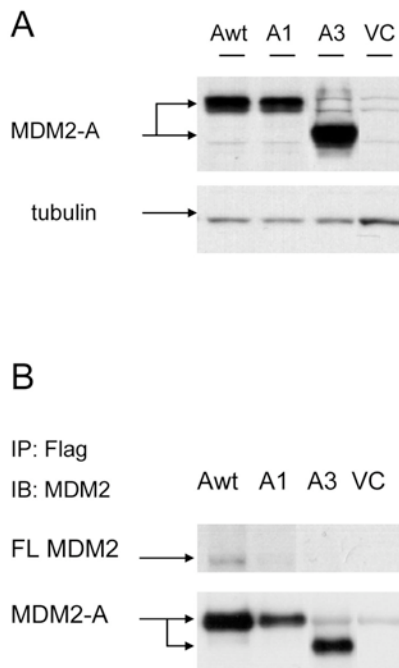


Figure 15

(A) MDM2-A expression in wild-type MEFs following retroviral transduction. Expression of MDM2-A variants and α -tubulin (loading control) are shown. Full-length MDM2 expression is not shown since this protein was almost undetectable in the whole cell lysates. (B) Immunoprecipitation of MDM2-A in wild-type MEFs. Anti-FLAG antibody was used to immunoprecipitate the FLAG-tagged MDM2-A proteins. An Anti-MDM2 antibody was used to visualize both the full-length MDM2 (FL) and MDM2-A proteins following western blot analysis. Wild-type MDM2-A complexes with full-length MDM2, however mutant MDM2-A proteins do not bind the full-length protein. The faint bands visible in the VC and A₃ lanes in the bottom panel are the antibody heavy chain.

4.7. Mutant MDM2-A proteins are unable to bind full-length MDM2

It was proposed that wild-type MDM2-A mediated growth inhibition occurs through binding to full-length MDM2. Such binding would result in enhanced p53 activity, as full-length MDM2 would no longer be able to regulate p53. To determine whether the mutations observed within the RING domain could prevent the formation of full-length MDM2/splice variant complexes, immunoprecipitation experiments were carried out as described in the Methods. FLAG epitope-tagged MDM2 splice variants were immunoprecipitated following expression in MEFs. Only wild-type MDM2-A formed a complex with full-length MDM2 (Figure 15B). These data are consistent with the growth inhibitory phenotype that was only observed upon expression of wild-type MDM2-A in wild-type MEFs. Full-length MDM2 did not co-precipitate with mutant MDM2-A₁ and A₃. Because the mutant proteins MDM2-A₁ and A₃ cannot bind full-length MDM2, p53 regulation by MDM2 was not affected.

4.8. Factors affecting development of a wild-type *Mdm2-a* transgenic mouse.

Despite the selection against wild-type MDM2-A during embryonic development and the p53-dependent growth inhibitory phenotype mediated by wild-type MDM2-A expression *in vitro*, a wild-type transgenic founder (A4) was generated. Three possible mechanisms were proposed that allowed this mouse to overcome the selective pressure against wild-type MDM2-A expression; 1) Loss of p53 function in this mouse, 2) Low level expression of the transgene and 3) a restricted pattern of tissue expression in tissues insensitive to increased p53-activity. Because p53 is essential for the observed MDM2-A mediated growth inhibition (Figure 10), loss of p53 function in mouse A4 may have allowed its survival. However, analysis of transgenic MEFs derived from this mouse line demonstrated that p53 was functional. p53 could be induced by ionizing radiation and in response to increasing p53 levels, p21 was induced (Figure 16A). In addition, transgenic MEFs isolated from A4 embryos were sensitive to expression of full-length MDM2 and MDM2-M3 proteins in the same manner as described for wild-type MEFs (Figure 16). A4 transgenic MEFs transduced with exogenous full-length MDM2 showed accelerated growth when compared to vector control transduced MEFs (Figure 16B) demonstrating that full-length MDM2 could inhibit endogenous p53 function and mediate proliferation of these cells. Overall, the growth rate of wild-type MEFs was faster than the A4 transgenic MEFs following transduction with each of the retroviral vectors demonstrating that p53 activity was being induced, mediated by a reduction in endogenous full-length MDM2 regulation (compare Figures 16C and 16B, respectively). In addition, functional p53 was suggested in the A4 mice by the fact that they

were not tumor prone and therefore loss of p53 function cannot be the reason for survival of mice expressing wild-type MDM2-A.

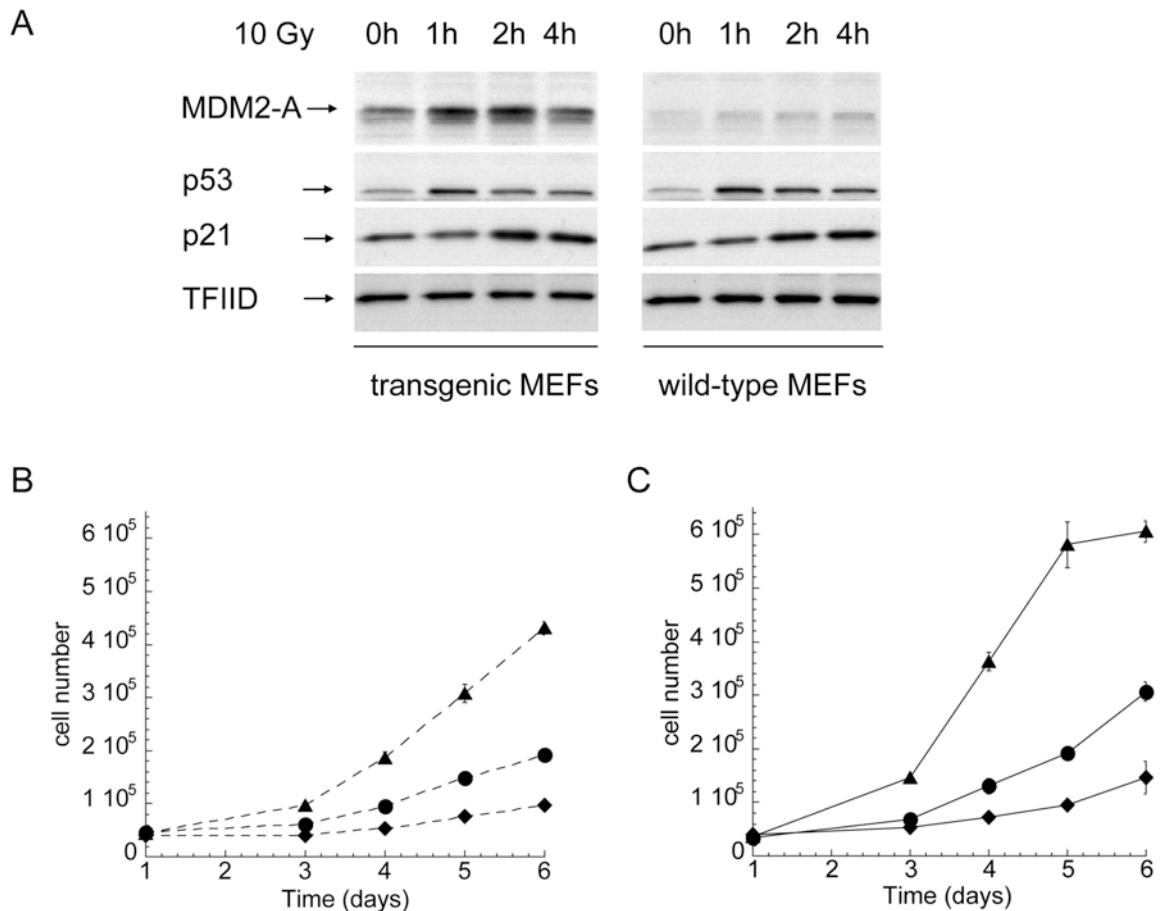


Figure 16

Western analysis and growth curves for wild-type and transgenic A4 MEFs demonstrating that p53 is functional in the wild-type *Mdm2-a* transgenic mouse line A4. (A) p53 western blot analysis following exposure of wild-type and transgenic MEFs to 10Gy ionizing radiation. p53 was induced 1h after treatment in both cell types and p21 induction was detected 2h after radiation in wild-type and transgenic MEFs suggesting that p53 is functional in the wild-type *Mdm2-a* transgenic mouse line. Transgenic (B) and wild-type (C) MEFs transduced with full-length MDM2, MDM2-M3 and vector control retroviral vectors; growth of both cell types was enhanced by expression of wild-type MDM2 due to inhibition of p53 activity. However, MDM2-A slightly decreased the growth promoting function of full-length MDM2 by partially activating p53. Expression of the truncated MDM2-M3 protein resulted in growth inhibition of both cell types. Symbols refer to the following: broken line – wild-type *Mdm2-a* transgenic MEFs isolated from mouse line A4; solid line – wild-type MEFs; (●) vector control; (▲) full-length MDM2; (◆) MDM2-M3.

The second potential reason for survival of mouse line A4 was a reduced level of MDM2-A protein expression. It was not possible to obtain any homozygous mice expressing wild-type MDM2-A suggesting that the lower level of MDM2-A expression in the

heterozygous mice mediated their survival. However, it is important to note that heterozygous wild-type MDM2-A is expressed in certain tissues (for example skeletal muscle) at a higher level in mouse A4 than mutant MDM2-A proteins in homozygous mice A1 and A3 (Figure 17). Therefore, elevated MDM2-A expression in certain tissues was not detrimental to survival, and the restricted pattern of MDM2-A expression in mouse line A4 also contributed to the survival of this mouse.

The pCAGGS plasmid¹⁰³ has previously been shown to allow expression of transgenes in a variety of tissues^{105, 106}. Equivalent expression patterns would have been expected in all three mouse lines unless the transgene integration site into the mouse genome influenced expression. In mouse line A1, MDM2-A₁ protein was expressed at high level in skeletal muscle and heart, while kidney and liver expressed the mutant MDM2-A₁ at lower levels (Figure 17A). MDM2-A₁ protein was not expressed in lung, skin, spleen, brain, salivary gland and ovaries. In mouse line A3, high level of mutant MDM2-A₃ was detected in lung, skeletal muscle, spleen, heart and ovarian tissue (Figure 17A). This mutant protein was also expressed at low levels in kidney, skin and brain. Mutant MDM2-A₃ expression could not be detected in salivary gland. Interestingly, the transgenic mouse lines A1 and A4 displayed a much more restricted pattern of tissue expression (Figure 17A). Wild-type MDM2-A (mouse line A4) could be detected at high level in skeletal muscle, heart and salivary gland, and at low level in kidney, lung and brain tissue. Wild-type MDM2-A could not be measured in liver, skin, spleen, and ovarian tissue. These data demonstrate that each *Mdm2-a* transgenic mouse line displayed a unique MDM2-A expression pattern likely dependent upon the transgene genomic integration site, and that the tissues expressing wild-type MDM2-A in mouse A4 appear to tolerate the growth-inhibitory effects selected against during development of the other transgenic founders.

4.9. Wild-type MDM2-A is expressed independently of full-length MDM2.

It was demonstrated that the growth inhibitory effect of wild-type MDM2-A is dependent upon inhibition of full-length MDM2 function. Therefore, it was hypothesized that MDM2-A could be tolerated in tissues of mouse A4 that expressed a higher level of full-length MDM2 protein. To test this hypothesis, the relative expression levels of MDM2-A and full-length MDM2 proteins were compared (Figure 17A). Full-length MDM2 was highly expressed in kidney and spleen, with lower expression observed in lung, brain and ovarian tissue. The amount of MDM2-A protein was not associated with the expression status of full-length MDM2 in any tissue. Low level wild-type MDM2-A was expressed together with a

high level of full-length protein in kidney and low level full length MDM2 in lung. In addition, tissues that expressed higher levels of wild-type MDM2-A (i.e. muscle, heart, and salivary gland) expressed lower levels of full-length MDM2. These data suggest that the level of MDM2-A expression was independent of full-length MDM2 expression in adult transgenic mice. In addition, expression of MDM2-A did not affect expression of full-length MDM2 as determined by a comparison of the amount of endogenous full-length MDM2 protein expressed in wild-type versus MDM2-A transgenic mice.

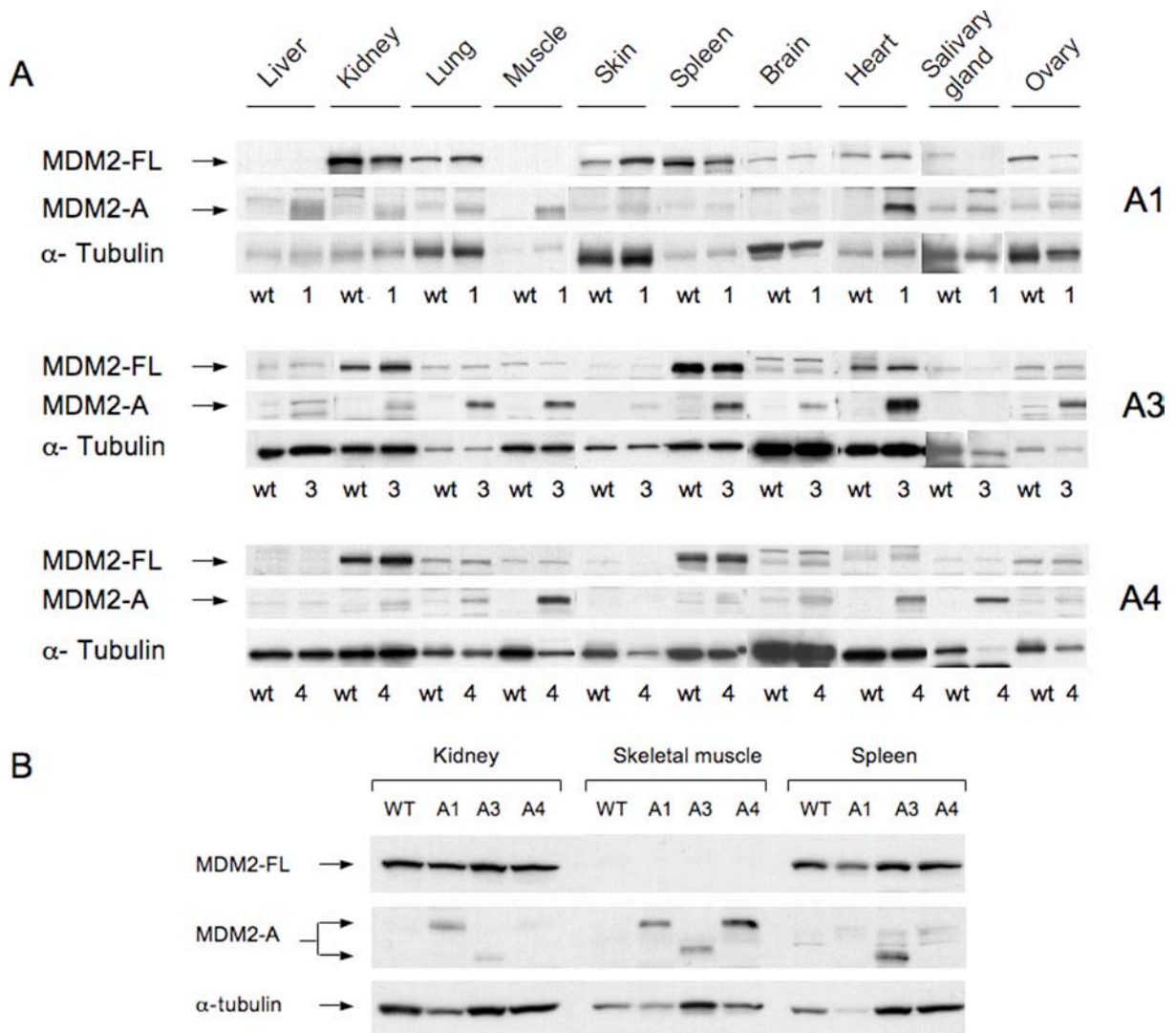


Figure 17

(A) Expression pattern of MDM2-A in homozygous transgenic mice A1, A3 and heterozygous A4 mice. Protein lysates were evaluated for MDM2-A, full-length MDM2 and α -tubulin expression. The tissues from each transgenic mouse were compared to the same tissues isolated from a non-transgenic animal (wt). (B) Direct comparison of MDM2-A expression in selected tissues from mice A1, A3 and A4. Mutant MDM2-A expressed in A3 is a smaller protein compared to the protein expressed in the A1 and A4 mouse lines owing to its C-terminal truncation (Figure 8).

4.10. Survival of *Mdm2-a* transgenic mice

The three MDM2-A founder mice, mutant A1, mutant A3 and wild-type A4 were bred in order to generate a homozygous mouse line. The mice were monitored for tumor development and disease with the help of Ms. June Bursi, Animal Research Center and Erin Volk, PhD, both at St. Jude. Animals were euthanized according to IACUC guidelines (Institutional Animal Care and Use Committee) when showing signs of pain or distress. Sacrificed mice were examined for lesions and tissue abnormalities by the Diagnostic Laboratory, St. Jude under supervision of Kelli Boyd, PhD.

Kaplan Meier curves for each mouse line are shown in Figure 18. Data demonstrate that survival of both heterozygous and homozygous mice of mouse lines A1 and A3 was identical to wild-type littermates (p value 0.28 and 0.69 respectively). For mouse line A1, 63 heterozygous and 36 homozygous animals were evaluated and compared to 72 wild-type animals. For mouse line A3, 41 heterozygous and 30 homozygous animals were compared to 19 wild-type littermates. Breeding of founder mouse A4 was unable to generate a homozygous line, as discussed above. The Kaplan Meier curve for the survival of this mouse line compared 64 heterozygous animals with 55 wild-type mice. The wild-type MDM2-A mice displayed a reduced survival (median survival 20 months, $p < 0.03$) compared to their non-transgenic littermates (median survival 25 months). Mice began to show common signs of aging FVB/NJ mice at about one year of age. Typical age-related problems included uterine hyperplasia, inguinal hernias and retinal degeneration. The limited number of tumors that were generated for each of the mouse lines compared to wild-type littermates is shown in Table 5. No transforming activity of either wild-type or mutant MDM2-A was observed.

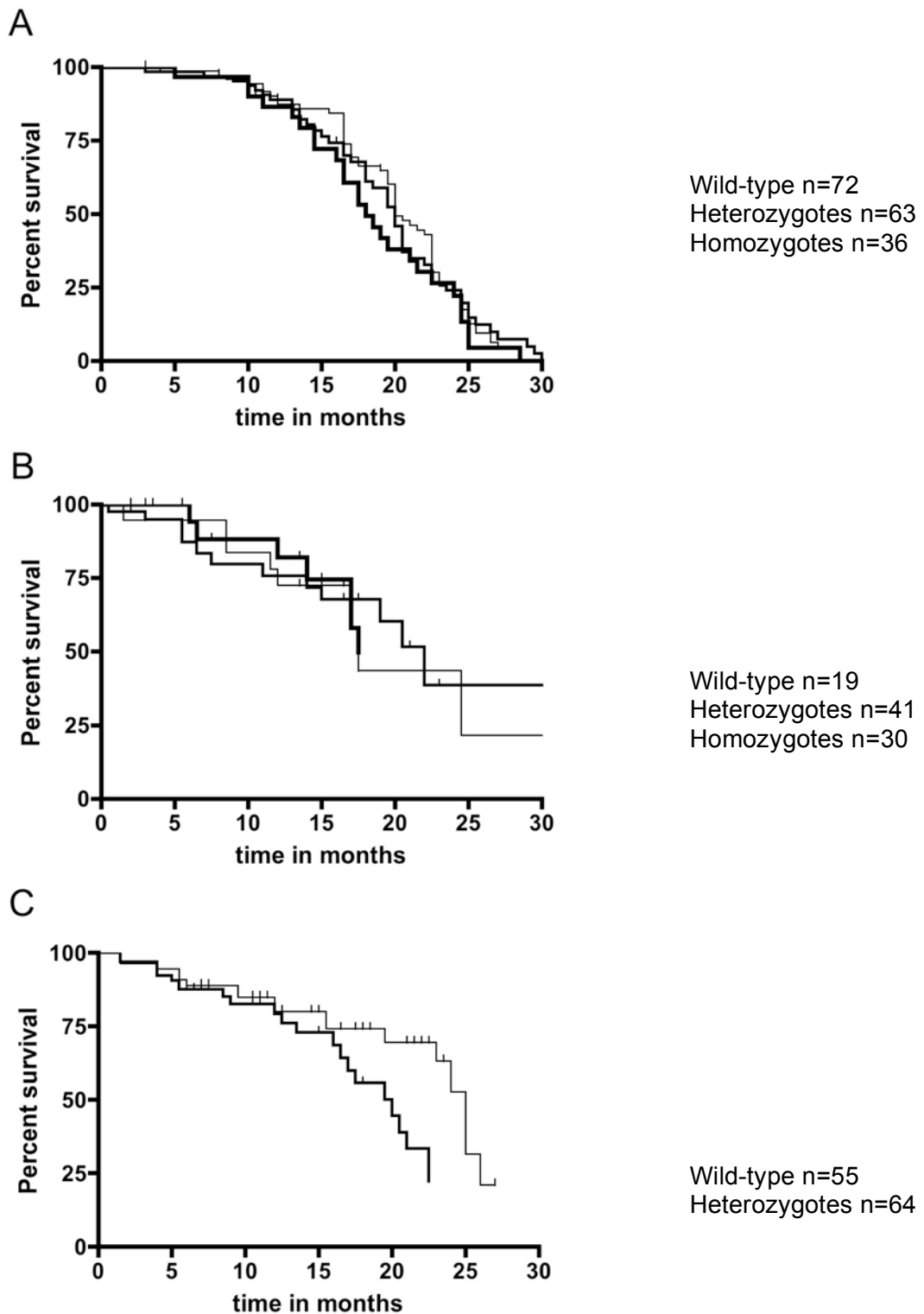


Figure 18

Kaplan Meier curves for *Mdm2-a* transgenic mice. (A) Mouse line A1. (B) Mouse line A3. (C) Mouse line A4. Wild-type, heterozygous and homozygous mice were monitored for disease and morbidity. The fine line represents non-transgenic littermates, the medium line heterozygous and the bold line homozygous animals. Survival was age-related and there was no significant difference between the survival of wild-type compared to the transgenic mice with the exception of mouse line A4 expressing wild-type MDM2-A ($p < 0.03$).

Mouse line	Number of animals with tumors/total number of animals (percentage)	Tumor types (number of animals)	Time of death of animal in months
A1			
wild-type	10/72 (14)	Soft tissue sarcoma (5) Soft tissue neoplasm (1) Lipoma (2)	20-28 25 24, 28
transgenic	9/99 (9)	Squamous cell carcinoma (2) Squamous cell carcinoma (5) Soft tissue sarcoma (1) Lipoma (1) Ovarian luteoma (1) Alveolar bronchiolar adenoma (1)	11-16 13-25 21 19 13 26
A3			
wild-type	2/19 (10)	Alveolar bronchiolar adenoma (1) Soft tissue mass ² leg (1)	15 17
transgenic	5/71 (7)	Ovarian teratoma (1) Alveolar bronchiolar adenoma (2) Squamous cell carcinoma ¹ (1) Hepatocellular adenoma ¹ (1) Soft tissue mass ² leg (1)	5 11, 11 17 17 17
A4			
wild-type	2/55 (4)	Squamous cell carcinoma (1) Soft tissue sarcoma (1) Alveolar bronchiolar adenoma (1)	25 24 12
transgenic	4/64 (6)	Soft tissue sarcoma (1) Osteoma (1) Soft tissue mass ² leg (1)	19 8 13

Table 5
Tumors detected in the *Mdm2-a* transgenic mouse lines compared to wild-type littermates, Footnotes:
¹ both tumors were found in the same animal, ² diagnosis unclear.

4.11. Discussion

Several studies have described MDM2 splice forms in human cancer⁷²⁻⁷⁶. Both growth inhibitory^{97, 98} and growth promoting functions^{78, 79} have been reported for different MDM2 splice variants¹⁰⁷ but the function of MDM2-A has not been evaluated. This chapter focused on the generation of MDM2-A transgenic mice. *MDM2-A* has been found in a variety of different tumor types and is the most common splice variant expressed in rhabdomyosarcoma tumors⁷⁵.

Despite its expression in tumors, data described here suggest that expression of wild-type MDM2-A is selected against during mouse development. Our data supporting this hypothesis are the following: 1) After multiple rounds of microinjection of wild-type *Mdm2-a* transgene, only four out of 75 mice tested positive for transgene integration. This proportion (5%) is lower than the average of 10-40% that has previously been described^{108, 109}. 2) Even though at least 97% of the *Mdm2-a* cDNA microinjected into the one-cell stage embryos was mutation free, only one of the four founders (25%) contained the wild-type *Mdm2-a* cDNA. 3) There was selection against the development of embryos containing the wild-type *Mdm2-a* sequence. The proportion of embryos containing wild-type *Mdm2-a* cDNA compared to those containing the mutant *Mdm2-a* cDNA decreased between day E10.5 and E12.5. During mouse development, organogenesis is observed at day E10 through E14¹⁰⁴, and at this time endogenous MDM2 and p53 expression is becoming tissue restricted^{110, 111}. The apparent loss of wild-type MDM2-A expressing embryos at this stage of development suggests that certain tissues may become more sensitive to the expression of wild-type MDM2-A, particularly as the level of endogenous MDM2 decreases, at approximately E10.5, leading to the termination of the embryo. Analysis of wild-type MDM2-A embryos at E10.5-12.5 did not reveal any tissue abnormalities that may have resulted in death of the embryos at this stage of development.

It was surprising that mutations were detected within the transgene cDNA in several transgenic embryos and mice. It is unlikely that these mutations occurred after microinjection because for the mutation to be present in every cell, mutagenesis would have to take place in the one cell stage embryo, prior to DNA replication. A more likely explanation is that the DNA used for microinjection contained mutations even though the plasmid DNA used for microinjection was grown from a single bacterial colony and no mutations could be detected within the *Mdm2-a* cDNA. Retransformation of the expanded transgenic plasmid and resequencing of selected colonies could not detect the presence of any mutations. However it is possible that the DNA used to microinject the fertilized eggs may have contained a

subpopulation of plasmids with mutant sequences generated during plasmid DNA replication within the *E. coli*. If so, the mutations were present at an extremely low level and appear to have been selected for during development of the transgenic mouse.

The observation of mutations within the cDNA inserted into transgenic animals is very unusual. If there was selection against expression of the transgene then the usual outcome would be for no transgenic founders to develop. However, it is unknown whether sequencing of the transgene following integration into the mouse genome is a common practice among investigators, and therefore the number of transgenic mice containing mutations may be much higher than is currently known. One example where mutations have been described within an integrated transgene was within *neu/c-erbB-2* transgenic mice¹¹². Deletion of 7-12 amino acids within the extracellular domain of this receptor tyrosine kinase was discovered. However, mutant sequences of *neu* were only detected within tumor tissue isolated from the transgenic mice, and could not be found in adjacent normal mammary tissue. Therefore these mutations were not generated during early embryonic development, but were somatic mutations within the mammary epithelial cells.

The mechanism by which MDM2-A is lethal during embryonic mouse development is mediated by wild-type p53. Expression of wild-type MDM2-A *in vitro* resulted in growth inhibition in MEFs in a p53 and p21 dependent manner (Figures 10 and 14) suggesting that p53-mediated growth inhibition was the reason for the selection against wild-type MDM2-A expression *in vivo*. A model for how MDM2-A functions, is shown in Figure 19. Full-length MDM2 binds p53 and regulates its activity resulting in a growth promoting phenotype (Figure 19A). Splice variants such as MDM2-A can bind full-length MDM2 through intact RING finger or acidic domains⁹⁸. Therefore, full-length MDM2 can no longer form a complex with p53, and p53 activity increases resulting in a growth inhibitory phenotype⁹⁷ (Figure 19B). Wild-type MDM2-A contains both the RING finger and acidic domains but the mutant transgenes in the founders and embryos (Figure 8) all contain mutations within at least one of these regions. Wild-type MDM2-A co-precipitates with full-length MDM2, but mutant proteins MDM2-A₁ and A₃ cannot. Therefore, when mutant MDM2-A proteins are expressed, full-length MDM2 can bind and regulate p53 appropriately (Figure 19C), and mice expressing mutant MDM2-A proteins develop normally. The variety of mutations observed within the MDM2-A sequence reflect the wide range of amino acids that can influence the binding of full-length MDM2 to splice variants such as MDM2-A.

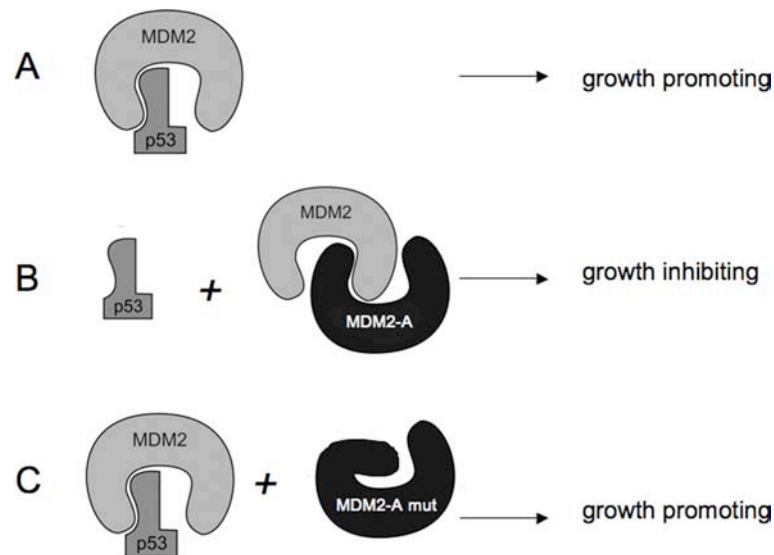


Figure 19

Model depicting full-length MDM2 and MDM2-A protein activities. (A) In a normal cell, full length MDM2 controls p53 activity through binding and ubiquitination, (B) Wild-type MDM2-A can bind full-length MDM2 and increase the growth inhibitory function of p53, (C) Mutations within the RING finger domain inhibit the binding of mutant MDM2-A to full-length MDM2. Therefore, full-length MDM2 function is unaffected and p53 activity can be controlled appropriately as in (A).

Expression of MDM2-A appears to be growth inhibitory both *in vivo* and *in vitro*. However, a single wild-type *Mdm2-a* transgenic mouse was generated, which expresses the transgene in several tissues. The reason for the survival of this mouse was evaluated, and appears to be due to a reduced level of MDM2-A expression in certain tissues. The evidence for this comes from the fact that it was not possible to generate homozygous MDM2-A mice from this line. Therefore, higher expression of MDM2-A in the homozygous mouse cannot be tolerated in mice that are wild-type for p53. It is proposed that only certain tissues are sensitive to elevated p53 activity mediated by MDM2-A since there are tissues from the heterozygous A4 mice in which expression of MDM2-A is greater than in the homozygous A1 and A3 mice, for example skeletal muscle (Figure 17). This hypothesis is not without precedent. In the study by Mendrysa *et al.* (2003), expression of hypomorphic MDM2 resulted in decreased endogenous MDM2 activity¹¹³. Transgenic mice expressing the hypomorphic MDM2 displayed elevated p53 activity in many tissues, however only cells of a proportion of these tissues died by p53-dependent apoptosis. These authors proposed that the surviving tissues have mechanisms to overcome p53-dependent apoptosis, which could also explain why elevated expression of MDM2-A is tolerated in certain tissues in mouse line A4. In addition, recent attempts to generate *Mdm2-b* transgenic mice expressing MDM2-B under the control of the β -actin promoter failed⁷⁹. It was only when these authors expressed

MDM2-B under the control of the glial fibrillary acidic protein (GFAP) promoter, and achieved a restricted pattern of tissue expression, that transgenic founders could be developed⁷⁹. These data support our hypothesis that expression of MDM2 splice variants that can bind full-length MDM2 are not well tolerated in certain tissues during mouse development. Restricting the tissues in which MDM2-A and B were expressed allowed the development of transgenic founders in our study and that of Steinman *et al.* (2004)⁷⁹, respectively.

It was demonstrated that MDM2-A displays a growth inhibitory phenotype both *in vitro* and *in vivo* during embryonic development but the question remains as to whether MDM2-A can mediate a different function during tumorigenesis. The *Mdm2-b* transgenic mice generated by Steinman *et al.* (2004)⁷⁹ were tumor prone and developed myeloid sarcomas and B-cell lymphomas. It is important to note that these tumors had a very long latency and were only observed between one and two years of age⁷⁹. This observation suggested that MDM2-B was a weak oncogene and that other genetic events were required before tumors could be formed. *MDM2-B* differs from *MDM2-A* by the deletion of an additional 78 amino acids containing of the acidic domain. It is possible that these two MDM2 splice variants may display different transforming activities as suggested by Fridman *et al.* (2003)⁷⁸. However if this were true, the frequent expression of each of these variants within tumors would be difficult to explain. The present study shows no evidence to support any transforming potential of MDM2-A.

The tissues of the wild-type *Mdm2-a* transgenic mice appear to have developed with activated p53. Therefore it is possible that these tissues might actually be protected against the tumor formation. This hypothesis is not without precedent. Recent studies have shown that higher levels of p53 and continuously activated p53 prevent the development of tumors in transgenic mice^{114, 115}. Garcia-Cao *et al.* (2002) evaluated mice, which contained three p53 alleles and these mice were resistant to tumor formation after treatment with carcinogenic chemicals¹¹⁴. These investigators suggested that upon DNA damage, the elevated p53 activity provided a more efficient control against propagation of damaged cells. This conclusion was supported by a report by Tyner *et al.* (2002) that evaluated mice that constitutively expressed activated endogenous p53 and as a consequence showed a tumor resistance phenotype¹¹⁵. Thus, elevated p53 activity may also prevent the development of tumors in the *Mdm2-a* transgenic mice generated in this study. These studies are ongoing by other members of the lab. On the other hand, it is also possible that if MDM2-A expression has only a weak oncogenic potential, this may only become apparent when *Mdm2-a* transgenic mice are crossed with mice with a tumor-prone genetic background such as p53-null or ARF-null mice.

Mice from line A4 were euthanized due to age-related problems as described in the results. However, death of these transgenic mice was quicker than that of the wild-type littermates (Figure 18, $p < 0.03$) suggesting that elevated p53 activity in these mice resulted in an enhanced rate of death. Reduced survival of mice expressing elevated p53 activity has also been previously reported. As described above¹¹⁵, mice expressing constitutively activated p53 showed resistance to tumorigenesis; however, these mice also showed reduced survival due to an aging phenotype. The authors proposed that constitutively activated p53 gradually reduces the number of dividing progenitor cells in organs with a high cell turnover. As a consequence these organs are incapable of maintaining homeostasis and no longer function, and the mice die prematurely¹¹⁵. This is probably the reason for the reduced life span of the *Mdm2-a* transgenic mice; although, the phenotype might not be quite as pronounced because these mice express MDM2-A in only a limited number of tissues.

MDM2 splice variants such as *MDM2-A* and *MDM2-B* have been detected primarily in tumor tissues^{72, 75, 97}, implicating that their expression may contribute to tumorigenesis. However, to date only MDM2-B has been shown to display transforming activities both *in vitro* and *in vivo*^{78, 79}. In this present report, no transforming activity mediated by MDM2-A was observed, instead MDM2-A expression was selected against during mouse development and inhibited cell growth *in vitro*. *MDM2-A* and *B* differ by 78 amino acids within their acidic domain suggesting that this structural difference is the reason for the observed contradictory activities⁷⁸. Therefore, MDM2-A may not cause transformation of a normal cell but may be expressed due to a dysfunctional splicing process in an already transformed cell.

In summary, four novel observations were made: 1) three of four *Mdm2-a* transgenic founders contained mutant *Mdm2-a* cDNAs 2) expression of wild-type MDM2-A is selected against during mouse development; 3) survival of wild-type *Mdm2-a* transgenic mice can be mediated by low level and restricted tissue expression of the transgene and 4) expression of wild-type MDM2-A is growth inhibitory in a p53 and p21 dependent manner. The growth inhibitory function of MDM2-A is in contrast to the growth promoting activities of other MDM2 splice variants^{78, 79}, but it is possible that loss of p53 function may be required before any transforming activities of MDM2-A can be observed. Alternatively, the enhanced p53 activity mediated by MDM2-A expression may result in an enhanced rate of loss of p53 activity contributing to tumorigenesis. It is clear that additional work is required to evaluate the complex phenotype of different MDM2 splice variants *in vivo* and to determine their role during tumorigenesis.

5. Results: Cellular localization of MDM2 splice variants

5.1. Introduction

Of the >40 alternative and aberrant splice variants of *MDM2* that have been described to date, the majority has lost both the nuclear localization signal and the nuclear export signal sequence. Therefore the goal of this study was to evaluate where splice variants might localize within the cell in order that potential functions might be predicted. The secondary goal of this study was to determine whether cellular localization of the splice variants is dependent upon expression of p53, p14^{ARF} and full-length MDM2.

Three splice variants were chosen for this project (Figure 20), *MDM2-B* which is the most common found variant in human cancer, *MDM2-A* the most common found splice variant in pediatric rhabdomyosarcoma and *MDM2-FB26*⁷⁵ one of only two splice variants described to date that contains the complete p53 binding domain. *MDM2-A* and *B* both lack

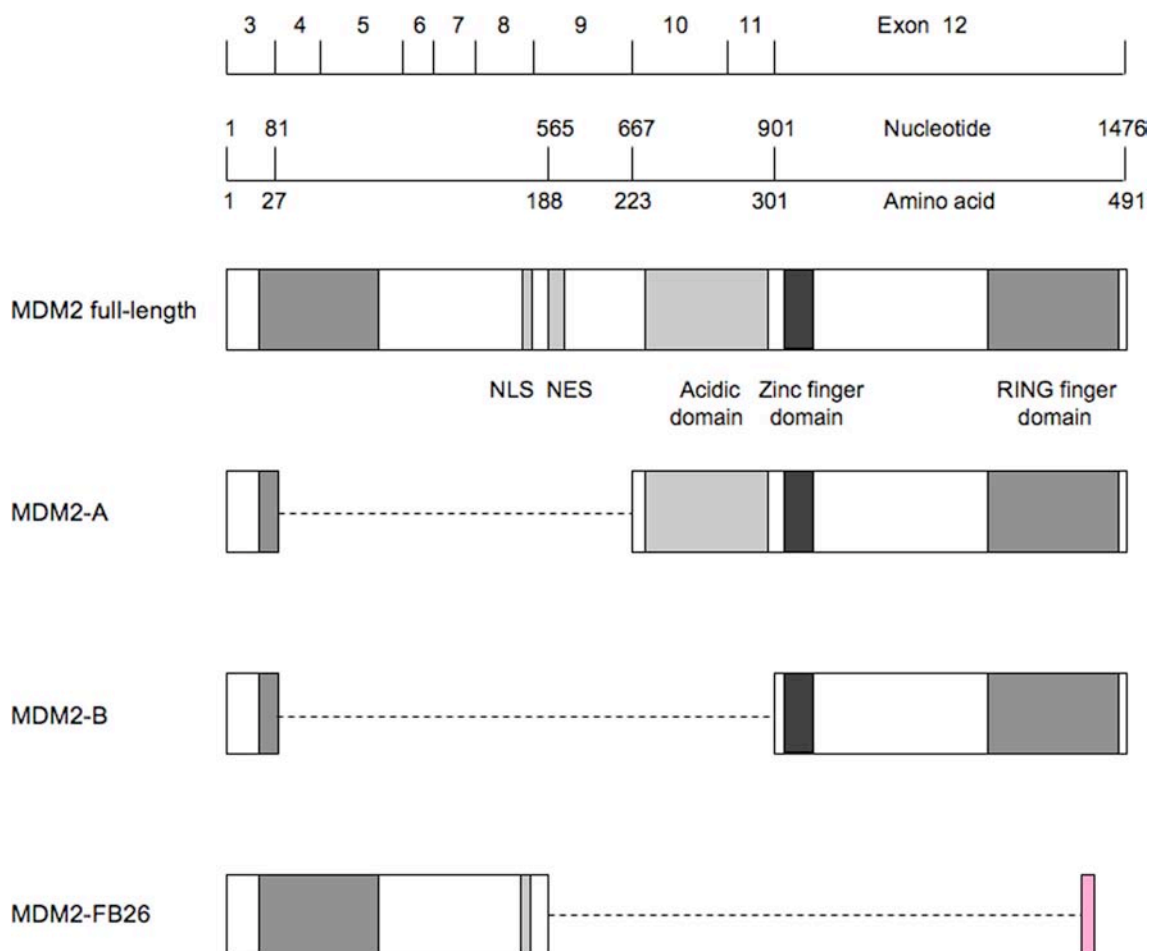


Figure 20

Structure of MDM2 and the splice variants evaluated in this study, MDM2-A, B and FB26. NLS- nuclear localization signal, NES- nuclear export signal. Numbers represent exons, nucleotides or amino acids of MDM2 as indicated.

most of the p53-binding domain, the nuclear localization signal (NLS) and the nuclear export signal (NES). However, the *MDM2-A* mRNA sequence contains an additional 234bp compared to *MDM2-B* that includes the acidic domain. The acidic domain is the p300/CREB and ARF binding region. In contrast, splice variant *MDM2-FB26* contains the complete p53-binding site and also the NLS. This variant lacks the C-terminus due to an out-of-frame sequence and a premature stop codon.

5.2. Generation of the *Mdm2* splice variant constructs

The DNA of splice variant *MDM2-FB26* cDNA was amplified from total mRNA of rhabdomyosarcoma samples as previously described ⁷⁵ and subcloned into helper plasmid pCR®2.1-TOPO® (Invitrogen). The cDNA of splice variant *B* was obtained from Dr. John Lunec (University Newcastle, UK). The cDNAs of *MDM2-A* and full-length *MDM2* were provided by Dr. Frank Bartel (Martin-Luther-University, Halle-Wittenberg, Germany). Sequencing analysis of the splice variants and full-length *MDM2* revealed mutations within various regions of the cDNA sequence (Table 6). Therefore, site-directed mutagenesis (Section 3.1.13) was performed to correct the base pair changes so that the *MDM2* sequences would match the entries in the GenBank (Table 6). The oligonucleotides used in the mutagenesis reactions are listed in Section 2.8.

The variants were cloned into a mammalian expression vector containing the sequence for the V5 epitope tag (pcDNA4/V5-his, Invitrogen) ¹¹⁶. Full-length *MDM2* was cloned into a mammalian vector and expressed as a fusion protein with the MYC epitope tag (pcDNA6/MYC-his, Invitrogen) ¹¹⁷. Large-scale plasmid DNA was isolated by Mrs. Misty D. Cheney, Technical Assistant, St. Jude as described in Method section 3.1.2.

Name	Mutation (bp)	Correct sequence (bp)	GenBank accession ID
<i>MDM2</i> full-length	C 1304	T 1304	AX057138
<i>MDM2-A</i>	G 325, G 586, A 742	A325, A586, G 742	U33199
<i>MDM2-B</i>	T 25, G 308, G 407	C 25, A 308, A 407	U33200
<i>MDM2-FB26</i>	T 394, T 491	G 394, C 491	AF385323

Table 6

Detected mutations in the cDNAs of *MDM2* splice variants and full-length *MDM2*. Oligonucleotides used for site-directed mutagenesis are listed under Section 2.8. bp-base pair.

The plasmids were stably transfected into knock out mouse embryonic fibroblasts that were either null for p53/MDM2 (double knock out, DKO); or null for p19^{ARF}/p53/MDM2 (triple knock out, TKO). The plasmids contained either the Zeocin™ or the Blasticidin resistance genes for selection of the stable cell lines transfected with the splice variant or the full-length *MDM2* vector, respectively. Cell lines were established that expressed each of the splice variants and full-length MDM2 independently. However, after several passages in culture expression of the MDM2 proteins was gradually reduced until expression could no longer be detected. For that reason, transiently transfected DKOs and/or TKOs were used in the following experiments. The cellular localization of the splice variants was visualized using fluorescence digital imaging microscopy.

5.3. Expression of MDM2 splice variants and full-length MDM2 in knockout mouse embryonic fibroblasts

In TKOs, the splice variants MDM2-A and B localized predominantly to the nucleus with faint expression in the cytoplasm (Figure 21A). FB26 localized to the nucleoplasm and was excluded from the cytoplasm and the nucleoli. As predicted, full-length MDM2 appeared to be exclusively expressed into the nucleoplasm and excluded from the nucleoli and the cytoplasm (Figure 21A). Similar results were observed when each of the four MDM2 proteins was separately expressed in DKOs (Figure 21B). However, previously published studies are contradictory with regards to where in the cell MDM2 splice variants lacking the NLS are expressed^{14, 97, 118, 119}. One potential explanation for the results above is that the fusion tag used in these experiments might affect the cellular transport of MDM2 splice variants. However, it is also possible that there may be alternate nuclear localization signals within the different MDM2 splice variants sufficient for the nuclear import.

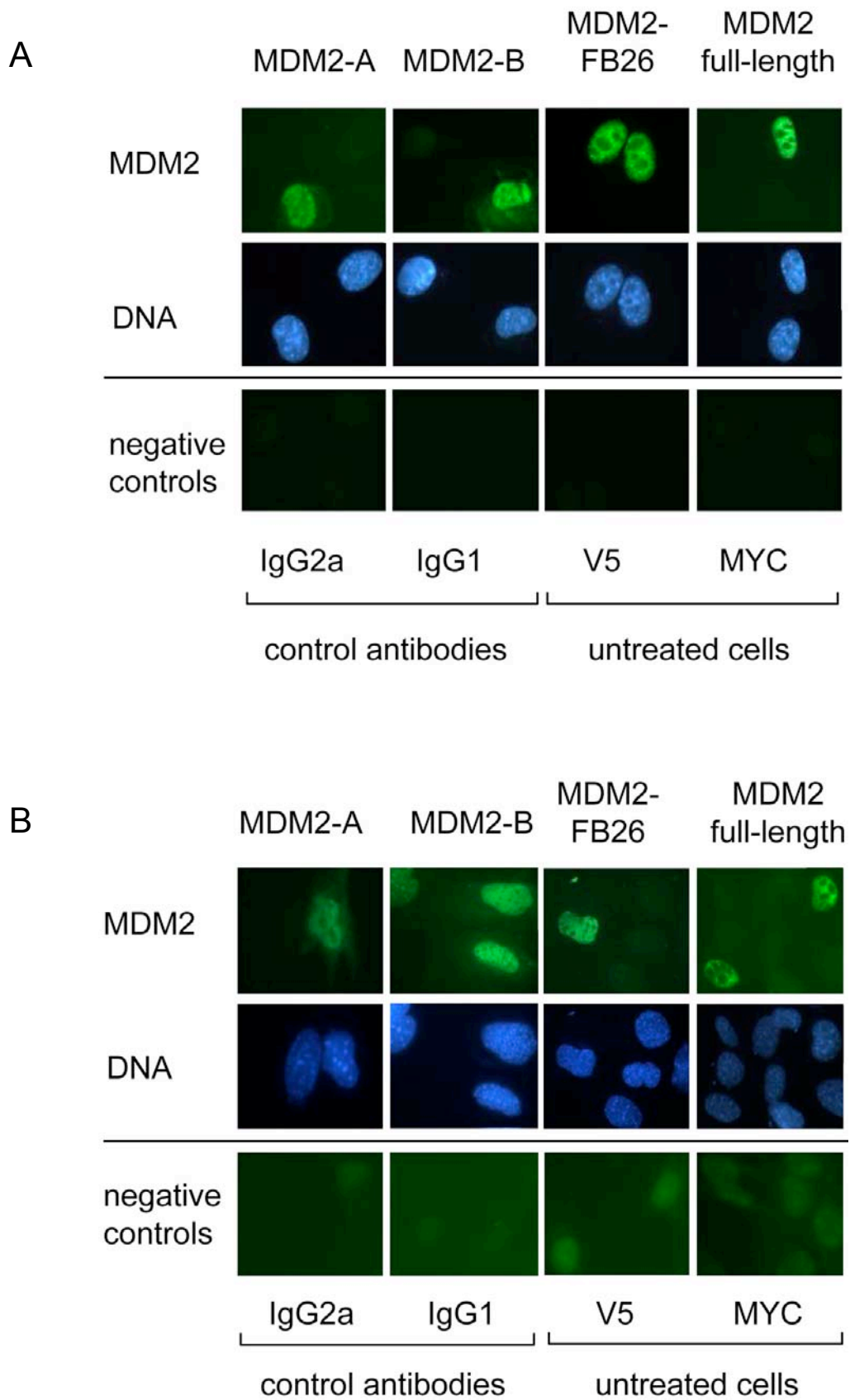


Figure 21
 Cellular localization of MDM2 splice variants and full-length MDM2 in (A) MDM2/p53/ARF null murine fibroblasts (TKOs) and (B) MDM2/p53 null murine fibroblasts (DKOs).

5.4. Fusion epitope tags do not influence the cellular localization

To determine whether the fusion epitope tag can affect cellular localization of MDM2 splice variants, MDM2-FB26 protein was expressed as fusion protein with a V5 epitope tag, a FLAG epitope tag¹²⁰ and without any fusion tag. In addition, MDM2 full-length was expressed with the MYC epitope tag and without fusion tag. The different proteins were either transiently transfected or transduced into the cells using retroviral vectors (see Method sections 3.2.3 and 3.2.4, respectively).

The fusion proteins FB26-V5, Flag-FB26 and FB26 were expressed predominantly in the nucleoplasm and excluded from the nucleoli and cytoplasm (Figure 22). These results suggest that the previously characterized nuclear localization signal (NLS) was responsible for the nuclear entry of FB26 and that the V5 epitope tag did not mediate nuclear localization. As shown in Figure 22, the fusion protein full-length MDM2-MYC and untagged full-length MDM2 were both expressed exclusively in the nucleus and excluded from the nucleoli and cytoplasm. These data demonstrate that the MYC epitope did not facilitate nuclear entry of the full-length protein.

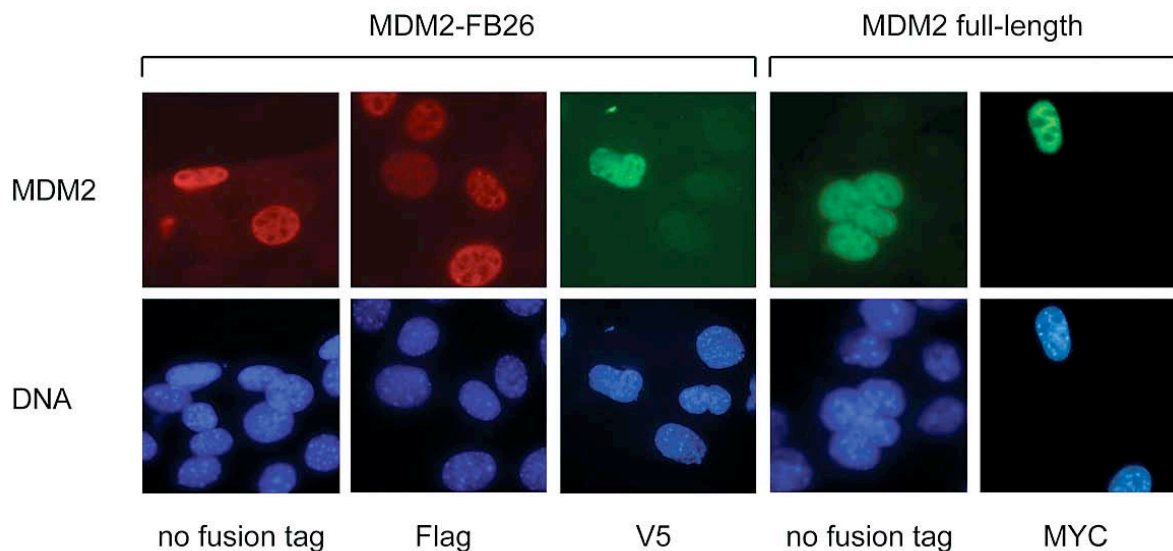


Figure 22
Cellular localization of MDM2-FB26 and full-length MDM2 with and without fusion epitope tags. Both MDM2 proteins were expressed in p53/MDM2/ARF null murine fibroblasts (TKOs).

5.5. Evaluation of alternate NLS sequences that could facilitate nuclear entry of MDM2 splice variants.

The nuclear localization of MDM2 splice variants MDM2-A and MDM2-B, which lack the previously characterized NLS, suggested that alternate sequences might facilitate their nuclear import. A nuclear localization signal has been confirmed within the N-terminal region of human full-length MDM2 ² (from now on called NLS1). However, a potential second nuclear localization signal appears to be contained within the RING finger domain ^{14, 121} (NLS2). A minimal feature of the majority of nuclear localization signals is the motif KXXXK/R (lysine-X-X-lysine/arginine) ¹²². NLS1 consists of amino acid numbers 181-185 with the motif RKRHK. The second potential transport signal (NLS2) consists of amino acid 466-473 resulting in three overlapping motifs within the same sequence KKLKCRNK. To determine whether both nuclear location signals are functional in MDM2, we introduced two mis-sense mutations into both transport signals, which changed the protein sequences as follows K182N and R183G for NLS1; and K469N and K470E for NLS2 (Figure 23A).

The splice variant MDM2-A, which lacks NLS1 was mutated to introduce the described mutations into NLS2 to generate MDM2-A_{NLS2}. The MDM2-A_{NLS2} protein was expressed predominately within the nucleus with faint expression in the cytoplasm of TKOs (Figure 24A) in an identical manner to the non-mutated protein. In addition, splice variant

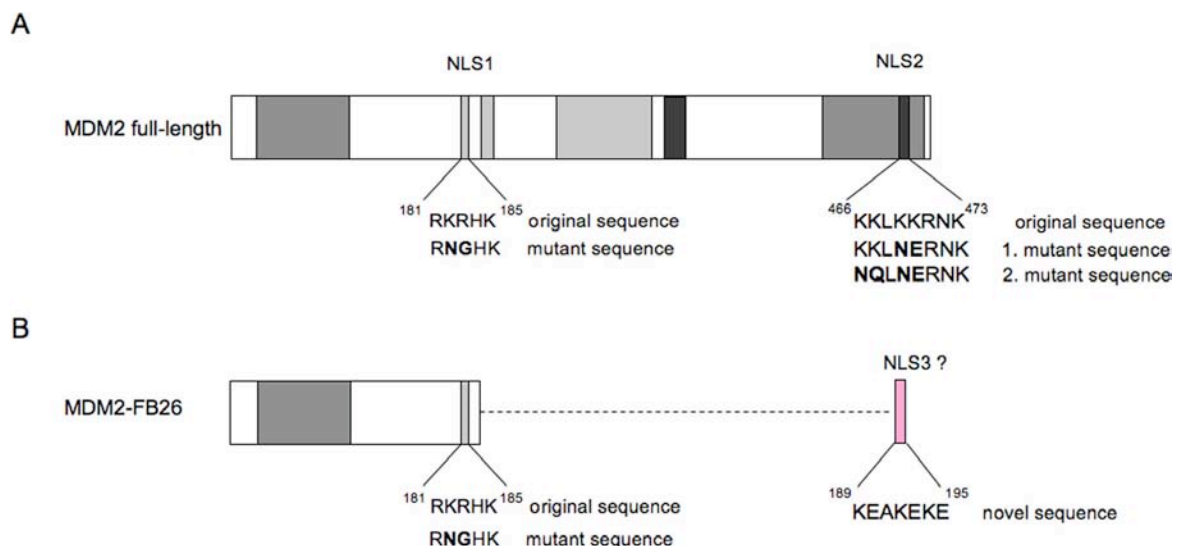


Figure 23

Introduction of mutations into the nuclear localization signals of MDM2 proteins. (A) For MDM2 full-length two nuclear localization signals have been predicted, NLS1 and NLS2. (B) The out-of-frame region of MDM2-FB26 contains a motif (NLS3) similar to the nuclear localization signals NLS1 and NLS2. Numbers represent amino acid positions. The resulting amino acid changes are shown in bold. R- arginine, K- lysine, H- histidine, N- asparagine, G- glycine, Q- glutamine, L- leucine, A- alanine.

MDM2-B, which also had mutations incorporated into NLS2 and lacks the NLS1, similarly localized predominantly in the nucleoplasm with visible expression in the cytoplasm of TKO cells (Figure 24A), as seen with the non-mutant proteins. Splice variant FB26, which contained NLS1 but lacked NLS2, had mutations introduced within the NLS1 sequence (FB26_{NLS1}). FB26_{NLS1} localized predominantly within the nucleus, but nucleolar and cytoplasmic expression of FB26_{NLS1} could also be detected (Figure 24A), which was not visible upon expression of wild-type FB26 (Figure 21A and B). MDM2 full-length_{NLS1} and full-length_{NLS2} each containing one intact localization signal expressed predominantly within the nucleus. Exclusion from the nucleoli was observed for each of these mutated full-length MDM2 proteins (Figure 24B). MDM2 full-length_{NLS1+2} had mutations introduced within both NLS1 and NLS2. However, this protein was still expressed predominantly in the nucleoplasm but was excluded from the nucleoli and the cytoplasm (Figure 24B). These results demonstrate that introduction of these mutations into the NLS motifs could not inhibit protein transport to the nucleus. However, the mutations created within the NLS1 of MDM2-FB26 slightly altered its cellular localization but it was still predominant nuclear, suggesting that other domains of this protein might substitute for the loss of NLS1.

These data suggested either that additional sequences are important for nuclear entry, or that the NLS signals had not been disrupted by the mutations that had been introduced. Introduction of mutations into the nuclear localization signal of large-T antigen of SV40 virus showed that of three contiguous lysine residues (amino acids 127-129) only lysine 128 was essential for the nuclear localization suggesting that different amino acids are of different importance for nuclear transport¹²². Therefore, additional site-directed mutagenesis was undertaken to further mutate NLS2 in the MDM2 splice variants to determine whether additional changes could interrupt the cellular transport of the splice variants to the nucleus. In addition to the amino acid changes at position 469 and 470 in NLS2 (Figure 23A, mutant sequence No.1), lysine residues 466 and 467 were also mutated (Figure 23A, mutant sequence No.2). The MDM2-A_{NLS2} protein sequence was changed as follows K466N, K467Q to generate MDM2-A_{NLS2+}. These additional mutations changed the cellular localization of MDM2-A. In TKOs, MDM2-A_{NLS2+} was now expressed predominantly in the cytoplasm with faint nuclear staining, which was not observed upon wild-type MDM2-A or mutant MDM2-A_{NLS2} expression. These data demonstrate that additional mutations within NLS2 were necessary to inhibit nuclear entry of MDM2-A_{NLS2+}.

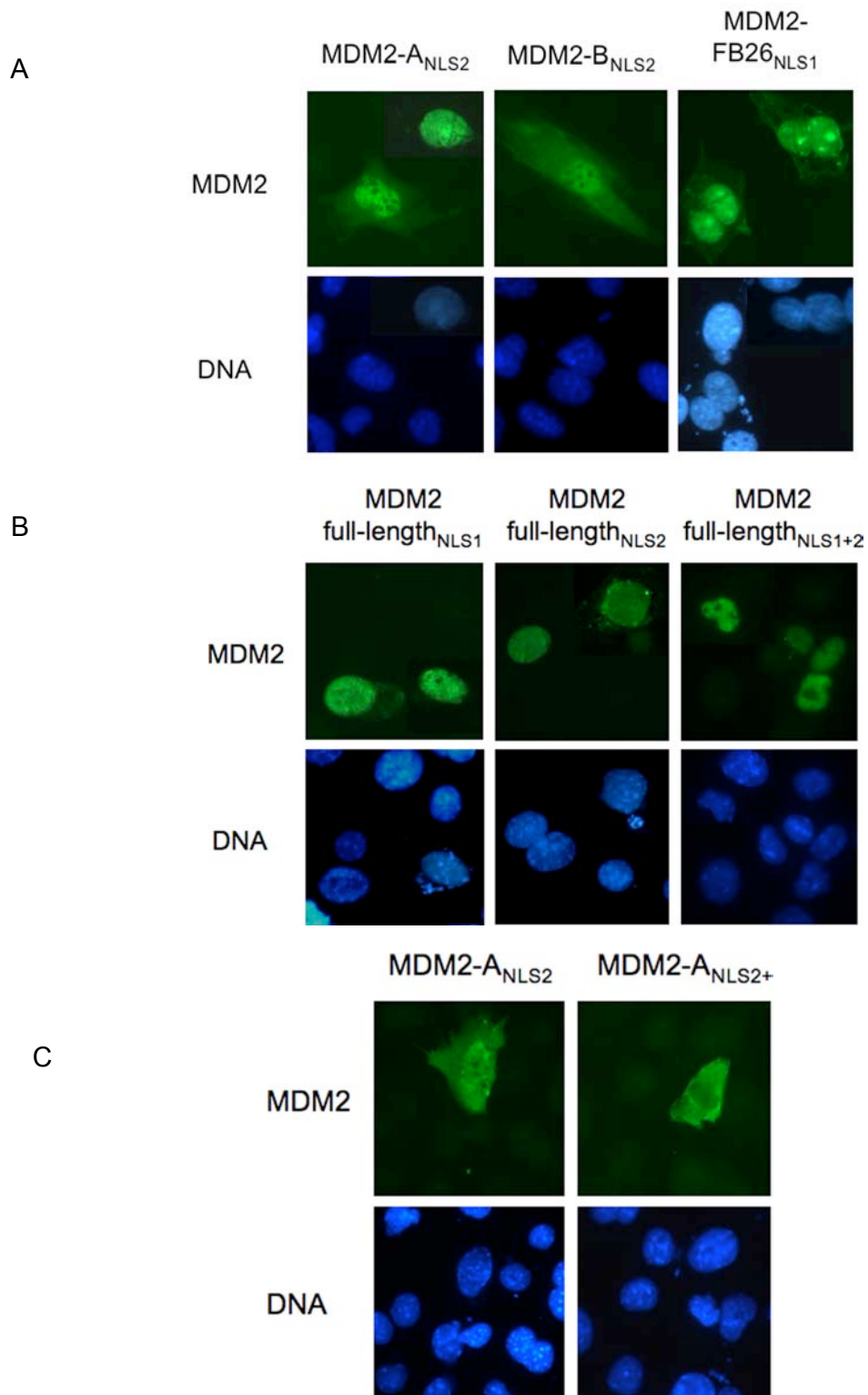


Figure 24

Cellular localization of MDM2 splice variants and full-length MDM2 mutated in their nuclear localization signals. (A) MDM2-A and B both lack the first nuclear localization signal (NLS1) and mutations have been introduced within a second nuclear localization signal (NLS2). MDM2-FB26 lacks NLS2 and is mutated within the first nuclear localization signal (NLS1). (B) Full-length MDM2 was expressed containing either a mutation within one of the two potential localization signals or within both. (C) Additional mutations were introduced into NLS2 of MDM2-A (NLS2+).

The splice variant FB26 is a rare MDM2 splice variant, which to date has only been detected in pediatric rhabdomyosarcomas⁷⁵. Evaluation of the C-terminal out-of-frame region of aberrant splice variant FB26 revealed a novel protein sequence consisting of seven amino acids ¹⁸⁹KEAKEKE¹⁹⁵ (MDM2-FB26 accession number AF385323). This novel sequence revealed a motif for a potential nuclear localization (NLS3?) consisting of amino acids ¹⁸⁹KEAKEK¹⁹⁴ (Figure 5.4B), which could have been responsible for nuclear localization of FB26. However, this novel sequence does not occur in other aberrantly spliced MDM2 variants, and therefore, the contribution of this novel potential NLS (NLS3?) to the nuclear localization of MDM2-FB26 was not pursued any further.

5.6. Co-expression of MDM2 splice variants with full-length MDM2

Another goal of this report was to determine if binding partners such as full-length MDM2, p53 and p14^{ARF} influence the cellular localization of MDM2 splice variants. To co-express full-length MDM2 with its splice variants, the plasmids encoding the different proteins as described in Section 5.2, were transiently transfected into mutant mouse embryonic fibroblasts (p53^{-/-}, MDM2^{-/-}, p19^{ARF}^{-/-}, TKOs). To distinguish between the different proteins when co-expressed, a secondary antibody conjugated to FITC (green fluorescence) was used to detect the primary antibody against the V5-tag of the splice variants, whereas a Texas Red (red fluorescence) conjugated secondary antibody was used to detect the primary antibody against the MYC-tagged full-length MDM2 protein (Section 3.3.6).

Dual staining to detect the three different MDM2 splice variants when co-expressed with full-length MDM2 revealed that as expected all three co-localized with full-length MDM2 in the nucleoplasm (Figure 25). Negative controls for antibody staining and staining of untransfected cells are shown in Figure 25 demonstrating that the observed staining was specific. In summary, full-length MDM2 co-localized with the MDM2 splice variant in the nucleoplasm.

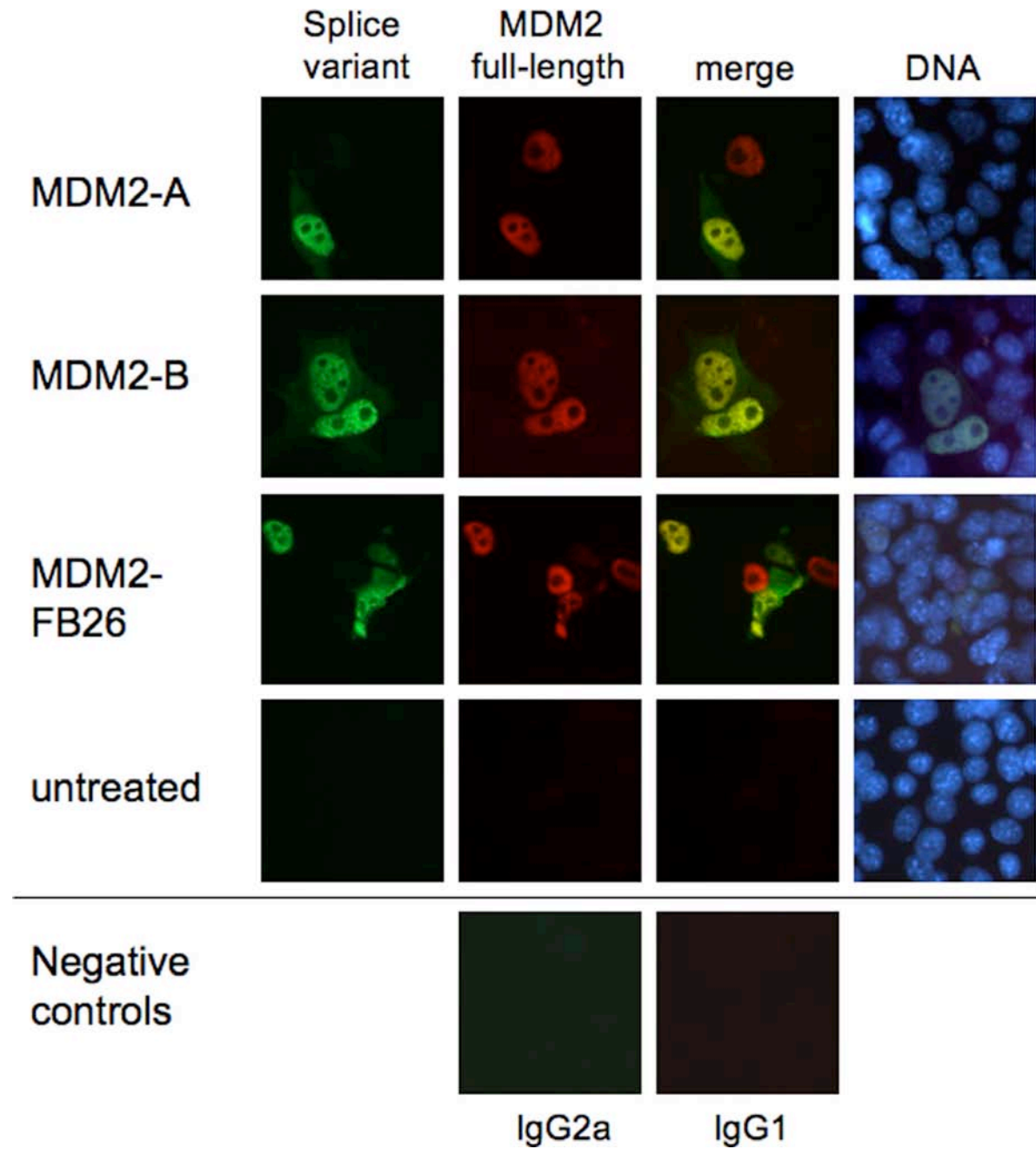


Figure 25

Co-expression of MDM2 splice variants with full-length MDM2. The MDM2 splice variants co-localized with full-length MDM2 within the nucleoplasm.

5.7. Co-expression of MDM2 splice variants with p53

To determine the effect of p53 expression on the cellular localization of MDM2 splice variants, p53 was expressed in the mutant mouse embryonic fibroblasts (p53^{-/-}, MDM2^{-/-}, ARF^{-/-} TKOs) together with the MDM2 splice variants. Expression of p53 was achieved by transduction with an adenoviral vector containing the p53 cDNA (refer to Method section 3.2.5). To visualize both proteins within the cell, a secondary antibody conjugated with FITC (green fluorescence) was used to detect the primary antibody against the V5-tagged splice variants, whereas a Texas Red (red fluorescence) conjugated secondary antibody was used to detect the primary antibody against p53 (Section 3.3.6). p53 expression was primarily detected in the nucleoplasm (Figure 26). As previously described splice variants A and B were predominately expressed within the nucleus, although these proteins were also detected in the nucleoli and the cytoplasm. MDM2-FB26 could only be detected in the nucleoplasm. Negative controls for antibody staining and negative staining of untreated cells are also shown in Figures 26 demonstrating that the observed staining was specific. These data indicate that p53 co-localizes with the different MDM2 isoforms within the nucleus of TKO cells.

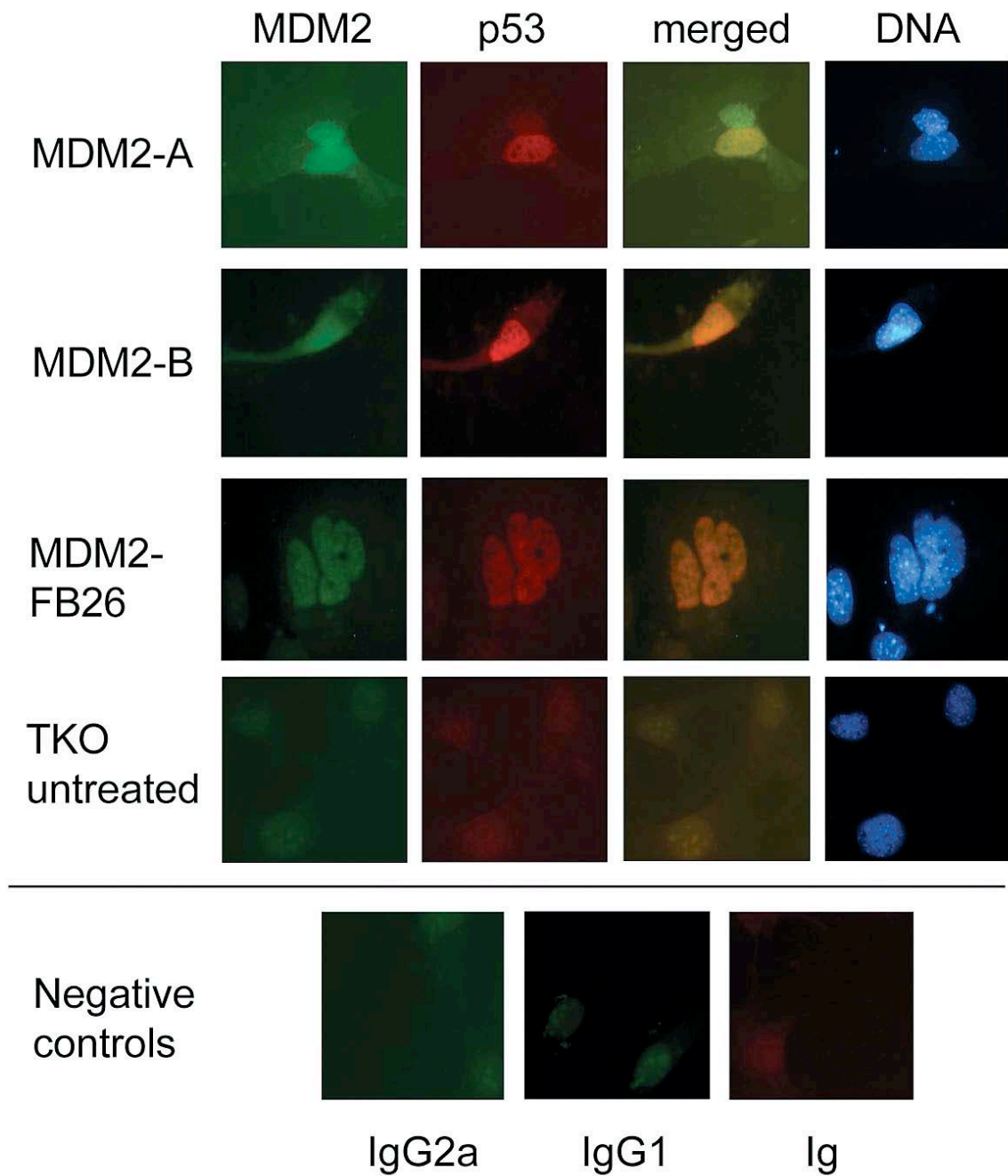


Figure 26

Co-expression of MDM2 splice variants and p53 in knock out fibroblasts (TKOs). MDM2 splice variants co-localize with p53 within the nucleoplasm. Negative control antibodies were used to ensure that the immunostaining is specific.

5.8. Co-expression of MDM2 splice variants with p14^{ARF}

To determine whether p14^{ARF} expression influenced the localization of MDM2 splice variants, a retroviral vector containing the p14^{ARF} cDNA was used to express ARF in knock out (p53^{-/-}, MDM2^{-/-}, ARF^{-/-}) MEFs. To distinguish between ARF and the MDM2 proteins, a secondary antibody conjugated with FITC (fluoresces green at 520nm) was used to detect the primary antibody against the splice variant V5 tag, whereas a Texas Red (fluoresces red at 620nm) conjugated secondary antibody was used to detect the primary p14^{ARF} antibody.

p14^{ARF} expressed predominantly within the nucleoli of p53/MDM2/ARF null murine fibroblasts (TKO) (Figure 27). However, upon ARF expression, MDM2-A, B and FB26 maintained their localization predominantly in the nucleoplasm (Figure 27). As previously observed, MDM2-A and B could faintly be detected in the cytoplasm. In summary, the co-expression of ARF with the splice variants did not result in co-localization within the cell demonstrating that ARF expression did not affect the cellular localization of MDM2-A, B and FB26.

5.9. Immunoprecipitation of MDM2 splice variants upon ARF expression

MDM2-A is the only splice variant that still contains the acidic domain that p14^{ARF} has previously been shown to bind. Therefore, immunoprecipitation analysis (IP) was undertaken to determine if MDM2-A and other MDM2 splice variants could form complexes with p14^{ARF}. ARF protein was immunoprecipitated following retroviral transduction of TKOs as described in the Methods (Section 3.3.5). MDM2 proteins were detected using an MDM2 specific antibody.

Full-length MDM2 formed a complex with ARF, as shown in Figure 28A. However, ARF binding to the MDM2 splice variants including MDM2-A could not be detected. If ARF bound to MDM2-A and B, then these proteins would have been visible following the IP. Unfortunately, due to the cross-reaction of the Horseradish peroxidase-conjugated secondary antibody with the ARF antibody used for the IP, any ARF binding to FB26 would have been obscured. Expression levels of full-length MDM2 (90kDa), MDM2-A (~53KDa), MDM2-B (~45KDa) and FB26 (~35KDa) in the TKO cell extracts before the IP are shown in Figure 28B.

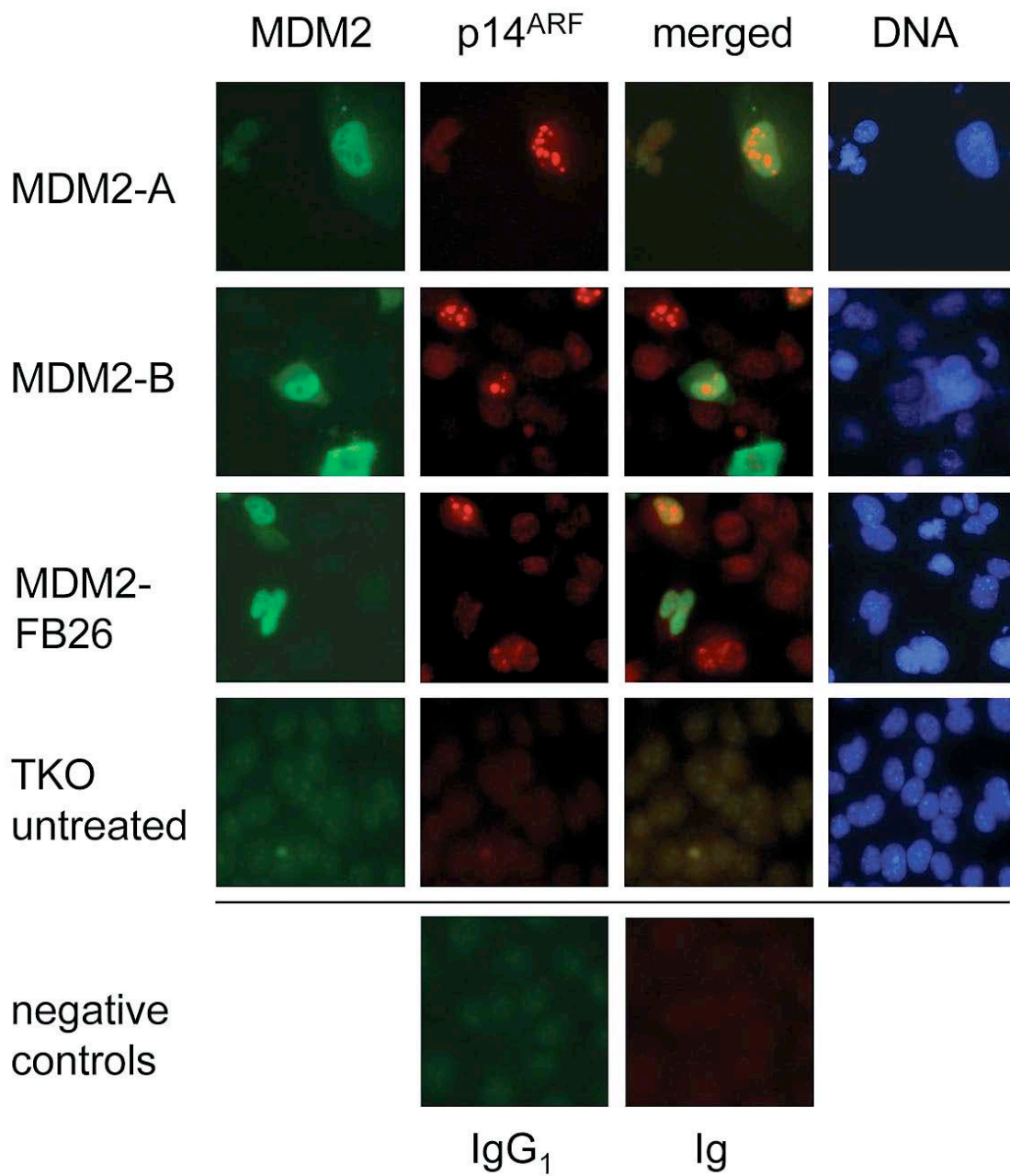


Figure 27

Co-expression of MDM2 splice variants and full-length MDM2 with p14^{ARF} in TKOs. ARF expressed predominantly within the nucleoli of the cell and was excluded from the nucleus and cytoplasm. MDM2-A, B and FB26 did not co-localize with ARF in the nucleoli. The splice variants maintained their predominantly nuclear localization.

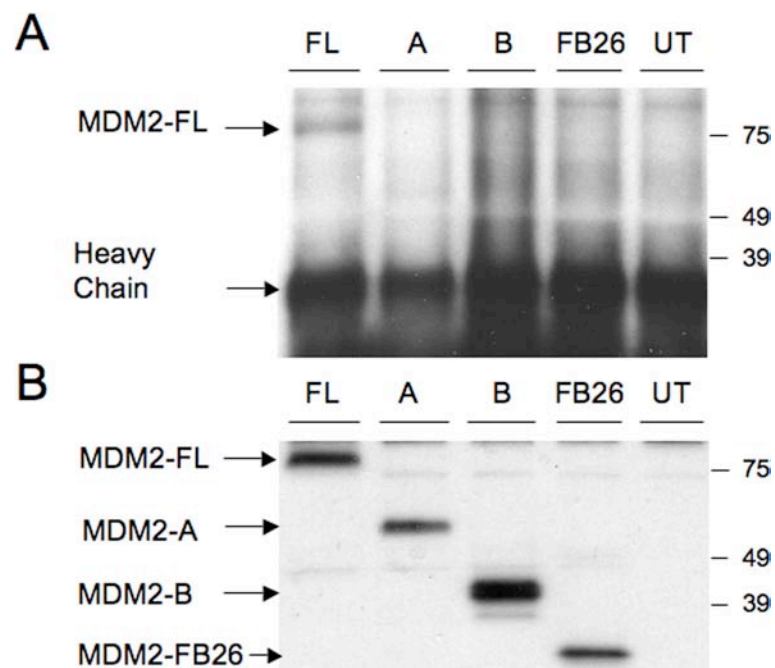


Figure 28

(A) Immunoprecipitation of MDM2 following retroviral transduction of ARF into TKO cells. An ARF specific antibody was used to immunoprecipitate p14^{ARF} protein. MDM2 antibody was used to visualize MDM2 proteins. Full-length MDM2 complexes with ARF. ARF binding to the MDM2 splice variants could not be detected. (B) MDM2 protein expression in the whole cell lysate before immunoprecipitation. FL- full-length MDM2; A- MDM2-A; B- MDM2-B; FB26- MDM2-FB26; UT- untreated and numbers represent the molecular weight markers (kDA-kilo Dalton).

5.10. Discussion

In this study, the cellular localization of human MDM2 splice variants was investigated in the presence and absence of potential binding partners; p53, p14^{ARF} and full-length MDM2. The splice variants and full-length MDM2 were expressed in knockout mouse embryonic fibroblasts (DKO, TKO) and all of the MDM2 proteins, including those that lacked the previously characterized NLS signal, localized predominately to the nucleus. At first, we proposed that the epitope tags V5 or MYC might have influenced the nuclear localization of the proteins. However, this possibility was discounted after showing that FB26 and full-length MDM2 could localize to the nucleus independent from the fusion tags expressed. Then, the mechanism by which the proteins localized to the nucleus was evaluated. Splice variants MDM2-A and B both lack the well-characterized NLS and NES (Figure 20) and yet they were detected predominantly in the nucleoplasm. These results suggested that MDM2-A and B may contain an alternative signal that mediated the nuclear localization of these proteins.

The small motif KXXK/R (lysine XX lysine/arginine) containing highly charged amino acids has been shown to mediate nuclear localization of several proteins including Lamin A, human C-MYC and SV40 large T¹²². This motif has been suggested to be the minimal feature required for a nuclear transport signal. This protein sequence was found three times within the RING finger region as ⁴⁶⁶KKLKRNK⁴⁷³ of MDM2^{14, 72, 119}. In order to test the hypothesis that the potential nuclear localization signal in the RING finger domain influenced nuclear localization of MDM2 and its splice variants, multiple mis-sense mutations were incorporated to disrupt all three possible transport motifs (NLS2) (Figure 23). The amino acid substitutions chosen were similar to mutations that had previously been introduced into the nuclear localization signal sequences of plant NPR1¹²³ and viral SV40 large T¹²² and were demonstrated to disrupt the ability of these proteins to localize to the nucleus. Two mutations were integrated into the original sequence of NLS2 (⁴⁶⁶KKLKRNK⁴⁷³) of MDM2-A and B changing lysine residues 469 and 470 into asparagine and glutamic acid, respectively (mutant sequence ⁴⁶⁶KKLNERNK⁴⁷³, Figure 23). However, this first set of mutations within the NLS2 did not interrupt the nucleoplasmic import of MDM2-A and B (Figure 24A). The mutants MDM2-A_{NLS2} and B_{NLS2} remained predominantly localized to the nucleoplasm with visible cytoplasmic staining in the same way as observed for the wild-type MDM2-A and B proteins (compare Figures 24A and 21, respectively). These data indicated that the amino acid changes in the three motifs ⁴⁶⁶KKLN⁴⁶⁹, ⁴⁶⁷KLNE⁴⁷⁰, or ⁴⁷⁰ERNK⁴⁷³ were not sufficient to disrupt the nuclear transport. Because the mutations within NLS2 of MDM2 were chosen so

that each of the three motifs would be mutated, it was not expected that the MDM2 proteins enter the nucleus. Therefore, it was proposed either that alternate regions of MDM2 protein were responsible for the nuclear localization or that the different lysine residues within the nuclear localization sequence of MDM2 are of different importance.

In support of the second hypothesis, the introduction of two additional mutations into MDM2-A_{NLS2} that changed lysine residues 466 and 467 to asparagine and glutamine, respectively (⁴⁶⁶NQLNERNK⁴⁷³) resulted in MDM2-A expression predominantly within the cytoplasm (Figure 24C). These data demonstrate that lysine 466 and lysine 467 are critical for nuclear localization of MDM2 proteins. This C-terminal NLS signal (NLS2) has previously been described, as a cryptic nucleolar localization signal that only becomes unmasked upon ARF binding to MDM2 facilitating nuclear entry¹¹⁹. This sequence has not previously been demonstrated to be a nuclear localization signal for full-length MDM2. However, we have demonstrated that NLS2 can also act as a NLS for full-length protein because when NLS1 is mutated, the full-length protein still enters the nucleus (Figure 24B).

Following mutation of NLS1 the localization of FB26 changed from being predominately nucleoplasmic to nucleolar, nucleoplasmic and faintly cytoplasmic (Figure 24A). FB26 contains seven novel amino acids at its C-terminus resulting from aberrant splicing and use of a different open reading frame (¹⁸⁹KEAKEKE¹⁹⁵). As described above, a minimal feature for a nuclear localization signal of various proteins is the amino acid sequence K-X-X-K/R¹²². This sequence can be found once in the out-of-frame region of FB26 (¹⁸⁹KEAK¹⁹²) and could be the reason for nuclear localization of mutant FB26_{NLS1}. The same motif might also be responsible for the observed nucleolar localization of FB26_{NLS1}. Comparison of nucleolar localization signals of proteins such as ARF^{60, 124}, HIV tat¹²⁵, and ribosomal proteins L5¹²⁶ and S6¹²⁷ suggested that the minimal feature for a nucleolar signal contains the following motif K/R-K/R-X-K/R¹²¹. However, this exact motif cannot be detected in the out-of-frame region of FB26 and therefore it is not clear whether it is responsible for the nucleolar localization of FB26_{NLS1}.

Another possible explanation for why FB26_{NLS1} localizes to the nucleoli of TKO cells might be that this out-of-frame region exerts a novel function. For example, this region could be a binding domain for an unknown protein that sequesters FB26 in the nucleoli. Because splice variant MDM2-FB26 is very rare and to date has only been detected in a single rhabdomyosarcoma tumor⁷⁵, the mechanism for nuclear and nucleolar localization of this protein was not pursued any further.

Our data were different compared to two previously published studies that evaluated cellular localization of MDM2 splice variants and truncated MDM2 proteins^{97, 119}. Data from one of those studies⁹⁷ showed predominately cytoplasmic expression of HDM2-ALT1 (human MDM2-B) in p53/MDM2 null mouse fibroblasts (DKO). In addition, truncated MDM2 isoforms, which lacked amino acids Δ 150-230 including the nuclear localization signal, were expressed only in the cytoplasm in U2OS cells (p14^{Arf}-/-)¹¹⁹. However, our data are in agreement with two other studies that evaluated MDM2 splice variants and MDM2 deletion mutants^{14, 118}. In one study¹¹⁸, an EGFP-MDM2-B fusion protein localized to the nucleus in human HEK293 cells. In addition, the deletion mutant MDM2- Δ 491-154 that does not contain NLS1 expressed predominantly in the nucleus of NIH3T3 cells¹⁴. A potential reason for the differences could be that expression of MDM2 proteins is influenced by the different cellular backgrounds in which these investigations have been carried out. However, a second reason for the observed differences could be that the different MDM2 proteins evaluated vary in their deleted domains and therefore may have lost the ability to bind to other proteins that could influence cellular localization.

However, the different results observed for MDM2-B in the present study and MDM2-ALT1 (MDM2-B) in the study by Evans *et al.* (2001)⁹⁷ are not easy to explain. In both cases, the splice variant was expressed in p53/MDM2 null mouse embryonic fibroblasts (DKO). However, in the present study MDM2-B predominantly expressed in the nucleoplasm whereas in contrast, in the study by Evans *et al.* (2001), MDM2-ALT1 primarily localized within the cytoplasm of DKO cells. One potential difference between the two studies is that the cells used differed in their passage number or in their clonal origin. These factors may influence the cellular localization of MDM2-B because they might change the characteristics of each cell line in culture. Also, the plasmid constructs used to express MDM2-B in both studies were not identical. In our study, MDM2-B was expressed with an V5 epitope tag and in the study by Evans *et al.* (2001), it appears that a CMV-His-MDM2-ALT1 plasmid construct was used. Therefore, different fusion tags used to express the same protein might be the cause for the observed differences in the cellular expression of MDM2-B. However, these suggestions are speculative and additional work would be required to determine the exact reasons for the differences.

To evaluate whether the cellular localization of MDM2 splice variants was influenced by p53, p14^{ARF} and full-length MDM2, each of these proteins was co-expressed with individual MDM2 splice variants in mutant MEFs (p53^{-/-}, MDM2^{-/-}, ARF^{-/-} TKO). In a

previously published report⁹⁷, MDM2 splice variants with an intact C-terminal RING finger domain such as MDM2-B, bound full-length MDM2 and sequestered it in the cytoplasm⁹⁷. However, we have not observed a predominantly cytoplasmic localization for any of the splice variants evaluated in our study, and co-expression of the three variants analyzed was observed together with full-length MDM2 in the nucleus (Figure 25). We have confirmed that MDM2-A can interact with full-length MDM2 through its RING finger domain (refer to Section 4.7) and therefore it appears that full-length MDM2 and the splice variants can interact through their RING finger domains without being exported to the cytoplasm. This hypothesis is supported by a previous study that showed that the interaction of full-length MDM2 with its splice variants occurs independent of the cellular compartment⁹⁸. Therefore, it was concluded that nuclear export is not necessary for the interaction of full-length MDM2 with MDM2-A and B, or for the activation of p53.

The p53 tumor suppressor protein was visualized in the nucleus as expected^{128, 129}, and co-localized with the MDM2 splice variants in the nucleoplasm (Figure 26). Full-length MDM2 has been shown to export p53 from the nucleus to the cytoplasm resulting in p53 proteasomal degradation⁶¹, however, the majority of MDM2 splice variants remains nucleoplasmic. Because the splice variant FB26 contains the p53-binding site, co-localization of this protein with p53 could be indicative of protein binding. However, MDM2 A and B both lack the p53 binding domain, and therefore co-expression of MDM2 A and B with p53 in the nucleus is independent of their binding to one another.

To determine whether p14^{ARF} influences the cellular localization of MDM2 splice variants, p14^{ARF} was expressed in the MEFs using a retroviral vector. p14^{ARF} as well as its murine equivalent p19^{ARF} have been shown to localize to the nucleolus independent of either p53 or MDM2 expression^{60, 61}. However, upon elevated levels of ARF expression, for example by oncogenic activation, ARF mediates the translocation of full-length MDM2 to the nucleolus, thereby releasing control of p53⁶⁰. In this manner cells are protected from oncogene-induced transformation by induction of p53-mediated apoptosis. Therefore, the question remained whether p14^{ARF} could bind and transfer MDM2 splice variants into the nucleolus?

MDM2-A, B and FB26 were expressed within the nucleoplasm and this did not change upon ARF expression. Of the three splice variants analyzed; MDM2-A was the only one that contains the central highly acidic domain to which ARF has been shown to bind (amino acids 210-304) and so MDM2-A would be predicted to bind and co-localize with ARF in the nucleoli. However, immunoprecipitation analysis revealed that even though MDM2-A

contained the ARF binding site it could not bind to the ARF protein, thus explaining the maintenance of its predominantly nucleoplasmic cellular localization upon ARF expression. MDM2-B and FB26 both lack the complete central acidic domain (amino acids 222-300 and 222-437, respectively) and these proteins also remained nucleoplasmic upon ARF expression, as expected.

In summary, all MDM2 splice variants evaluated predominantly localized to the nucleus in mouse embryonic fibroblasts. This mechanism appears to involve two nuclear localization signals within the protein. Even though the localization of the splice variants was not altered by the expression of full-length MDM2 or p53, their co-localization within the cell is probably important for their function. MDM2-A and B co-localization with full-length MDM2 in the nucleoplasm would allow their binding and subsequent activation of p53. FB26 does not contain the C-terminal RING finger domain but does contain the p53-binding site, which would facilitate its binding to p53 protein in the nucleoplasm. Like full-length MDM2, FB26 would be predicted to inactivate p53 protein, although this hypothesis was not tested. It was interesting that MDM2-A that contained the ARF-binding site did not bind ARF protein and localize to the nucleoli. However, maintenance of MDM2-A in the nucleoplasm would allow its binding to full-length MDM2 and subsequent activation of p53 as confirmed in Section 4.7.

6. Summary

6.1. English Summary

MDM2 has been characterized as an oncogene because transforming activities have been observed upon *MDM2* overexpression². In addition, more than 40 potentially oncogenic *MDM2* splice variants have been detected in a variety of human tumor types. The majority of *MDM2* splice variants lacks part of the N-terminal region including the p53-binding domain, the nuclear localization and export signal. Therefore, the main goal of this report was to evaluate the function of *MDM2* splice variants *in vivo* and *in vitro*. This study was divided into two projects:

Project 1. *MDM2-A* is one of the most commonly found *MDM2* splice variants in human tumors; therefore an *Mdm2-a* transgenic mouse model was generated to evaluate the function of *MDM2-A* *in vivo* and *in vitro*.

Murine *Mdm2-a* cDNA was created based on the human *MDM2-A* homolog, which lacks exons 4-9 of the full-length *MDM2* sequence. Expression of the transgene was under the control of the β -actin promoter and CMV enhancer to allow ubiquitous expression in all tissues. However, multiple rounds of microinjection of the *Mdm2-a* transgene resulted in a low transgenic founder rate (5%) suggesting that *MDM2-A* expression might be lethal for mouse development. Surprisingly, three of the four transgenic founder mice contained unique mis-sense mutations within their *Mdm2-a* sequences even though no mutations could be detected within the *Mdm2-a* transgenic plasmid. Evaluation of DNA from multiple organs of the mice revealed that mutant *Mdm2-a* sequence was present in each tissue. For the mutant *Mdm2-a* sequence to be present in different cell types the transgene must have integrated into the genome of a one-cell stage embryo before replication. Therefore, it is likely that the DNA used for the generation of the transgenic mice contained a small population of mutant *Mdm2-a* copies that were initially injected into the embryo, but could not be detected. Nevertheless, expression of wild-type *MDM2-A* was selected against during embryonic development. These data are supported by the fact that the ratio of wild-type *Mdm2-a* to mutant *Mdm2-a* transgenic embryos decreased *in utero* suggesting that *MDM2-A* expression was lethal during mouse development.

Consistent with these findings, expression of *MDM2-A* mediated growth inhibition of mouse embryonic fibroblast *in vitro* in a p53 and p21^{Waf1/Cip1} dependent manner. Immunoprecipitation data determined that *MDM2-A* bound full-length *MDM2* through its

RING finger domain and as a consequence p53 activity was elevated resulting in growth arrest. In contrast, mutant MDM2-A proteins have lost their growth inhibitory activity. Mutations within the RING finger domains of the mutant MDM2-A proteins interfered with the binding to full-length MDM2 resulting in appropriate regulation of p53 activity by full-length MDM2.

Despite the growth inhibitory activity of MDM2-A, one wild-type *Mdm2-a* transgenic mouse line was generated. MDM2-A protein was expressed in only a few tissues suggesting that these cell types might tolerate enhanced p53 function.

The evaluation of sick and moribund mice revealed no transforming phenotype for either wild-type or the mutant *Mdm2-a* transgenic mice. Interestingly, a reduced survival was observed for the wild-type *Mdm2-a* transgenic mice compared to wild-type littermates. This shortened life span was not observed for transgenic mice of the mutant *Mdm2-a* mouse lines suggesting that the elevated p53 activity in the tissues of the wild-type *Mdm2-a* transgenic mice was the reason for the reduced longevity. In summary, MDM2 splice variants with an intact RING finger domain inhibit growth *in vitro* and reduce the life-span of mice when expressed *in vivo*.

Project 2. This project focused on the cellular localization of MDM2 splice variants, and whether the lack of different protein domains interfered with cellular transport of these variants. In addition, this project evaluated the co-expression of MDM2 splice variants with known binding partners.

The majority of MDM2 splice variants has lost the N-terminal region of the protein that includes domains such as the p53 binding domain, the nuclear localization signal (NLS1) and the nuclear export signal (NES). In contrast, other splice variants have lost the C-terminal region including the RING finger domain containing a second potential nuclear localization signal (NLS2). Full-length MDM2 and splice variants MDM2-A, B (without NLS1) and FB26 (without NLS2) were expressed with fusion tags *in vitro* in mouse embryonic fibroblasts; the MDM2 splice variants and full-length MDM2 localized predominately within the nucleoplasm. In addition, MDM2-A and B were faintly expressed within the cytoplasm. Because some previously published reports proposed that the loss of NLS1 resulted in predominantly cytoplasmic expression of MDM2 proteins. The initial thought was that the fusion tags might have facilitated the nuclear sequestration of the different MDM2 proteins. However, MDM2-FB26 and full-length MDM2 expression both with and without fusion tags had identical cellular localization demonstrating that nucleoplasmic expression of the splice

variants was not dependent upon the fusion tag. Site directed mutagenesis of the C-terminal NLS2 sequence resulted in MDM2-A protein re-localizing to the cytoplasm. These data demonstrated the importance of the second less-well characterized NLS2 sequence, and further supported the conclusion that the epitope tag had not mediated the nucleoplasmic localization of the MDM2 splice variants.

Additional experiments were carried out to determine whether cellular localization of the MDM2 splice variants was affected by co-expression of full-length MDM2, p53 and p14^{ARF}. Full-length MDM2 and p53 predominantly localized to the nucleus as expected, and therefore they co localized with the MDM2 splice variants. Because MDM2 splice variants with an intact C-terminal RING finger domain such as MDM2-A and B can bind full-length MDM2, their co-expression in the nucleoplasm likely facilitated their interaction. In addition, even though FB26 does not contain a C-terminal RING finger, it does contain an intact p53-binding domain that probably bound and inactivated nuclear p53 expressed in MEFs.

ARF expression was predominantly nucleolar, but ARF expression did not influence the nucleoplasmic localization of the MDM2 splice variants. It was predicted that MDM2A, with an intact ARF binding site may have bound and co-localized with ARF. However, *in vitro* immunoprecipitation experiments could not demonstrate binding of these two proteins, which likely explains why they did not co-localize within the cell. In summary, MDM2 splice variants localize predominantly in the nucleus mediated by one of two nuclear localization signals. Co-localization of MDM2 splice variants with full-length MDM2 and p53 in the nucleoplasm is important for their ability to bind full-length MDM2 and activate the p53 pathway.

The majority of MDM2 splice variants has been detected in human tumors. However, studies evaluating their function are contradictory because both transforming^{78,79} and growth inhibitory activities⁹⁸ have been observed. It appears that the function of MDM2 splice variants is dependent upon the cellular background in which they are expressed. It is therefore possible that MDM2 splice variants may contribute to the development of tumors in one tissue but may not have an effect in another. The growth inhibitory activity that has been observed for MDM2-A with an intact C-terminal RING finger domain suggests that MDM2-A and similar splice variants may not be involved in tumorigenesis but arise as a consequence of a defective splicing machinery within a transformed cell⁹⁰.

The detection of specific *MDM2* splice variants in tumors could be a significant diagnostic marker for treatment and therapy of patients with cancer. For example, tumors with

functional p53 that express splice variants such as MDM2-A could be more sensitive to chemotherapy because of a higher p53 activity. Furthermore, splice variants with growth promoting activities might be a useful target for future cancer therapies.

6.2. Deutsche Zusammenfassung

Das Onkogen *MDM2* kodiert für ein Phosphoprotein, welches an maligner Transformation beteiligt ist ². Mehr als 40 *MDM2* Spleißvarianten wurden in verschiedenen Tumoren des Menschen identifiziert. Das Hauptziel dieser Arbeit war es deshalb die Funktionen von *MDM2* Spleißvarianten *in vivo* und *in vitro* zu untersuchen. Die vorliegende Studie wurde in zwei Projekte unterteilt:

Projekt 1. *MDM2-A* ist eine der am meist detektierten *MDM2* Spleißvarianten in menschlichen Tumoren. Deshalb wurde in der vorliegenden Arbeit ein *Mdm2-a* transgenes Maus Modell entwickelt, um die Funktion und Aufgabe von *MDM2-A* *in vivo* und *in vitro* zu untersuchen.

Die *Mdm2-a* cDNA wurde anhand der menschlichen *MDM2-A* mRNA entwickelt, welcher im Vergleich zum vollständigen *MDM2* mRNA Transkript (full-length *MDM2*) die Exone 4 bis 9 fehlen. Das *MDM2-A* Protein wurde mit Hilfe des β -Actin Promoters und des CMV Enhancers exprimiert, um die Expression in allen Geweben zu ermöglichen. Nach mehreren Mikroinjektionen der Transgen DNA in Mausembryonen, wurde nur eine geringe Anzahl von *Mdm2-a* transgenen Mäusen (5%, 4/75) detektiert. Deshalb wurde angenommen, dass die Expression von *MDM2-A* Protein letal für die Entwicklung der Maus ist. Überraschend war auch, dass drei der vier transgenen Mäuse mis-sense Mutationen in der *Mdm2-a* DNA Sequenz aufwiesen, obwohl keine Mutationen im *Mdm2-a* Transgen Plasmid detektiert werden konnten. DNA Sequenzierungen mehrerer Organe der transgenen Mäuse ergab, dass die Mutationen in jedem Zellgewebe vorhanden waren. Das ist nur möglich, wenn ein mutiertes Transgen in das Genom eines einzelligen Embryonen integriert wurde, bevor DNA Replikation einsetzen konnte. Es wird daher postuliert, dass die DNA für die Herstellung der transgenen Mäuse eine sehr geringe Anzahl mutierter *Mdm2-a* DNA Kopien enthielt, und diese mit Wildtyp *Mdm2-a* Kopien in die Embryonen injiziert wurde. Da drei von vier transgenen Mäuse eine mutierte *Mdm2-a* Sequenz aufwiesen, spricht alles für eine Selektion gegen die Expression des Wildtyp *MDM2-A* Proteins. Diese Tatsache wird auch

dadurch unterstützt, dass sich die Rate von Wildtyp *Mdm2-a* zu mutierten *Mdm2-a* transgenen Embryonen während der embryonalen Entwicklung der Mäuse verringerte.

In Zellkulturexperimenten konnte gezeigt werden, dass die Expression von MDM2-A das Wachstum von embryonalen Maus-Fibroblasten (MEFs) hemmt, wobei diese Wachstumsinhibierung dabei von dem Tumor Suppressor p53 und dem Kinase Hemmer p21^{Waf1/Cip1} abhängig ist. Immunopräzipitation von MDM2-A Proteinen ergab, dass MDM2-A mit Hilfe der RING Finger Domäne an full-length MDM2 binden kann, dadurch wird p53 aktiviert, und das Wachstum der Fibroblasten verhindert. Im Vergleich dazu, haben die mutierten MDM2-A Proteine die Fähigkeit der Wachstumsinhibierung verloren. Die Mutationen in den MDM2-A Mutanten wurden in der RING Finger Domäne detektiert und verhindern deshalb eine Bindung zwischen MDM2-A und full-length MDM2.

Trotz der wachstumsinhibierende Aktivität des MDM2-A Proteins konnte eine einzige Wildtyp *Mdm2-a* transgene Mauslinie erzeugt werden. Diese Mauslinie exprimiert das MDM2-A Protein nur in bestimmten Organen. Darum wurde vermutet, dass verschiedenen Zelltypen eine erhöhte p53 Aktivität tolerieren können.

Bei der Untersuchung erkrankter oder toter Mäuse, konnte weder für Wildtyp *Mdm2-a* noch für die mutierten *Mdm2-a* transgenen Mauslinien ein transformierender Phänotyp festgestellt werden. Interessant war aber, dass Wildtyp *Mdm2-a* Mäuse im Vergleich zu nicht transgenen Geschwistermäusen eine verkürzte Lebenserwartung hatten. Der Grund dafür könnte die erhöhte p53 Aktivität sein. Zusammenfassend lässt sich sagen, dass MDM2 Spleißvarianten mit einer intakten RING Finger Domäne das Wachstum von Zellen in der Kultur verhindern können. Außerdem kann die Expression dieser Spleißvarianten tödlich für die Entwicklung von Mäusen sein.

Projekt 2. In diesem Teil der vorliegenden Arbeit sollte die zelluläre Lokalisation von verschiedenen MDM2 Spleißvarianten untersucht werden. Es wurde geprüft, ob der Verlust von Proteindomänen die Proteinverteilung in einer Zelle stören kann. Des Weiteren wurde die Koexpression von MDM2 Spleißvarianten mit bekannten Bindungsproteinen untersucht.

Den meisten MDM2 Spleißvarianten fehlt die N-terminale Proteinregion, welche aus einer p53-Bindedomäne, einem Kernlokalisierungssignal (NLS1) und einem Kernexportsignal (NES) besteht. Anderen Spleißvarianten fehlt die C-terminale Proteinregion, welche aus einer RING-Finger-Domäne und einem zweiten Kernlokalisierungssignal (NLS2) aufgebaut ist. Full-length MDM2 und MDM2-A, B (ohne NLS1) und FB26 (ohne NLS2) wurden als Epitop-Fusionsproteine in MEFs (p53/MDM2/ARF null) exprimiert. Die Spleißvarianten

und full-length MDM2 waren im Plasma des Zellkerns detektierbar. Zusätzlich lokalisierten MDM2-A und B auch im Zytoplasma. Zu erst wurde vermutet, dass das Fusions-epitop für die nukleare Verteilung der MDM2 Proteine verantwortlich war, weil in früheren Studien ^{97, 119} der Verlust von NLS1 zu einer zytoplasmatischen Verteilung führte. Weiter Versuche zeigten jedoch, das MDM2-FB26 und full-length MDM2 im Kernplasma lokalisieren, unabhängig davon, ob die Proteine mit und ohne Fusionsmarkierung exprimiert wurden. Gezielte Mutagenese der C-terminalen NLS2 Sequenz führte dazu, das MDM2-A ausschließlich in das Zytoplasma lokalisierte. Diese Ergebnisse zeigen, dass NLS2 wichtig für die zelluläre Lokalisation ist, und dass das Fusions-epitop keinen störenden Einfluss auf die zelluläre Verteilung der MDM2 Proteinen hatte.

In weiteren Experimenten wurde bestimmt, welchen Einfluss Koexpression von full-length MDM2, p53 und p14^{ARF} auf die zelluläre Lokalisation der Spleißvarianten hatte. Full-length MDM2 und p53 wurden ausschließlich im Kernplasma detektiert und co-lokalisierten mit A, B und FB26. MDM2 Spleißvarianten mit einer intakten RING-Finger-Domäne, wie z.B. MDM2-A und B, können mit full-length MDM2 binden ⁹⁸. MDM2-A und B lagen zusammen mit full-length MDM2 im Plasma des Zellkerns vor und machen eine Protein-Protein-Interaktion sehr wahrscheinlich. Im Unterschied dazu, besitzt MDM2-FB26 die RING-Finger-Domäne nicht sondern nur die p53-Bindedomäne und könnte somit p53 binden und dessen Aktivität in den Fibroblasten inaktivieren.

p14^{ARF} war ausschließlich in den Nukleoli verteilt und beeinflusste die Lokalisation der MDM2 Spleißvarianten nicht. Weil MDM2-A die ARF-Bindedomäne besitzt, wurde vermutet, dass MDM2-A an ARF bindet und mit ARF in den Nukleoli lokalisiert. Aber in Immunopräzipitationsversuchen wurde keine ARF/MDM2-A Bindung nachgewiesen. Das ist auch der Grund warum beide Proteine nicht zusammen in den Nukleoli detektiert wurden. Zusammenfassend lässt sich sagen, dass MDM2 Spleißvarianten ausschließlich im Zellkern lokalisieren und dass diese zelluläre Verteilung von einem der zwei Kernlokalisierungssignale vermittelt wird. Die Kolokalisation der Spleißvarianten mit full-length MDM2 und p53 könnte dazu führen, dass full-length MDM2 negativ inhibiert und p53 aktivieren wird.

Die Mehrheit der MDM2 Spleißvarianten wurde in Tumorgewebe entdeckt. Trotzdem sind Angaben über deren Funktion sehr widersprüchlich, da transformierende ^{78, 79} und wachstumshemmende ⁹⁸ Funktionen beschrieben sind. Es ist sehr wahrscheinlich, dass die Funktion der MDM2 Spleißvarianten davon abhängt in welchem zellulären Hintergrund

sie exprimiert werden. Zum Beispiel, können Spleißvarianten in einem speziellen Gewebe mit ihren Bindungspartnern interagieren. In einem Zelltypen, der diese Bindungsproteine nicht exprimiert, hätten diese MDM2 Spleißvarianten keine Funktion. Die Schlussfolgerung ist, dass MDM2 Spleißvarianten sehr wohl zur Bildung von malignen Tumoren in einem sensitiven Zelltyp beitragen könnten. Auf der anderen Seite werden einige der MDM2 Spleißvarianten auf Grund eines defekten Spleißmechanismus in einer transformierten Zelle exprimiert.

Das Vorhandensein von MDM2 Spleißvarianten könnte ein wichtiger diagnostischer Marker für die Behandlung und Therapie von Tumorpatienten sein. Zum Beispiel könnten Tumore, die p53 und MDM2-A zusammen exprimieren sensitiver auf die Behandlung mit Chemotherapeutischen Medikamenten reagieren, da p53 stärker aktiviert würde. MDM2 Spleißvarianten mit wachstumsanregenden Funktionen könnten ein Ziel für zukünftige Krebstherapien sein.

7. References

1. Cahilly-Snyder, L., Yang-Feng, T., Francke, U. & George, D. L. Molecular analysis and chromosomal mapping of amplified genes isolated from a transformed mouse 3T3 cell line. *Somat Cell Mol Genet* 13, 235-44 (1987).
2. Fakharzadeh, S. S., Trusko, S. P. & George, D. L. Tumorigenic potential associated with enhanced expression of a gene that is amplified in a mouse tumor cell line. *Embo J* 10, 1565-9 (1991).
3. Oliner, J. D., Kinzler, K. W., Meltzer, P. S., George, D. L. & Vogelstein, B. Amplification of a gene encoding a p53-associated protein in human sarcomas. *Nature* 358, 80-3 (1992).
4. Ladanyi, M. et al. MDM2 gene amplification in metastatic osteosarcoma. *Cancer Res* 53, 16-8 (1993).
5. Corvi, R. et al. Non-syntenic amplification of MDM2 and MYCN in human neuroblastoma. *Oncogene* 10, 1081-6 (1995).
6. Reifenberger, G., Liu, L., Ichimura, K., Schmidt, E. E. & Collins, V. P. Amplification and overexpression of the MDM2 gene in a subset of human malignant gliomas without p53 mutations. *Cancer Res* 53, 2736-9 (1993).
7. Marechal, V. et al. Conservation of structural domains and biochemical activities of the MDM2 protein from *Xenopus laevis*. *Oncogene* 14, 1427-33 (1997).
8. Piette, J., Neel, H. & Marechal, V. Mdm2: keeping p53 under control. *Oncogene* 15, 1001-10 (1997).
9. Leng, P., Brown, D. R., Shivakumar, C. V., Deb, S. & Deb, S. P. N-terminal 130 amino acids of MDM2 are sufficient to inhibit p53-mediated transcriptional activation. *Oncogene* 10, 1275-82 (1995).
10. Chen, J., Marechal, V. & Levine, A. J. Mapping of the p53 and mdm-2 interaction domains. *Mol Cell Biol* 13, 4107-14 (1993).
11. Roth, J., Dobbelstein, M., Freedman, D. A., Shenk, T. & Levine, A. J. Nucleocytoplasmic shuttling of the hdm2 oncoprotein regulates the levels of the p53 protein via a pathway used by the human immunodeficiency virus rev protein. *Embo J* 17, 554-64 (1998).
12. Argentini, M., Barboule, N. & Wasylyk, B. The contribution of the acidic domain of MDM2 to p53 and MDM2 stability. *Oncogene* 20, 1267-75 (2001).
13. Boddy, M. N., Freemont, P. S. & Borden, K. L. The p53-associated protein MDM2 contains a newly characterized zinc-binding domain called the RING finger. *Trends Biochem Sci* 19, 198-9 (1994).

14. Brown, D. R., Thomas, C. A. & Deb, S. P. The human oncoprotein MDM2 arrests the cell cycle: elimination of its cell-cycle-inhibitory function induces tumorigenesis. *Embo J* 17, 2513-25 (1998).
15. Barak, Y., Gottlieb, E., Juven-Gershon, T. & Oren, M. Regulation of mdm2 expression by p53: alternative promoters produce transcripts with nonidentical translation potential. *Genes Dev* 8, 1739-49 (1994).
16. Landers, J. E., Cassel, S. L. & George, D. L. Translational enhancement of mdm2 oncogene expression in human tumor cells containing a stabilized wild-type p53 protein. *Cancer Res* 57, 3562-8 (1997).
17. Mendrysa, S. M. & Perry, M. E. The p53 tumor suppressor protein does not regulate expression of its own inhibitor, MDM2, except under conditions of stress. *Mol Cell Biol* 20, 2023-30 (2000).
18. Lin, D., Shields, M. T., Ullrich, S. J., Appella, E. & Mercer, W. E. Growth arrest induced by wild-type p53 protein blocks cells prior to or near the restriction point in late G1 phase. *Proc Natl Acad Sci U S A* 89, 9210-4 (1992).
19. Shaw, P. et al. Induction of apoptosis by wild-type p53 in a human colon tumor-derived cell line. *Proc Natl Acad Sci U S A* 89, 4495-9 (1992).
20. Chen, J., Wu, X., Lin, J. & Levine, A. J. mdm-2 inhibits the G1 arrest and apoptosis functions of the p53 tumor suppressor protein. *Mol Cell Biol* 16, 2445-52 (1996).
21. Meek, D. W. & Knippschild, U. Posttranslational modification of MDM2. *Mol Cancer Res* 1, 1017-26 (2003).
22. Honda, R., Tanaka, H. & Yasuda, H. Oncoprotein MDM2 is a ubiquitin ligase E3 for tumor suppressor p53. *FEBS Lett* 420, 25-7 (1997).
23. Fang, S., Jensen, J. P., Ludwig, R. L., Vousden, K. H. & Weissman, A. M. Mdm2 is a RING finger-dependent ubiquitin protein ligase for itself and p53. *J Biol Chem* 275, 8945-51 (2000).
24. Buschmann, T., Lerner, D., Lee, C. G. & Ronai, Z. The Mdm-2 amino terminus is required for Mdm2 binding and SUMO-1 conjugation by the E2 SUMO-1 conjugating enzyme Ubc9. *J Biol Chem* 276, 40389-95 (2001).
25. Miyauchi, Y., Yogosawa, S., Honda, R., Nishida, T. & Yasuda, H. Sumoylation of Mdm2 by protein inhibitor of activated STAT (PIAS) and RanBP2 enzymes. *J Biol Chem* 277, 50131-6 (2002).
26. Xirodimas, D. P., Chisholm, J., Desterro, J. M., Lane, D. P. & Hay, R. T. P14ARF promotes accumulation of SUMO-1 conjugated (H)Mdm2. *FEBS Lett* 528, 207-11 (2002).

27. Hay, T. J. & Meek, D. W. Multiple sites of *in vivo* phosphorylation in the MDM2 oncoprotein cluster within two important functional domains. *FEBS Lett* 478, 183-6 (2000).
28. Mayo, L. D., Turchi, J. J. & Berberich, S. J. Mdm-2 phosphorylation by DNA-dependent protein kinase prevents interaction with p53. *Cancer Res* 57, 5013-6 (1997).
29. Khosravi, R. et al. Rapid ATM-dependent phosphorylation of MDM2 precedes p53 accumulation in response to DNA damage. *Proc Natl Acad Sci U S A* 96, 14973-7 (1999).
30. Maya, R. et al. ATM-dependent phosphorylation of Mdm2 on serine 395: role in p53 activation by DNA damage. *Genes Dev* 15, 1067-77 (2001).
31. Sionov, R. V. et al. c-Abl regulates p53 levels under normal and stress conditions by preventing its nuclear export and ubiquitination. *Mol Cell Biol* 21, 5869-78 (2001).
32. Sionov, R. V. et al. c-Abl neutralizes the inhibitory effect of Mdm2 on p53. *J Biol Chem* 274, 8371-4 (1999).
33. Goldberg, Z. et al. Tyrosine phosphorylation of Mdm2 by c-Abl: implications for p53 regulation. *Embo J* 21, 3715-27 (2002).
34. Zhang, T. & Prives, C. Cyclin a-CDK phosphorylation regulates MDM2 protein interactions. *J Biol Chem* 276, 29702-10 (2001).
35. Zhou, B. P. et al. HER-2/neu induces p53 ubiquitination via Akt-mediated MDM2 phosphorylation. *Nat Cell Biol* 3, 973-82 (2001).
36. Mayo, L. D. & Donner, D. B. A phosphatidylinositol 3-kinase/Akt pathway promotes translocation of Mdm2 from the cytoplasm to the nucleus. *Proc Natl Acad Sci U S A* 98, 11598-603 (2001).
37. Graeber, T. G. et al. Hypoxia-mediated selection of cells with diminished apoptotic potential in solid tumours. *Nature* 379, 88-91 (1996).
38. Linke, S. P., Clarkin, K. C., Di Leonardo, A., Tsou, A. & Wahl, G. M. A reversible, p53-dependent G0/G1 cell cycle arrest induced by ribonucleotide depletion in the absence of detectable DNA damage. *Genes Dev* 10, 934-47 (1996).
39. Kastan, M. B., Onyekwere, O., Sidransky, D., Vogelstein, B. & Craig, R. W. Participation of p53 protein in the cellular response to DNA damage. *Cancer Res* 51, 6304-11 (1991).
40. Harris, S. L. & Levine, A. J. The p53 pathway: positive and negative feedback loops. *Oncogene* 24, 2899-908 (2005).
41. Sugrue, M. M., Shin, D. Y., Lee, S. W. & Aaronson, S. A. Wild-type p53 triggers a rapid senescence program in human tumor cells lacking functional p53. *Proc Natl Acad Sci U S A* 94, 9648-53 (1997).

42. Hollstein, M., Sidransky, D., Vogelstein, B. & Harris, C. C. p53 mutations in human cancers. *Science* 253, 49-53 (1991).
43. Malkin, D. et al. Germ line p53 mutations in a familial syndrome of breast cancer, sarcomas, and other neoplasms. *Science* 250, 1233-8 (1990).
44. Srivastava, S., Zou, Z. Q., Pirollo, K., Blattner, W. & Chang, E. H. Germ-line transmission of a mutated p53 gene in a cancer-prone family with Li-Fraumeni syndrome. *Nature* 348, 747-9 (1990).
45. Li, F. P. & Fraumeni, J. F., Jr. Soft-tissue sarcomas, breast cancer, and other neoplasms. A familial syndrome? *Ann Intern Med* 71, 747-52 (1969).
46. Bartel, F., Taubert, H. & Harris, L. C. Alternative and aberrant splicing of MDM2 mRNA in human cancer. *Cancer Cell* 2, 9-15 (2002).
47. Barak, Y., Juven, T., Haffner, R. & Oren, M. mdm2 expression is induced by wild type p53 activity. *Embo J* 12, 461-8 (1993).
48. Wu, X., Bayle, J. H., Olson, D. & Levine, A. J. The p53-mdm-2 autoregulatory feedback loop. *Genes Dev* 7, 1126-32 (1993).
49. Kussie, P. H. et al. Structure of the MDM2 oncoprotein bound to the p53 tumor suppressor transactivation domain. *Science* 274, 948-53 (1996).
50. Oliner, J. D. et al. Oncoprotein MDM2 conceals the activation domain of tumour suppressor p53. *Nature* 362, 857-60 (1993).
51. Li, M. et al. Mono- versus polyubiquitination: differential control of p53 fate by Mdm2. *Science* 302, 1972-5 (2003).
52. Zhu, Q., Yao, J., Wani, G., Wani, M. A. & Wani, A. A. Mdm2 mutant defective in binding p300 promotes ubiquitination but not degradation of p53: evidence for the role of p300 in integrating ubiquitination and proteolysis. *J Biol Chem* 276, 29695-701 (2001).
53. Jones, S. N., Roe, A. E., Donehower, L. A. & Bradley, A. Rescue of embryonic lethality in Mdm2-deficient mice by absence of p53. *Nature* 378, 206-8 (1995).
54. Montes de Oca Luna, R., Wagner, D. S. & Lozano, G. Rescue of early embryonic lethality in mdm2-deficient mice by deletion of p53. *Nature* 378, 203-6 (1995).
55. Donehower, L. A. et al. Mice deficient for p53 are developmentally normal but susceptible to spontaneous tumours. *Nature* 356, 215-21 (1992).
56. Jones, S. N. et al. The tumorigenic potential and cell growth characteristics of p53-deficient cells are equivalent in the presence or absence of Mdm2. *Proc Natl Acad Sci U S A* 93, 14106-11 (1996).

57. McDonnell, T. J. et al. Loss of one but not two mdm2 null alleles alters the tumour spectrum in p53 null mice. *J Pathol* 188, 322-8 (1999).
58. Momand, J., Wu, H. H. & Dasgupta, G. MDM2--master regulator of the p53 tumor suppressor protein. *Gene* 242, 15-29 (2000).
59. Chin, L., Pomerantz, J. & DePinho, R. A. The INK4a/ARF tumor suppressor: one gene--two products--two pathways. *Trends Biochem Sci* 23, 291-6 (1998).
60. Weber, J. D., Taylor, L. J., Roussel, M. F., Sherr, C. J. & Bar-Sagi, D. Nucleolar Arf sequesters Mdm2 and activates p53. *Nat Cell Biol* 1, 20-6 (1999).
61. Tao, W. & Levine, A. J. P19(ARF) stabilizes p53 by blocking nucleo-cytoplasmic shuttling of Mdm2. *Proc Natl Acad Sci U S A* 96, 6937-41 (1999).
62. Tanimura, S. et al. MDM2 interacts with MDMX through their RING finger domains. *FEBS Lett* 447, 5-9 (1999).
63. Badciong, J. C. & Haas, A. L. MdmX is a RING finger ubiquitin ligase capable of synergistically enhancing Mdm2 ubiquitination. *J Biol Chem* 277, 49668-75 (2002).
64. Sharp, D. A., Kratowicz, S. A., Sank, M. J. & George, D. L. Stabilization of the MDM2 oncoprotein by interaction with the structurally related MDMX protein. *J Biol Chem* 274, 38189-96 (1999).
65. Linares, L. K., Hengstermann, A., Ciechanover, A., Muller, S. & Scheffner, M. HdmX stimulates Hdm2-mediated ubiquitination and degradation of p53. *Proc Natl Acad Sci U S A* 100, 12009-14 (2003).
66. Daujat, S., Neel, H. & Piette, J. MDM2: life without p53. *Trends Genet* 17, 459-64 (2001).
67. Ganguli, G. & Wasylyk, B. p53-independent functions of MDM2. *Mol Cancer Res* 1, 1027-35 (2003).
68. Cordon-Cardo, C. et al. Molecular abnormalities of mdm2 and p53 genes in adult soft tissue sarcomas. *Cancer Res* 54, 794-9 (1994).
69. Lu, M. L. et al. Impact of alterations affecting the p53 pathway in bladder cancer on clinical outcome, assessed by conventional and array-based methods. *Clin Cancer Res* 8, 171-9 (2002).
70. Shibagaki, I. et al. p53 mutation, murine double minute 2 amplification, and human papillomavirus infection are frequently involved but not associated with each other in esophageal squamous cell carcinoma. *Clin Cancer Res* 1, 769-73 (1995).
71. Momand, J., Jung, D., Wilczynski, S. & Niland, J. The MDM2 gene amplification database. *Nucleic Acids Res* 26, 3453-9 (1998).

72. Sigalas, I., Calvert, A. H., Anderson, J. J., Neal, D. E. & Lunec, J. Alternatively spliced mdm2 transcripts with loss of p53 binding domain sequences: transforming ability and frequent detection in human cancer. *Nat Med* 2, 912-7 (1996).
73. Matsumoto, R. et al. Short alternative splice transcripts of the mdm2 oncogene correlate to malignancy in human astrocytic neoplasms. *Cancer Res* 58, 609-13 (1998).
74. Kraus, A. et al. Expression of alternatively spliced mdm2 transcripts correlates with stabilized wild-type p53 protein in human glioblastoma cells. *Int J Cancer* 80, 930-4 (1999).
75. Bartel, F., Taylor, A. C., Taubert, H. & Harris, L. C. Novel mdm2 splice variants identified in pediatric rhabdomyosarcoma tumors and cell lines. *Oncol Res* 12, 451-7 (2000).
76. Lukas, J. et al. Alternative and aberrant messenger RNA splicing of the mdm2 oncogene in invasive breast cancer. *Cancer Res* 61, 3212-9 (2001).
77. Tamborini, E. et al. Analysis of the molecular species generated by MDM2 gene amplification in liposarcomas. *Int J Cancer* 92, 790-6 (2001).
78. Fridman, J. S. et al. Tumor promotion by Mdm2 splice variants unable to bind p53. *Cancer Res* 63, 5703-6 (2003).
79. Steinman, H. A. et al. An alternative splice form of Mdm2 induces p53-independent cell growth and tumorigenesis. *J Biol Chem* 279, 4877-86 (2004).
80. Jones, S. N., Hancock, A. R., Vogel, H., Donehower, L. A. & Bradley, A. Overexpression of Mdm2 in mice reveals a p53-independent role for Mdm2 in tumorigenesis. *Proc Natl Acad Sci U S A* 95, 15608-12 (1998).
81. Harbour, J. W. & Dean, D. C. Rb function in cell-cycle regulation and apoptosis. *Nat Cell Biol* 2, E65-7 (2000).
82. Harbour, J. W. & Dean, D. C. The Rb/E2F pathway: expanding roles and emerging paradigms. *Genes Dev* 14, 2393-409 (2000).
83. Xiao, Z. X. et al. Interaction between the retinoblastoma protein and the oncoprotein MDM2. *Nature* 375, 694-8 (1995).
84. Loughran, O. & La Thangue, N. B. Apoptotic and growth-promoting activity of E2F modulated by MDM2. *Mol Cell Biol* 20, 2186-97 (2000).
85. Shan, B., Farmer, A. A. & Lee, W. H. The molecular basis of E2F-1/DP-1-induced S-phase entry and apoptosis. *Cell Growth Differ* 7, 689-97 (1996).
86. Juven-Gershon, T. et al. The Mdm2 oncoprotein interacts with the cell fate regulator Numb. *Mol Cell Biol* 18, 3974-82 (1998).

87. Gu, L., Findley, H. W. & Zhou, M. MDM2 induces NF-kappaB/p65 expression transcriptionally through Sp1-binding sites: a novel, p53-independent role of MDM2 in doxorubicin resistance in acute lymphoblastic leukemia. *Blood* 99, 3367-75 (2002).
88. Faustino, N. A. & Cooper, T. A. Pre-mRNA splicing and human disease. *Genes Dev* 17, 419-37 (2003).
89. Garcia-Blanco, M. A., Baraniak, A. P. & Lasda, E. L. Alternative splicing in disease and therapy. *Nat Biotechnol* 22, 535-46 (2004).
90. Venables, J. P. Aberrant and alternative splicing in cancer. *Cancer Res* 64, 7647-54 (2004).
91. Broeks, A. et al. ATM-heterozygous germline mutations contribute to breast cancer-susceptibility. *Am J Hum Genet* 66, 494-500 (2000).
92. Clarke, L. A. et al. Pathological exon skipping in an HNPCC proband with MLH1 splice acceptor site mutation. *Genes Chromosomes Cancer* 29, 367-70 (2000).
93. Jurica, M. S. & Moore, M. J. Pre-mRNA splicing: awash in a sea of proteins. *Mol Cell* 12, 5-14 (2003).
94. Nilsen, T. W. The spliceosome: the most complex macromolecular machine in the cell? *Bioessays* 25, 1147-9 (2003).
95. Bartel, F. et al. Amplification of the MDM2 gene, but not expression of splice variants of MDM2 mRNA, is associated with prognosis in soft tissue sarcoma. *Int J Cancer* 95, 168-75 (2001).
96. Bartel, F. et al. Expression of alternatively and aberrantly spliced transcripts of the MDM2 mRNA is not tumor-specific. *Int J Oncol* 24, 143-51 (2004).
97. Evans, S. C. et al. An alternatively spliced HDM2 product increases p53 activity by inhibiting HDM2. *Oncogene* 20, 4041-9 (2001).
98. Dang, J. et al. The RING domain of Mdm2 can inhibit cell proliferation. *Cancer Res* 62, 1222-30 (2002).
99. Zindy, F., Quelle, D. E., Roussel, M. F. & Sherr, C. J. Expression of the p16INK4a tumor suppressor versus other INK4 family members during mouse development and aging. *Oncogene* 15, 203-11 (1997).
100. Jackson Laboratory Catalog, Jax® Mice, T. J. L. in *Setting the Gold Standard for Genetic Purity*, page 45 (Bar Harbor, Maine, 2005-2007).
101. Persons, D. A. et al. Retroviral-mediated transfer of the green fluorescent protein gene into murine hematopoietic cells facilitates scoring and selection of transduced progenitors in vitro and identification of genetically modified cells in vivo. *Blood* 90, 1777-86 (1997).

102. Horton, R. M. et al. Gene splicing by overlap extension. *Methods Enzymol* 217, 270-9 (1993).
103. Niwa, H., Yamamura, K. & Miyazaki, J. Efficient selection for high-expression transfectants with a novel eukaryotic vector. *Gene* 108, 193-9 (1991).
104. Hogan, B. B., R; Costnatini, F; Lacy, E. *Manipulating the Mouse Embryo : A Laboratory Manual* (Cold Spring Harbor Laboratory Press, Plainview, New York, 1994).
105. Ray, P. S. et al. Transgene overexpression of alphaB crystallin confers simultaneous protection against cardiomyocyte apoptosis and necrosis during myocardial ischemia and reperfusion. *Faseb J* 15, 393-402 (2001).
106. Sunaga, S., Maki, K., Komagata, Y., Ikuta, K. & Miyazaki, J. I. Efficient removal of loxP-flanked DNA sequences in a gene-targeted locus by transient expression of Cre recombinase in fertilized eggs. *Mol Reprod Dev* 46, 109-13 (1997).
107. Harris, L. C. MDM2 splice variants and their therapeutic implications. *Curr Cancer Drug Targets* 5, 21-6 (2005).
108. Brinster, R. L. et al. Somatic expression of herpes thymidine kinase in mice following injection of a fusion gene into eggs. *Cell* 27, 223-31 (1981).
109. Palmiter, R. D. et al. Dramatic growth of mice that develop from eggs microinjected with metallothionein-growth hormone fusion genes. *Nature* 300, 611-5 (1982).
110. Leveillard, T., Gorry, P., Niederreither, K. & Wasylyk, B. MDM2 expression during mouse embryogenesis and the requirement of p53. *Mech Dev* 74, 189-93 (1998).
111. de Oca Luna, R. M. et al. The organization and expression of the *mdm2* gene. *Genomics* 33, 352-7 (1996).
112. Siegel, P. M., Dankort, D. L., Hardy, W. R. & Muller, W. J. Novel activating mutations in the *neu* proto-oncogene involved in induction of mammary tumors. *Mol Cell Biol* 14, 7068-77 (1994).
113. Mendrysa, S. M. et al. *mdm2* Is critical for inhibition of p53 during lymphopoiesis and the response to ionizing irradiation. *Mol Cell Biol* 23, 462-72 (2003).
114. Garcia-Cao, I. et al. "Super p53" mice exhibit enhanced DNA damage response, are tumor resistant and age normally. *Embo J* 21, 6225-35 (2002).
115. Tyner, S. D. et al. p53 mutant mice that display early ageing-associated phenotypes. *Nature* 415, 45-53 (2002).
116. Southern, J. A., Young, D. F., Heaney, F., Baumgartner, W. K. & Randall, R. E. Identification of an epitope on the P and V proteins of simian virus 5 that distinguishes between two isolates with different biological characteristics. *J Gen Virol* 72 (Pt 7), 1551-7 (1991).

117. Evans, L. H. & Cloyd, M. W. Friend and Moloney murine leukemia viruses specifically recombine with different endogenous retroviral sequences to generate mink cell focus-forming viruses. *Proc Natl Acad Sci U S A* 82, 459-63 (1985).
118. Evdokiou, A. et al. Expression of alternatively-spliced MDM2 transcripts in giant cell tumours of bone. *Int J Oncol* 19, 625-32 (2001).
119. Lohrum, M. A., Ashcroft, M., Kubbutat, M. H. & Vousden, K. H. Identification of a cryptic nucleolar-localization signal in MDM2. *Nat Cell Biol* 2, 179-81 (2000).
120. Chiang, C. M. & Roeder, R. G. Expression and purification of general transcription factors by FLAG epitope-tagging and peptide elution. *Pept Res* 6, 62-4 (1993).
121. Weber, J. D. et al. Cooperative signals governing ARF-mdm2 interaction and nucleolar localization of the complex. *Mol Cell Biol* 20, 2517-28 (2000).
122. Roberts, B. Nuclear location signal-mediated protein transport. *Biochim Biophys Acta* 1008, 263-80 (1989).
123. Kinkema, M., Fan, W. & Dong, X. Nuclear localization of NPR1 is required for activation of PR gene expression. *Plant Cell* 12, 2339-2350 (2000).
124. Zhang, Y. & Xiong, Y. Mutations in human ARF exon 2 disrupt its nucleolar localization and impair its ability to block nuclear export of MDM2 and p53. *Mol Cell* 3, 579-91 (1999).
125. Dang, C. V. & Lee, W. M. Nuclear and nucleolar targeting sequences of c-erb-A, c-myc, N-myc, p53, HSP70, and HIV tat proteins. *J Biol Chem* 264, 18019-23 (1989).
126. Michael, W. M. & Dreyfuss, G. Distinct domains in ribosomal protein L5 mediate 5 S rRNA binding and nucleolar localization. *J Biol Chem* 271, 11571-4 (1996).
127. Schmidt, C., Lipsius, E. & Kruppa, J. Nuclear and nucleolar targeting of human ribosomal protein S6. *Mol Biol Cell* 6, 1875-85 (1995).
128. Shaulsky, G., Goldfinger, N., Peled, A. & Rotter, V. Involvement of wild-type p53 protein in the cell cycle requires nuclear localization. *Cell Growth Differ* 2, 661-7 (1991).
129. Shaulsky, G., Goldfinger, N., Tosky, M. S., Levine, A. J. & Rotter, V. Nuclear localization is essential for the activity of p53 protein. *Oncogene* 6, 2055-65 (1991).
130. Liang, H., Atkins, H., Abdel-Fattah, R., Jones, S. N. & Lunec, J. Genomic organisation of the human MDM2 oncogene and relationship to its alternatively spliced mRNAs. *Gene* 338, 217-23 (2004).
131. Schlott, T. et al. Point mutations and nucleotide insertions in the MDM2 zinc finger structure of human tumours. *J Pathol* 182, 54-61 (1997).

8. Appendix

8.1. Alignment of the human and murine *MDM2* coding sequence

GenBank Accession number: human *MDM2* mRNA AX057138

murine *Mdm2* mRNA U40145

```

human      1  ATGTGCAATACCAACATGTCTGTACCTACTGATGGTGCTGTAACCACCTC  50
          |||
murine    203 ATGTGCAATACCAACATGTCTGTGTCTACCGAGGGTGCTGCAAGCACCTC  252
          .
human     51  ACAGATTCCAGCTTCGGAACAAGAGACCCTGGTTAGACCAAAGCCATTGC  100
          |||
murine    253  ACAGATTCCAGCTTCGGAACAAGAGACTCTGGTTAGACCAAAACCATTGC  302
          .
human    101  TTTTGAAGTTATTAAAGTCTGTTGGTGCACAAAAGACACTTATACTATG  150
          |||
murine    303  TTTTGAAGTTGTTAAAGTCCGTTGGAGCGCAAACGACACTTACACTATG  352
          .
human    151  AAAGAGGTTCTTTTTTATCTTGGCCAGTATATTATGACTAAACGATTATA  200
          |||
murine    353  AAAGAGATTATATTTTATATTGGCCAGTATATTATGACTAAGAGGTTATA  402
          .
human    201  TGATGAGAAGCAACAACATATTGTATATTGTTCAAATGATCTTCTAGGAG  250
          |||
murine    403  TGACGAGAAGCAGCAGCACATTGTGTATTGTTCAAATGATCTCCTAGGAG  452
          .
human    251  ATTTGTTTGGCGTGCCAAGCTTCTCTGTGAAAGAGCACAGGAAAATATAT  300
          |||
murine    453  ATGTGTTTGGAGTCCCGAGTTTCTCTGTGAAGGAGCACAGGAAAATATAT  502
          .
human    301  ACCATGATCTACAGGAACTTGGTAGTAGTCAATCAGCAGGAATCATCGGA  350
          |
murine    503  GCAATGATCTACAGAAATTTAGTGGCTGTAAGTCAGCA.....AGA  543
          .
human    351  CTCAGGTACATCTGTGAGTGAGAACAGGTGTCACCTTGAAGGTGGGAGTG  400
          |||
murine    544  CTCTGGCACATCGCTGAGTGAGAGCAGACGTCAGCCTGAAGGTGGGAGTG  593
          .
human    401  ATCAAAAGGACCTTGTACAAGAGCTTCAGGAAGAGAAACCTTCATCTTCA  450
          |||
murine    594  ATCTGAAGGATCCTTTGCAAGCGCCACCAGAAGAGAAACCTTCATCTTCT  643
          .
human    451  CATTGGTTTCTAGACCATCTACCTCATCTAGAAGGAGAGCAATTAGTGA  500
          |||
murine    644  GATTTAATTTCTAGACTGTCTACCTCATCTAGAAGGAGATCCATTAGTGA  693
          .
human    501  GACAGAAGAAAATTCAGATGAATTATCTGGTGAACGACAAAGAAAACGCC  550
          |||
murine    694  GACAGAAGAGAACACAGATGAGCTACCTGGGGAGCGGCACCGGAAGCGCC  743

```

```

human 551 ACAAATCTGATAGTATTTCCCTTTCCCTTTGATGAAAGCCTGGCTCTGTGT 600
          | | | | | | | | | | | | | | | | | | | | | | | | | | | |
murine 744 .....GCAGGTCCTGTCCCTTTGATCCGAGCCTGGGTCTGTGT 781
          | | | | | | | | | | | | | | | | | | | | | | | | | | | |
human 601 GTAATAAGGGAGATATGTTGTG.....AAAGAAGCAGTAG 635
          | | | | | | | | | | | | | | | | | | | | | | | | | | | |
murine 782 GAGCTGAGGGAGATGTGCAGCGGCGGCAGCAGCAGCAGTAGCAGCAGCAG 831
          | | | | | | | | | | | | | | | | | | | | | | | | | | | |
human 636 CAGTGAATCTACAGGGACGCCATCGAATCCGGATCTTGATGCTGGTGTAA 685
          | | | | | | | | | | | | | | | | | | | | | | | | | | | |
murine 832 CAGCGAGTCCACAGAGACGCCCTCGCATCAGGATCTTGACGATGGCGTAA 881
          | | | | | | | | | | | | | | | | | | | | | | | | | | | |
human 686 GTGAACATTCAGGTGATTGGTTGGATCAGGATTCAGTTTCAGATCAGTTT 735
          | | | | | | | | | | | | | | | | | | | | | | | | | | | |
murine 882 GTGAGCATTCTGGTGATTGCCTGGATCAGGATTCAGTTTCTGATCAGTTT 931
          | | | | | | | | | | | | | | | | | | | | | | | | | | | |
human 736 AGTGTAGAATTTGAAGTTGAATCTCTCGACTCAGAAGATTATAGCCTTAG 785
          | | | | | | | | | | | | | | | | | | | | | | | | | | | |
murine 932 AGCGTGGAATTTGAAGTTGAGTCTCTGGACTCGGAAGATTACAGCCTGAG 981
          | | | | | | | | | | | | | | | | | | | | | | | | | | | |
human 786 TGAAGAAGGACAAGAACTCTCAGATGAAGATGATGAGGTATATCAAGTTA 835
          | | | | | | | | | | | | | | | | | | | | | | | | | | | |
murine 982 TGACGAAGGGCACGAGCTCTCAGATGAGGATGATGAGGTCTATCGGGTCA 1031
          | | | | | | | | | | | | | | | | | | | | | | | | | | | |
human 836 CTGTGTATCAGGCAGGGGAGAGTGATACAGATTCATTTGAAGAAGATCCT 885
          | | | | | | | | | | | | | | | | | | | | | | | | | | | |
murine 1032 CAGTCTATCAGACAGGAGAAAGCGATACAGACTCTTTTGAAGGAGATCCT 1081
          | | | | | | | | | | | | | | | | | | | | | | | | | | | |
human 886 GAAATTTCCCTTAGCTGACTATTGGAAATGCACTTCATGCAATGAAATGAA 935
          | | | | | | | | | | | | | | | | | | | | | | | | | | | |
murine 1082 GAGATTTCCCTTAGCTGACTATTGGAAAGTGTACCTCATGCAATGAAATGAA 1131
          | | | | | | | | | | | | | | | | | | | | | | | | | | | |
human 936 TCCCCCCTTCCATCACATTGCAACAGATGTTGGGCCCTTCGTGAGAATT 985
          | | | | | | | | | | | | | | | | | | | | | | | | | | | |
murine 1132 TCCTCCCCCTTCCATCACACTGCAAAAGATGCTGGACCCTTCGTGAGAACT 1181
          | | | | | | | | | | | | | | | | | | | | | | | | | | | |
human 986 GGCTTCCTGAAGATAAAAGGGAAAGATAAAGGGGAAATCTCTGAGAAAGCC 1035
          | | | | | | | | | | | | | | | | | | | | | | | | | | | |
murine 1182 GGCTTCCAGACGATAAAGGGGAAAGATAAAGTGGAAATCTCTGAAAAAGCC 1231
          | | | | | | | | | | | | | | | | | | | | | | | | | | | |
human 1036 AAACTGGAAAACCTCAACACAAGCTGAAGAGGGCTTTGATGTTCCCTGATTG 1085
          | | | | | | | | | | | | | | | | | | | | | | | | | | | |
murine 1232 AAACTGGAAAACCTCAGCTCAGGCAGAAGAAGGCTTGGATGTGCCTGATGG 1281
          | | | | | | | | | | | | | | | | | | | | | | | | | | | |
human 1086 TAAAAAACTATAGTGAATGATTCCAGAGAGTCATGTGTT...GAGGAAA 1132
          | | | | | | | | | | | | | | | | | | | | | | | | | | | |
murine 1282 CAAAAAGCTGACAGAGAATGATGCTAAAGAGCCATGTGCTGAGGAGGACA 1331
          | | | | | | | | | | | | | | | | | | | | | | | | | | | |
human 1133 ATGATGATAAAATTACACAAGCTTCACAATCACAAGAAAGTGAAGACTAT 1182
          | | | | | | | | | | | | | | | | | | | | | | | | | | | |
murine 1332 GCGAGGAGAAGGCCGAACAGACGCCCTGTCCCAGGAGAGTGACACTAT 1381
          | | | | | | | | | | | | | | | | | | | | | | | | | | | |
human 1183 TCTCAGCCATCAACTTCTAGTAGCATTATTTATAGCAGCCAAGAAGATGT 1232
          | | | | | | | | | | | | | | | | | | | | | | | | | | | |
murine 1382 TCCCAACCATCGACTTCCAGCAGCATTGTTTATAGCAGCCAAGAAAGCGT 1431
          | | | | | | | | | | | | | | | | | | | | | | | | | | | |

```

```

human  1233  GAAAGAGTTT·GAAAGGG·AAGAAACCCA·AGACAA·AGAAGAGAGTGTGGAAT 1282
         | | | | | | | | | | | | | | | | | | | | | | | | | | | | | | | | | | | | |
murine 1432  GAAAGAGTT...GAAGGAGGAAACGCAGGACAAAGACGAGAGTGTGGAAT 1478
         .
human  1283  CTAGTTTGCCCCTTAATGCCATTGAACCTTGTGTGATTTGTCAAGGTCGA 1332
         | | | | | | | | | | | | | | | | | | | | | | | | | | | | | | | | |
murine 1479  CTAGCTTCTCCCTGAATGCCATCGAACCATGTGTGATCTGCCAGGGGCGG 1528
         .
human  1333  CCTAAAAATGGTTGCATTGTCCATGGCAAACAGGACATCTTATGGCCTG 1382
         | | | | | | | | | | | | | | | | | | | | | | | | | | | | | | | | |
murine 1529  CCTAAAAATGGCTGCATTGTTACGGCAAGACTGGACACCTCATGTCATG 1578
         .
human  1383  CTTTACATGTGCAAAGAAGCTAAAGAAAAGGAATAAGCCCTGCCCAGTAT 1432
         | | | | | | | | | | | | | | | | | | | | | | | | | | | | | | | | |
murine 1579  TTTCACGTGTGCAAAGAAGCTAAAAAAAAAGAAACAAGCCCTGCCCAGTGT 1628
         .
human  1433  GTAGACAACCAATTCAAATGATTGTGCTAACTTATTTCCCCTAG 1476
         | | | | | | | | | | | | | | | | | | | | | | | | | | | | | | | |
murine 1629  GCAGACAGCCAATCCAAATGATTGTGCTAAGTTACTTCAACTAG 1672

```

The exons in the MDM2 coding sequence are high-lighted in gray, starting with exon 3. The start and stop codons are shown in bold.¹³⁰

8.3. Commonly used Oligonucleotides for human *MDM2*

```

1   ATGtgcaata ccaacatgtc tgtacctact gatggtgctg taaccacctc
----- MdmKS1 ----->
51  acagattcca gcttcggaac aagagaccct ggtagacca aagccattgc
101 ttttgaagtt attaaagtct gttggtgcac aaaaagacac ttatactatg
151 aaagaggttc ttttttatct tggccagtat attatgacta aacgattata
201 tgatgagaag caacaacata ttgtatattg ttcaaagatg cttctaggag
251 atttgtttgg cgtgccaagc ttctctgtga aagagcacag gaaaatatat
301 accatgatct acaggaactt ggtagtagtc aatcagcagg aatcatcggg
351 ctcaggtaca tctgtgagtg agaacagggtg tcaccttgaa ggtgggagtg
401 atcaaaagga ccttgtacaa gagcttcagg aagagaaacc tcatcttca
451 catttggttt ctagaccatc tacctcatct agaaggagag caattagtga
501 gacagaagaa aattcagatg aattatctgg tgaacgacaa agaaaacgcc
----- MutAS182/183 -----
551 acaaatctga tagtatttcc ctttcctttg atgaaagcct ggctctgtgt
----->
601 gtaataaggg agatatgttg tgaagaagc agtagcagtg aatctacagg
651 gacgccatcg aatccggatc ttgatgctgg tgtaagtga cttcagggtg
701 attggttggg tcaggattca gtttcagatc agtttagtgt agaatttgaa
751 gttgaatctc tcgactcaga agattatagc cttagtgaag aaggacaaga
801 actctcagat gaagatgatg aggtatatca agttactgtg taccaggcag
851 gggagagtga tacagattca tttgaagaag atcctgaaat ttccttagct
901 gactattgga aatgcacttc atgcaatgaa atgaatcccc cccttccatc
951 acattgcaac agatggttggg cccttcgtga gaattggctt cctgaagata
1001 aagggaaaga taaaggggaa atctctgaga aagccaaact ggaaaactca
1051 acacaagctg aagagggcct tgatgttcct gattgtaaaa aaactatagt
1101 gaatgattcc agagagtcac gtgttgagga aatgatgatg aaaattacac
1151 aagcttcaca atcacaagaa agtgaagact attctcagcc atcaacttct
1201 agtagcatta tttatagcag ccaagaagat gtgaaagagt ttgaaagggg
1251 agaaacccaa gacaaagaag agagtgtgga atctagtttg ccccttaatg
1301 ccattgaacc ttgtgtgatt tgtcaaggtc gacctaaaaa tggttgcatt
1351 gtccatggca aaacaggaca tcttatggcc tgctttacat gtgcaaagaa
-----<-----
----- MutAS466/467 -----
1401 gctaaagaaa aggaataagc cctgcccagt atgtagacaa ccaattcaaa
----- MdmKS2 -----
----- MutAS469/470 ----->
----->
1451 tgattgtgct aacttatttc cccTAG
<----- MdmKS3 -----

```

Oligonucleotides are represented as dashed lines. Aligning sequences are shown in bold, italic or are underlined. Start and Stop codons are shown in capital letters.

8.4. Commonly used Oligonucleotids of murine *Mdm2*

```

203   ATGtgcaa taccaacatg tctgtgtcta ccgaggggtgc tgcaagcacc
      ----- Mouse5end ---->
251   tcacagattc cagcttcgga acaagagact ctgggttagac caaaaccatt
      <----- Super3ex -----
301   gcttttgaag ttgttaaagt ccgttggagc gcaaaaacgac acttacacta
351   tgaaagagat tatattttat attggccagt atattatgac taagaggtta
401   tatgacgaga agcagcagca cattgtgtat tgttcaaagt atctcctagg
451   agatgtgttt ggagtcccga gtttctctgt gaaggagcac aggaaaatat
501   atgcaatgat ctacagaaat ttagtggctg taagtcagca agactctggc
551   acatcgctga gtgagagcag acgtcagcct gaaggtggga gtgatctgaa
601   ggatcccttg caagcgccac cagaagagaa accttcatct tctgatttaa
651   tttctagact gtctacctca tctagaagga gatccattag tgagacagaa
701   gagaacacag atgagctacc tggggagcgg caccggaagc gccgcaggtc
751   cctgtccttt gatccgagcc tgggtctgtg tgagctgagg gagatgtgca
801   gcggcggcag cagcagcagt agcagcagca gcagcagtc cacagagacg
851   ccctcgcatc aggatcttga cgatggcgta agtgagcatt ctgggtgattg
      ----- Super10ex ----->
901   cctggatcag gattcagttt ctgatcagtt tagcgtggaa tttgaagttg
951   agtctctgga ctcggaagat tacagcctga gtgacgaagg gcacgagctc
1001  tcagatgagg atgatgaggc ctatcggggtc acagtctatc agacaggaga
1051  aagcgataca gactcttttg aaggagatcc tgagatttcc ttagctgact
1101  attggaagtg tacctcatgc aatgaaatga atcctcccct tccatcacac
1151  tgcaaaagat gctggaccct tctgtgagaac tggcttccag acgataaagg
1201  gaaagataaa gtggaaatct ctgaaaaagc caaactggaa aactcagctc
1251  aggcagaaga aggcttggat gtgcctgatg gcaaaaagct gacagagaat
1301  gatgctaaag agccatgtgc tgaggaggac agcgaggaga aggccgaaca
1351  gacgccctg tcccaggaga gtgacgacta ttccaacca tcgacttcca
1401  gcagcattgt ttatagcagc caagaaagcg tgaaagagtt gaaggaggaa
1451  acgcaggaca aagacgagag tgtggaatct agcttctccc tgaatgccat
1501  cgaaccatgt gtgatctgcc aggggcggcc taaaaatggc tgcattgttc
1551  acggcaagac tggacacctc atgtcatggt tcacgtgtgc aaagaagcta
1601  aaaaaaagaa acaagccctg cccagtgtgc agacagccaa tccaaatgat
1651  tgtgctaagt tacttcaact AG
      <----- Mouse3end -----

```

Oligonucleotids are represented as dashed lines. Aligning sequence is shown bold. Start and Stop codons are shown in capital letters.

Acknowledgement

This work would have not been written without the help of dear friends, coworkers and peers who helped, encouraged and supported me during the past four years.

Linda Harris, PhD, thank you so much for being my mentor and friend, and for your trust in my work and my abilities. I am grateful that you gave me the opportunity to investigate such an interesting and exciting science project. Your optimism is contagious, and I truly enjoyed being a member of your research lab.

Ich möchte mich bei Ihnen, Herrn Prof. Dr. Rainer Rudolph recht herzlich für Ihre Betreuung meiner Dissertation von Seiten der Martin-Luther-Universität Halle-Wittenberg bedanken.

I would like to show my sincerest gratitude to the members of my lab. Misty D. Cheney, thank you for being my friend and a great help. Your daily “Guten Morgen” made me feel at home. Pam McKenzie, PhD, thanks for setting the bar high, I realize that sciences can be fun but also hard and discouraging. And your saying “Science sucks!” is ever so true. Queen Rodgers, I am forever indebted to you for teaching me the basics in lab etiquette and sharing all your knowledge about adenoviruses. Erin Volk, PhD, I enjoyed our helpful discussions about scientific and other topics. If you ever need a break from the bench, let me know, we can still change careers and write a soap opera about science drama. Justin Marlar and Katie Nemeth, thank you very much for bringing in a breeze of fresh air. My research would have never been completed without the help of three special lab members, Jerry, Bianca and of course Rudi.

Department chair Peter Houghton, PhD, thank you very much for supporting my stay in the United States and for all your help during my work. Thanks to the members of the department of Molecular Pharmacology at St. Jude Children’s Research Hospital, I am grateful for your help and your kindness. I am especially grateful to all the members of the laboratories of Philip Potter, PhD, and Mary Danks, PhD. Thanks for always being helpful and sharing your knowledge and your lab supplies.

I also want to acknowledge Martine Roussel, PhD, for providing plasmid constructs and for helpful discussions. Furthermore, I would like to thank John Raucchi, George Heath, and the Transgenic Core Facility at St. Jude for the generation of the transgenic mice; June Bursi and the Animal Resource Center for the technical assistance; Kelli Boyd and the Diagnostic Lab for evaluating the mouse tissues. I also acknowledge the St. Jude Hartwell Center for primer production and sequencing analysis and the St. Jude Flow cytometry Lab

for sorting the GFP positive cells and performing cell cycle analysis. This work was supported by NIH grants CA92401, CA21765, and the American Lebanese Syrian Associated Charities (ALSAC).

Vielen herzlichen Dank lieber Herr PD Dr. Helge Taubert und Herr Dr. Frank Bartel (Institut für Pathologie der Martin-Luther-Universität in Halle/Saale) für Ihr Interesse und Ihre Unterstützung an meiner Arbeit.

Liebe Maminki, lieber Paps und liebe Anni, vielen Dank für Eure offenen Ohren und Eure Neugier an meiner Arbeit und meinem Leben. Ihr habt mich angespornt, mich aufgemuntert und von mir verlangt. Liebe Ola, ich vermisse Dich. An meine Freundinnen Paula und Jana, vielen lieben Dank dass Ihr immer für mich da seid. Steve, thanks for your encouragement, your trust and your love.

Curriculum vitae

Katja Schuster

Anschrift Deutschland	Lindenstr. 15 03096 Guhrow
Anschrift USA	985 Oakmont Place Apt. 1 Memphis, TN 38107
Familienstand	ledig
Geboren am	31.12.1975 in Cottbus
1982-1990	Besuch der 6. Polytechnischen Oberschule „Alexander Puschkin“, Cottbus.
1990-1992	Besuch der 17. Oberschule „Ernst Schneller“, Cottbus.
1992-1996	Besuch der gymnasialen Oberstufe des Oberstufenzentrums 1, Cottbus.
1993-1994	Austauschschüler, Besuch der Fredericksburg High School, Fredericksburg, TX, USA.
1996	Abitur

Wissenschaftlicher Werdegang

1996-2001	Studium der Biochemie, Martin-Luther-Universität, Halle-Wittenberg.
2001	Abschluss als Diplom-Biochemikerin, Institut für Pathologie, Abteilung Molekularpathologie, Halle-Wittenberg. Diplom Thema: „Untersuchung von Weichteilsarkomen auf genomische Instabilität“
seit 2001	Doktorandin, Research Scholar, Department für Molekulare Pathologie, St. Jude Children’s Research Hospital, Memphis, TN, USA. Projekt: “Characterization of MDM2 splice variants“

Memphis, den 24. Februar 2006

Katja Schuster

List of publications

Published:

1. Taubert H, Schuster K, Brinck U, Bartel F, Kappler M, Lautenschläger C, Bache M, Trump C, Schmidt H, Holzhausen H.J. Würll P, and Schlott T. (2003a). Loss of heterozygosity at 12q14-15 often occurs in stage I soft tissue sarcomas and is associated with MDM2 amplification in tumors at various stages. *Mod Pathol* 16, 1109-1116.
2. Taubert H, Bartel F, Kappler M, Schuster K, Meye A, Lautenschläger C, Thamm-Mucke B, Bache M, Schmidt H, Holzhausen HJ, and Würll P. (2003b). Reduced expression of hMSH2 protein is correlated to poor survival for soft tissue sarcoma patients. *Cancer* 97, 2273-2278.
3. Hoefling C, Schmidt H, Meinhardt M, Lohse A, Taubert H, Fuessel S, Schmidt U, Schuster K, Baretton G, Wirth MP, and Meye A. (2004). Comparative evaluation of microsatellite marker, AP-PCR and CGH studies in primary renal cell carcinoma. *Int J Mol Med* 13, 835-842.

Published abstracts and posters:

1. Schuster K, McKenzie PP, Cheney MD, Harris LC. The effects of p14ARF, p53 and full-length MDM2 on the cellular localization of MDM2 splice variants. 94th meeting of the American Association for Cancer Research, Washington, DC. July 11-14. *Proc. AACR* 44:403, 2003.
2. Schuster K, Cheney MD, Harris LC. Selection for mutations in Mdm2-a transgenic mice. 95th meeting of the American Association for Cancer Research, Orlando, Florida. March 27-31. *Proc. AACR* 45:2543, 2004.
3. Schuster K, Cheney MD, McKenzie PP, Harris LC. MDM2-A is growth inhibitory in a transgenic mouse model. 96th meeting of the American Association for Cancer Research, Anaheim, California. April 16-20. *Proc. AACR* 46:1070, 2005.

Submitted:

1. Schuster K, Volk EL, Cheney MD, McKenzie PP, Harris LC. Expression of a common tumor MDM2 splice variant results in embryonic lethality and selection for mutations in transgenic mice.
2. Taylor AC, Schuster K, McKenzie PP, Harris LC. Differential cooperation of oncogenes to induce p53-mediated apoptosis of rhabdomyosarcoma cells.

In preparation:

1. Schuster K, McKenzie PP, Harris LC. MDM2 splice variants predominantly localize to the nucleoplasm of the cell mediated by a C-terminal nuclear localization signal.
2. Cheney MD, McKenzie PP, Schuster K, Harris LC. Growth of tumor cells with a constitutively active NFκB pathway can be suppressed by MDM2-mediated suppression of NFκB p65RelA subunit.

Selbstständigkeitserklärung

Ich erkläre hiermit, die vorliegende Arbeit selbstständig und ohne unerlaubte fremde Hilfe angefertigt zu haben. Alle benutzten Quellen und Textstellen aus veröffentlichten und unveröffentlichten Schriften sind als solche gekennzeichnet und im Referenzverzeichnis aufgeführt. Ebenso sind alle bereitgestellten Materialien und erbrachten Leistungen anderer Personen als solche gekennzeichnet.

Ich erkläre, dass diese Dissertationsschrift an keiner anderen Einrichtung oder Universität zur Begutachtung eingereicht worden ist.

Memphis, den 24. Februar 2006

Katja Schuster